AD-A118 518 DELAWARE UNIV NEWARK DEPT OF CIVIL ENGINEERING F/G 8/3
NUMERICAL MODELING OF THE NEARSHORE REGION.(U)
JUN 82 J T KIRBY, R A DALRYMPLE N00014-81-K-0297
UNCLASSIFIED CE-82-24 NL

1 OF 2
AD A
118518

AD-A118518

# NUMERICAL MODELING OF THE NEARSHORE REGION


by

**James T. Kirby, Jr.**

and

**Robert A. Dalrymple**



Technical Report No. 11

Contract No. N00014-81-K-0297

with the OFFICE OF NAVAL RESEARCH, GEOGRAPHY PROGRAMS

Research Report CE-82-24

June 1982


OCEAN ENGINEERING PROGRAM


DEPARTMENT OF CIVIL ENGINEERING

UNIVERSITY OF DELAWARE

NEWARK, DELAWARE

19711

# NUMERICAL MODELLING OF THE NEARSHORE REGION

by

JAMES T. KIRBY, Jr.

and

ROBERT A. DALRYMPLE

Technical Report No. 11

Contract No. N00014-81-K-0297

with the Office of Naval Research, Geography Programs

RESEARCH REPORT CE-82-24

June 1982

Ocean Engineering Program

Department of Civil Engineering

University of Delaware

Newark, Delaware

19711

SECURITY CLASSIFICATION OF THIS PAGE (When Data Entered)

# REPORT DOCUMENTATION PAGE

READ INSTRUCTIONS BEFORE COMPLETING FORM

| | |
|---|---|
| 1. REPORT NUMBER: ONR TR. No. 11 | 2. GOVT ACCESSION NO. |
| 3. RECIPIENT'S CATALOG NUMBER | |
| 4. TITLE (and Subtitle): Numerical Modelling of the Nearshore Region | 5. TYPE OF REPORT & PERIOD COVERED |
| | 6. PERFORMING ORG. REPORT NUMBER |
| 7. AUTHOR(s): James T. Kirby, Jr. and Robert A. Dalrymple | 8. CONTRACT OR GRANT NUMBER(s): N00014-81-K-0297 |
| 9. PERFORMING ORGANIZATION NAME AND ADDRESS | 10. PROGRAM ELEMENT, PROJECT, TASK AREA & WORK UNIT NUMBERS |
| 11. CONTROLLING OFFICE NAME AND ADDRESS: Department of Civil Engineering, University of Delaware, Newark, DE 19711 | 12. REPORT DATE: June 1982 |
| | 13. NUMBER OF PAGES: 163 |
| 14. MONITORING AGENCY NAME & ADDRESS (if different from Controlling Office) | 15. SECURITY CLASS. (of this report) |
| | 15a. DECLASSIFICATION/DOWNGRADING SCHEDULE |

16. DISTRIBUTION STATEMENT (of this Report)

This report has been approved for public release and sale; its distribution is unlimited

17. DISTRIBUTION STATEMENT (of the abstract entered in Block 20, if different from Report)

18. SUPPLEMENTARY NOTES

19. KEY WORDS (Continue on reverse side if necessary and identify by block number)

Numerical models, nearshore circulation, longshore currents, rip currents

20. ABSTRACT (Continue on reverse side if necessary and identify by block number)


The thoeretical background and numerical formulation for two finite-difference models for predicting nearshore circulation are reviewed. The models are based on the time- and depth-averaged equations of continuity and momentum, with momentum flux terms derived from linear wave theory. Wave shoaling and refraction are determined by the method of Noda et al. (1974). The first model,


DD FORM 1 JAN 73 1473 EDITION OF 1 NOV 65 IS OBSOLETE

Unclassified

SECURITY CLASSIFICATION OF THIS PAGE (When Data Entered) referred to as linear, neglects the effects of convective acceleration and lateral mixing, and calculates bottom friction using the small mean current assumption. The second, nonlinear model includes the neglected effects, and uses the full bottom stress relation as given by Liu and Dalrymple (1978). Both models solve iteratively for mean currents and mean free surface displacement at discrete grid points.

A calibration of both models is described based on comparison with field data obtained from the NSTS Torrey Pines experiment (Gable, 1979). Finally, various results obtained during previous studies utilizing the models are presented and discussed.

AD A118 518

Blank pages

p. ii, vi

p. 28, 44, 76, 110, 114, 126, 140

DTIC DDAB
6 Oct 82

## ABSTRACT

The theoretical background and numerical formulation for two finite-difference models for predicting nearshore circulation are reviewed. The models are based on the time- and depth-averaged equations of continuity and momentum, with momentum flux terms derived from linear wave theory. Wave shoaling and refraction are determined by the method of Noda et al. (1974). The first model, referred to as linear, neglects the effects of convective acceleration and lateral mixing, and calculates bottom friction using the small mean current assumption. The second, nonlinear model includes the neglected effects, and uses the full bottom stress relation as given by Liu and Dalrymple (1978). Both models solve iteratively for mean currents and mean free surface displacement at discrete grid points.

A calibration of both models is described based on comparison with field data obtained from the NSTS Torrey Pines experiment (Gable, 1979). Finally, various results obtained during previous studies utilizing the models are presented and discussed.

TABLE OF CONTENTS

Page

Abstract . . . . . . . . . . . . . . . . . . . . . . . . . . i

List of Figures . . . . . . . . . . . . . . . . . . . . . . . vii

Chapter I. Introduction . . . . . . . . . . . . . . . . . . . . 1

Chapter II. Theoretical Development of the Models . . . . . . . . 3

1. Introduction . . . . . . . . . . . . . . . . . . . . . . 3

2. Theoretical Framework of the Models . . . . . . . . . . . 3

2.1 Specification of the Boundary Value Problem . . . 5

2.2 Depth and Time Averaged Forms of the Equations . . 9

2.3 Radiation Stresses . . . . . . . . . . . . . . . . 12

2.4 Wind Stress . . . . . . . . . . . . . . . . . . . . 13

2.5 Bottom Stress . . . . . . . . . . . . . . . . . . . 14

2.6 Wave Refraction and Shoaling Including Wave-Current Interaction . . . . . . . . . . . . . . 15

2.7 Wave Breaking Criteria . . . . . . . . . . . . . . 19

2.8 Lateral Mixing . . . . . . . . . . . . . . . . . . 20

2.9 Wave Height Decay . . . . . . . . . . . . . . . . . 22

3. Overview of the Linear and Nonlinear Models . . . . . . 25

Chapter III. Formulation of the Numerical Models . . . . . . . . . 29

1. Introduction . . . . . . . . . . . . . . . . . . . . . . 29

2. The Grid Scheme and Location of the Unknown Quantities . . . . . . . . . . . . . . . . . . . . . . . 30

3. Boundary Conditions . . . . . . . . . . . . . . . . . . . 34

Page

4. Finite Difference Operators and Notation . . . . . . . 36

5. Finite Difference Forms of the Governing Equations - Linear Model . . . . . . . . . . . . . . . . 37

6. Finite Difference Forms of the Governing Equations - Nonlinear Model . . . . . . . . . . . . . . 40

7. The Numerical Scheme for Refraction and the Wave Height Field . . . . . . . . . . . . . . . . . . . . . . 45

Chapter IV. Calibration of the Nearshore Circulation Models . . . 49

1. Field Data Used for Calibration . . . . . . . . . . . . . 49

1.1 Choice of Field Data Used for Calibration . . . . 51

2. Calibration of the Models . . . . . . . . . . . . . . . . 61

2.1 Linear Model Calibration . . . . . . . . . . . . . . 63

2.2 Nonlinear Model Calibration . . . . . . . . . . . 65

2.3 Response of Both Models Using Data Set 2 . . . . . 68

3. Discussion of the Calibrated Coefficients . . . . . . . 72

Chapter V. Examples of Numerical Results Using the Nearshore Circulation Models . . . . . . . . . . . . . . . . . . . 77

1. Introduction . . . . . . . . . . . . . . . . . . . . . . . 77

2. Specific Applications of the Linear and Nonlinear Models . . . . . . . . . . . . . . . . . . . . . . . . . 77

2.1 Plane Beach Applications . . . . . . . . . . . . . . 78

2.2 Barred Profile Applications . . . . . . . . . . . 86

2.3 Applications to the Laboratory Wave Basin . . . . 90

2.4 Periodic Bottom Topography . . . . . . . . . . . . . 91

2.5 Intersecting Waves Applications . . . . . . . . . 102

Chapter VI. Conclusions . . . . . . . . . . . . . . . . . . . . . . . 111

Page

References . . . . . . . . . . . . . . . . . . . . . . . . . . . . 115

Appendix I. Using the Nearshore Circulation Program . . . . . . . 119

Listing of Linear Model . . . . . . . . . . . . . . . . . . . 125

Listing of Nonlinear Model . . . . . . . . . . . . . . . . . 143

LIST OF FIGURES


| Figure No. | Title | Page |
|---|---|---|
| 2-1 | Plan Definition Sketch For Coordinate System | 6 |
| 2-2 | Longuet-Higgins' Analytical Solution for Oblique Wave Attack on a Plane Beach | 21 |
| 3-1 | Grid Scheme | 31 |
| 3-2 | Velocity Components for Grid Block (i,j) | 33 |
| 3-3 | General Leapfrog Solution Scheme | 43 |
| 4-1 | Location of NSTS Torrey Pines Experiment | 50 |
| 4-2 | Instrumentation for NSTS Torrey Pines Experiment | 52 |
| 4-3 | Torrey Pines Nearshore Bathymetry, November 9, 1978 | 53 |
| 4-4 | Torrey Pines Nearshore Bathymetry, November 18, 1978 | 54 |
| 4-5 | Time Averaged Current Measurements, November 10, 1978 | 57 |
| 4-6 | Average Field Velocity Profile, Data Set 1 | 58 |
| 4-7 | Angular Distribution of Spectral Density, November 15, 1978 | 60 |
| 4-8 | Average Field Velocity Profile, Data Set 2 | 62 |
| 4-9 | Currents Induced in Model Using Nov. 9 Bathymetry. Nonlinear Model: Data Set 1 | 64 |
| 4-10 | Longshore Average Depth Profile, Torrey Pines, Nov. 9 | 66 |
| 4-11 | Variation of Longshore Current with Friction Factor in the Linear Model | 67 |
| 4-12 | Variation of Longshore Current with Lateral Mixing in the Nonlinear Model. f = 0.015 | 69 |
| 4-13 | Variation of Longshore Current with Lateral Mixing in the Nonlinear Model. f = 0.010 | 70 |
| 4-14 | Longshore Current in the Linear and Nonlinear Models. Data Set 2 | 71 |

| Figure No. | Title | Page |
|---|---|---|
| 4-15 | Currents Induced in Model Using Nov. 18 Bathymetry. Nonlinear Model: Data Set 2 | 73 |
| 5-1 | Set-up on a Plane Beach | 79 |
| 5-2 | Set-up at Shoreline Due to a Wave Group with a Period of 18 Seconds | 81 |
| 5-3 | Resonance of Wave Channel Due to Forcing at Seiche Period | 82 |
| 5-4 | Inshore Mean Free Surface Displacement Versus Time for the Nonlinear Model Application to a Plane Beach | 83 |
| 5-5 | Longshore Current Profile for Plane Beach. Linear Model | 84 |
| 5-6 | Longshore Current Profile for Plane Beach. Nonlinear Model | 85 |
| 5-7 | Barred and Plane Beach Profiles | 87 |
| 5-8 | Longshore Current Profile for Barred Beach. Linear Model | 88 |
| 5-9 | Longshore Current Profile for Barred Beach. Nonlinear Model | 89 |
| 5-10 | Experimental Streamlines in the Wave Basin (From Dalrymple et al., 1977) | 92 |
| 5-11 | Currents in Model Basin Corresponding to Dalrymple et al. (1977) | 93 |
| 5-12 | Predicted and Measured Longshore Velocities for the Basin Test Case | 94 |
| 5-13 | Depth Contours for the Periodic Bottom of Noda (1973) | 96 |
| 5-14 | Current Vectors for Noda Topography. Linear Model | 97 |
| 5-15 | Current Vectors for Noda Topography. Nonlinear Model | 98 |
| 5-16 | Currents Induced by Bulge on a Plane Beach. Linear Model | 100 |
| 5-17 | Currents Induced by Bulge on a Plane Beach. Nonlinear Model | 101 |

| Figure No. | Title | Page |
|---|---|---|
| 5-18 | Definition Sketch for the Intersecting Wave Application | 102 |
| 5-19 | Current Vector Plot for a Rip Current Perpendicular to the Shoreline | 108 |
| 5-20 | Current Vector Plot for the Meandering Circulation Pattern | 109 |

## Chapter I

## INTRODUCTION

The need for methods to accurately predict the magnitude and spatial distribution of nearshore currents is central to the present research efforts aimed at quantifying the transport of marine sediment in the beach and nearshore environment. Investigators have made significant strides in describing the mean wave-induced motions in the surf zone in the twenty years since the correct formulation of the averaged equations of motion. Using the concept of wave momentum flux, or radiation stress (see Longuet-Higgins and Stewart, 1964), it has become possible to analytically predict the wave set-up, longshore currents, and spacing of rip currents on beaches of simple planform. Recent strides have also been made towards predicting the dynamic response of the surf zone to fluctuating driving forces with time scales larger than that of the incident wind waves, such as surf beat (see, for example, Symonds, Huntley, and Bowen, 1982).

In general, however, the nearshore environment is a complex system which is not amenable to analytic treatment. Even in simple situations, the presence of a physical feature predicted by one mechanism, such as the longshore current, will greatly complicate the prediction of a separate feature, such as rip currents. In addition, the action of waves and currents on the bottom can create complex topographies, making a reduction of the analytic problems to one space dimension impossible.

This report represents a review and conclusion of several studies conducted at the University of Delaware with the aim of providing a numerical model for calculating nearshore wave-induced currents and mean water level fluctuations. The purpose of constructing a numerical model rests on the need to extend our predictive capabilities into situations which lie beyond the scope of analytic methods. In the end, all numerical models, as well as analytic formulations, are limited in scope by the simplifying assumptions incorporated in their theoretical framework; in this regard, the present models represent an attempt to extend present analytic treatments to the case of a complex topography in two dimensions. The models do not consider the associated sediment transport problem, although this capability can be added (see McDougal, 1979, and Paddock and Ditmars, 1981). Also, the models require that the incident wave field be regarded as monochromatic, or, after some model modifications, narrow banded enough to be represented as a modulated wave train at a single carrier frequency.

The models described here utilize a wave refraction scheme developed by Noda et al. (1974). Using this scheme, Birkemeier and Dalrymple (1976) developed a circulation model, referred to here as the linear model, which neglected the effect of convective accelerations and lateral mixing. The model of Ebersole and Dalrymple (1979), referred to here as the nonlinear model, extended the treatment to include these effects.

In Chapter II, the theoretical framework for the two models is described, followed by an outline of the numerical formulations in Chapter III. In Chapter IV, we present a calibration of the models using field data from the NSTS Torrey Pines experiment (Gable, 1979). Chapter V gives a summary of applications of the models presented in Birkemeier and Dalrymple (1976) and Ebersole and Dalrymple (1979).

## Chapter II

## THEORETICAL DEVELOPMENT OF THE MODELS

### 1. INTRODUCTION

In this chapter the theoretical framework for the development of time averaged governing equations for the problem of waves and currents in the nearshore zone is outlined. The development of the numerical circulation models in either the "linear" or "nonlinear" form is then described in Chapter III based on the theoretical framework.

In general, the development of each model has been described in previous technical reports; the linear model in Birkemeier and Dalrymple (1976), and the nonlinear model in Ebersole and Dalrymple (1979). For this reason, some of the derivations and intermediate steps needed to develop the governing equations are not described in detail in the present report. The reader can refer to the previous work for missing details. However, both models now include the option of calculating wave energy decay due to interaction with the bottom, which has not been included in previous reports. The theory and implementation of this option is described in detail.

### 2. THEORETICAL FRAMEWORK FOR THE MODELS

The basis for any fluid dynamic model rests on the principle of conservation of mass, conservation of momentum (the Navier-Stokes equations), and conservation of energy. The resulting system of equations, together with boundary conditions which quantify the interaction of the fluid continuum with its solid and free bounding surfaces, give a mathematical representation of the physical problem of interest. The problem may then be further simplified by assumptions which are consistent with the physical processes involved.

Here, we are interested in the effect of waves propagating towards shore over a complex bathymetry and breaking, and the mean currents driven by changes in the flux of wave momentum. The problem has two apparent time-scales; a fast time scale associated with the oscillation of the incident waves, and a slower time scale over which the characteristics of the incident wave, such as height and angle of incidence, may vary. The longer time scale may also include the effect of changes in wind, tidal oscillation, and, in models, which include sediment transport, gradual shift of the bottom. Since our attention here is towards mean quantities which are reasonably steady in time, the set of equations may be averaged over the faster time scale of the wave oscillation to remove the direct effect of the oscillation. The effect of the waves then is represented by a stress-like term acting on the slowly varying mean flow pattern. In addition, since we are mainly interested in net transport quantities rather than detailed structure of the velocity profiles over depth, the equations may be averaged over depth, reducing the entire problem to a two dimensional problem in the horizontal plane together with appropriate boundary conditions. This averaged model can then be solved using numerical procedures, as discussed in Chapter III. The quantities to be determined are: the horizontal components of mean wave-induced current, the local wave height and angle of incidence, and the set-up, or wave-induced deviation of the mean water surface from its still-water level.

## 2.1 Specification of the Boundary Value Problem

A right-handed coordinate system is defined with x in the offshore direction, normal to the coastline, y in the longshore direction, and z vertically upward (see Figure 1). The continuity equation is

$$\frac{\partial \rho}{\partial t} + \frac{\partial(\rho u)}{\partial x} + \frac{\partial(\rho v)}{\partial y} + \frac{\partial(\rho w)}{\partial z} = 0 \tag{2.1}$$

where $\rho$ is the water density and (u,v,w) are the (x,y,z) components of velocity, respectively. The continuity equation can be further reduced to the form

$$\frac{\partial u}{\partial x} + \frac{\partial v}{\partial y} + \frac{\partial w}{\partial z} = 0 \tag{2.2}$$

consistent with an assumption of constant water density $\rho$.

The momentum equations are, in the x direction

$$\frac{\partial u}{\partial t} + \frac{\partial u^2}{\partial x} + \frac{\partial uv}{\partial y} + \frac{\partial uw}{\partial z} = -\frac{1}{\rho}\frac{\partial P}{\partial x} + \frac{1}{\rho}\left\{\frac{\partial \tau_{xx}}{\partial x} + \frac{\partial \tau_{yx}}{\partial y} + \frac{\partial \tau_{zx}}{\partial z}\right\} \quad , \tag{2.3}$$

in the y direction,

$$\frac{\partial v}{\partial t} + \frac{\partial uv}{\partial x} + \frac{\partial v^2}{\partial y} + \frac{\partial vw}{\partial z} = -\frac{1}{\rho}\frac{\partial P}{\partial y} + \frac{1}{\rho}\left\{\frac{\partial \tau_{xy}}{\partial x} + \frac{\partial \tau_{yy}}{\partial y} + \frac{\partial \tau_{zy}}{\partial z}\right\} \quad , \tag{2.4}$$

and in the z direction,

$$\frac{\partial w}{\partial t} + \frac{\partial uw}{\partial x} + \frac{\partial vw}{\partial y} + \frac{\partial w^2}{\partial z} = -\frac{1}{\rho}\frac{\partial}{\partial z}(P + gz) + \frac{1}{\rho}\left(\frac{\partial \tau_{xz}}{\partial x} + \frac{\partial \tau_{yz}}{\partial y} + \frac{\partial \tau_{zz}}{\partial z}\right), \tag{2.5}$$

after substitution of the continuity equation into the convective acceleration terms.

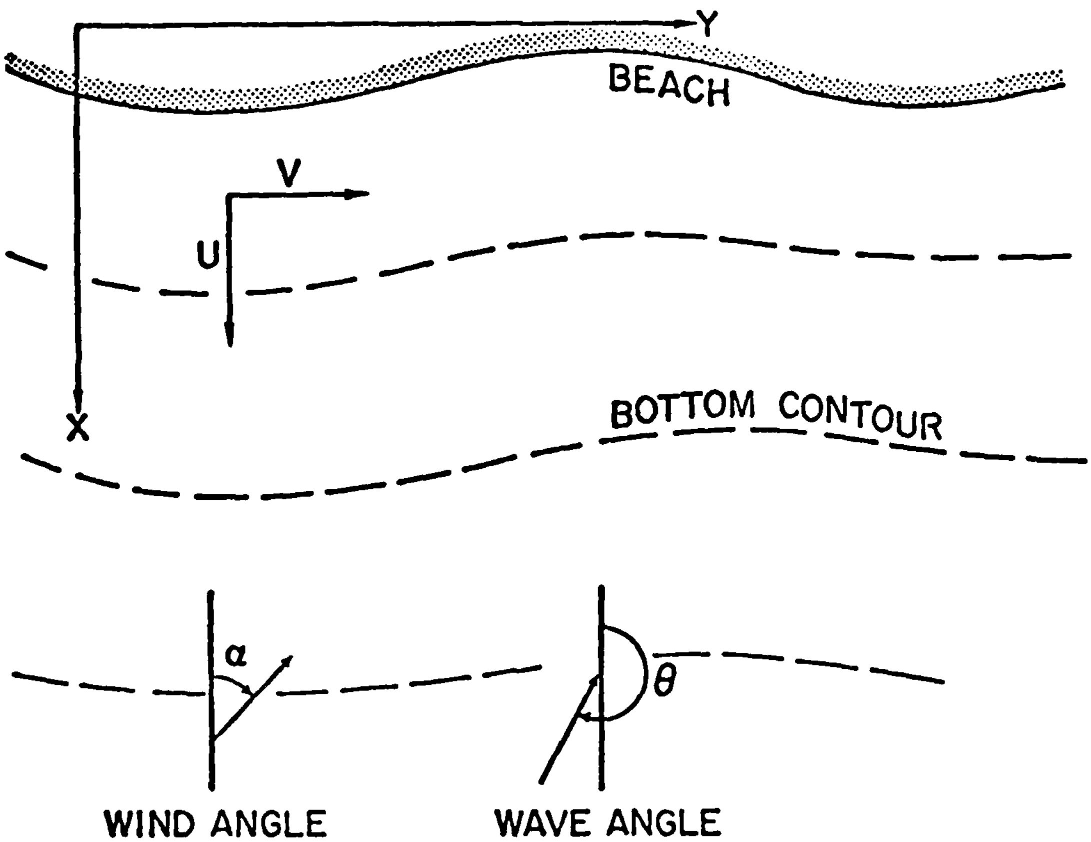


Figure 2-1. Plan Definition Sketch For Coordinate System.

## Boundary Conditions

Certain boundary conditions are required at the physical boundary of the water body in question in order to correctly specify the problem. First, kinematic conditions are specified at the free surface and rigid bottom, which state that water particles may not cross the boundary surface, whether it be rigid or moving.

The equation of a surface of the fluid domain is given by

$$F(x,y,z,t) = 0 \quad .$$

A water particle cannot flow across the surface, otherwise the surface would cease to exist. Mathematically, this condition is expressed by the total time rate of change of the function $F(x,y,z,t)$ being equal to zero.

$$\frac{D}{Dt}\left(F(x,y,z,t)\right) = 0 \quad .$$

At the free surface the boundary is given by

$$F_1(x,y,z,t) = z - \eta(x,y,t) = 0$$

and at the bottom

$$F_2(x,y,z,t) = z + h(x,y,t) = 0 \quad .$$

Therefore, for the kinematic free surface boundary condition (KFSBC),

$$\frac{\partial F_1}{\partial t} + u\frac{\partial F_1}{\partial x} + v\frac{\partial F_1}{\partial y} + w\frac{\partial F_1}{\partial z} = 0 \qquad z = \eta$$

or

$$\frac{\partial \eta}{\partial t} + u_\eta\frac{\partial \eta}{\partial x} + v_\eta\frac{\partial \eta}{\partial y} - w_\eta = 0 \quad . \tag{2.6}$$

For the bottom boundary condition (BBC) we get,

$$\frac{\partial h}{\partial t} + u_{-h} \frac{\partial h}{\partial x} + v_{-h} \frac{\partial h}{\partial y} + w_{-h} = 0 \tag{2.7}$$

where u,v,w are the velocity components in the x,y and z directions and the subscripts denote the evaluation of a specific term at the bottom, $z = -h$, or at the free surface, $z = \eta$.

In addition to the kinematic free surface boundary condition, a dynamic free surface boundary condition is required as well, which states that

$$P = \text{constant} \qquad z = \eta$$

This condition is satisfactory if we neglect the local generation of waves by wind or the deformation of the free surface due to barotropic effects. Then, using Bernoulli's equation expanded to the free surface, we obtain

$$-\frac{\partial \phi_\eta}{\partial t} + \frac{(u_\eta^2 + v_\eta^2 + w_\eta^2)}{z} + g\eta = 0 \qquad z = \eta \tag{2.8}$$

after setting $P = 0$, where $\phi(x,y,z,t)$ is the velocity potential for the wave motion.

The model also requires lateral boundary conditions. In the y (longshore) direction, the bathymetry, given by the surface $h(x,y)$ will be required to be periodic. Since the offshore wave conditions will be assumed uniform, lateral periodicity conditions for wave and currents are also assumed.

Offshore in the x direction, the usual boundary condition for a wave problem would be to assume that all waves at the boundary other than the incident wave are propagating away from shore, the radiation condition (Sommerfeld (1949)). However, the circulation model does not directly calculate an actual wave field. Rather, a somewhat arbitrary condition,

$$u = 0 \quad ; \quad x = \text{furthest offshore grid}$$

is imposed, which serves to put a bound on the horizontal extent of the flow under consideration.

Specification of an onshore boundary condition is an uncertain task, due to the complexity of the surf zone. In general, it is likely that some wave energy survives the breaking process and reflects from the beach, leading to waves propagated back into the region of the model. However, it is assumed for the purpose of modelling that all wave energy decays in the surf zone, reducing the wave height to a value of zero at the shoreline. In addition, both u and v are set equal to zero at the shoreline.

## 2.2 Depth and Time Averaged Forms of the Equations

By integrating the equations of motion and continuity over depth and substituting the boundary conditions, the problem is reduced to equations in two horizontal dimensions, with lateral boundary conditions prescribed. Secondly, the quantities of principal interest are average in nature, i.e., mean currents, wave height and wave angle, and mean water level. The equations can then be time averaged over a wave period to remove consideration of instantaneous wave induced motions. The quantities remaining would be free to vary slowly in time in response to changing offshore conditions.

Integrating Eq. (2.2) over depth from $z = -h(x,y,t)$ to $z = \eta(x,y,t)$, using *Leibnitz rule (Hildebrand (1976), p. 365) to remove partial derivatives* from within the integrals, and substituting Eqs. (2.5) and (2.6), the continuity equation becomes

$$\frac{\partial}{\partial t} \int_{-h}^{\eta} \rho dz + \frac{\partial}{\partial x} \int_{-h}^{\eta} \rho u dz + \frac{\partial}{\partial y} \int_{-h}^{\eta} \rho v dz = 0 \qquad (2.9)$$

Let both u and v be comprised of a time independent mean flow and a wave induced flow.

$$u = \overline{U} + \hat{u}$$

$$v = \overline{V} + \hat{v} \quad .$$

By substituting the above expressions for u and v into Eq. (2.7) and time averaging over one wave period so as to eliminate the wave induced fluctuations, the continuity equation can be written as

$$\frac{\partial}{\partial t} \{\rho(h + \overline{\eta})\} + \frac{\partial}{\partial x} \{\rho\overline{U}(h + \overline{\eta})\} + \frac{\partial}{\partial x} \overline{\int_{-h}^{\eta} \rho\hat{u}dz}$$

$$+ \frac{\partial}{\partial y} \{\rho\overline{V}(h + \overline{\eta})\} + \frac{\partial}{\partial y} \overline{\int_{-h}^{\eta} \rho\hat{v}dz} = 0 \qquad (2.10)$$

where the symbol "$\overline{\quad\quad}$" denotes the time average over one wave period and $\overline{\eta}$ the time independent mean free surface displacement. Note that the time averages of the vertically integrated wave induced velocities $\hat{u}$ and $\hat{v}$ are not zero.

Defining $\quad U \equiv \overline{U} + \tilde{u}$

$$V \equiv \overline{V} + \tilde{v} \quad ,$$

where $\tilde{u} = \dfrac{\overline{\int_{-h}^{\eta} \rho \hat{u} dz}}{\rho(h + \bar{\eta})}$ and $\tilde{v} = \dfrac{\overline{\int_{-h}^{\eta} \rho \hat{v} dz}}{\rho(h + \bar{\eta})}$

are the wave induced mass transport velocities, and substituting the total depth D for $(h + \bar{\eta})$, the time averaged, depth integrated continuity equation is, in its final form

$$\frac{\partial \bar{\eta}}{\partial t} + \frac{\partial}{\partial x} (UD) + \frac{\partial}{\partial y} (VD) = 0 \quad . \tag{2.11}$$

Inherent in the derivation are the assumptions that the bottom is constant with time and the density is constant in space and time.

Momentum Equations

The x and y momentum equations are manipulated in the same way as the continuity equation in order to achieve equations which are independent of wave induced oscillations, i.e., they are integrated over depth and time averaged over a wave period. Details of this derivation may be found in Ebersole and Dalrymple (1979). The resulting equations are equivalent to those given by Phillips (1977), but are written explicitly in terms of depth averaged mean velocities. The equations contain terms for mean bottom shear stress, mean surface shear stress due to wind, mean lateral friction (not used in the linear model), and excess mean momentum stress due to wave action (the radiation stress, see Longuet-Higgins and Stewart (1964)). The x momentum equation in its final form can be written as,

$$\frac{\partial}{\partial t} (UD) + \frac{\partial}{\partial x} (U^2 D) + \frac{\partial}{\partial y} (UVD) = -gD \frac{\partial \bar{\eta}}{\partial x} - \frac{D}{\rho} \frac{\partial \tilde{\tau}_{\ell}}{\partial y}$$

$$- \frac{1}{\rho} \frac{\partial S_{xx}}{\partial x} - \frac{1}{\rho} \frac{\partial S_{xy}}{\partial y} + \frac{1}{\rho} \overline{\tau_{sx}} - \frac{1}{\rho} \overline{\tau_{bx}} \tag{2.12}$$

and the final form of the y momentum equation can be written as

$$\frac{\partial}{\partial t}(VD) + \frac{\partial}{\partial x}(UVD) + \frac{\partial}{\partial y}(V^2D) = -gD\frac{\partial\bar{\eta}}{\partial y} - \frac{D}{\rho}\frac{\partial\bar{\tau}_\ell}{\partial x}$$

$$-\frac{1}{\rho}\frac{\partial S_{xy}}{\partial x} - \frac{1}{\rho}\frac{\partial S_{yy}}{\partial y} + \frac{1}{\rho}\overline{\tau_{sy}} - \frac{1}{\rho}\overline{\tau_{by}} \quad . \tag{2.13}$$

Wave Energy Equation

Following Phillips (1977), an equation expressing the conservation of averaged wave energy may be written as

$$\frac{\partial E}{\partial t} + \frac{\partial}{\partial x}\{E(U + C_g\cos\theta)\} + \frac{\partial}{\partial y}\{E(V + C_g\sin\theta)\}$$

$$+ S_{xx}\frac{\partial U}{\partial x} + S_{xy}\left(\frac{\partial V}{\partial x} + \frac{\partial U}{\partial y}\right) + S_{yy}\frac{\partial V}{\partial y} = \varepsilon \tag{2.14}$$

Here, $C_g$ is the wave group velocity and $\theta$ is the local wave angle. The quantity $\varepsilon$ represents the dissipation of wave energy, and is identically zero in a conservative wave field. It can be given a non-zero value to include the effect of wave damping, as described below.

## 2.3 Radiation Stresses

The radiation stresses included in Eqs. (2.12), (2.13) and (2.14) represent the stress on the water column induced by wave action. Neglecting the effects of small scale turbulent velocities, the stresses have been given in simple form by Longuet-Higgins and Stewart (1964) as

$$S_{xx} = E\,[(2n - 1/2)\cos^2\theta + (n - 1/2)\sin^2\theta] \tag{2.15}$$

$$S_{yy} = E\ [(2n - 1/2)\sin^2\theta + (n - 1/2)\cos^2\theta] \tag{2.16}$$

$$S_{xy} = S_{yx} = \frac{E}{2}\ n\ \sin\ (2\theta) \tag{2.17}$$

where E is the wave energy, $\theta$ is the wave angle, and n = ratio of group velocity ($C_g$), to wave celerity (C). To second order for a progressive small amplitude wave, E and n are given by

$$E = \frac{1}{8}\ \rho g\ H^2 \tag{2.18}$$

$$n = \frac{C_g}{C} = \frac{1}{2}\ [1 + \frac{2kh}{\sinh(2kh)}] \tag{2.19}$$

k = wave number ($= \frac{2\pi}{L}$)

h = depth

L = wave length

H = wave height.

## 2.4 Wind Stress

Although other methods exist for computing the surface stress due to the wind (see Wu (1968)), the one suggested in the Shore Protection *Manual* (1977) has been utilized. This form was first developed by Van Dorn (1953) and gives a fairly good fit to the existing experimental data. The form of the surface stress is quadratic in the wind speed and is given by

$$\bar{\tau}_{sx} = \rho K|W|W_x \tag{2.20}$$

$$\bar{\tau}_{sy} = \rho K|W|W_y \tag{2.21}$$

where W is the wind speed, and $W_x$, $W_y$ are wind velocity components in the x and y directions, as determined by the wind angle, $\alpha$.

The wind stress coefficient K is determined empirically to be dependent on the magnitude of the wind velocity such that

$$K = \begin{cases} K_1 & W < W_{cr} \\ K_1 + K_2 \, (1 + W_{cr}/W)^2 & W > W_{cr} \end{cases} \qquad (2.22)$$

and $$K_1 = 1.1 \times 10^{-6} \quad ; \quad K_2 = 2.5 \times 10^{-6}$$

$$W_{cr} = 7.2 \text{ meters/second}$$

A comparison of the wind stress coefficient given here with experimental data is given in Pearce (1972).

## 2.5 Bottom Stress

The correct method for specifying the effect of a rigid bottom on waves and currents is still a matter of lively debate. For the purpose of modelling hydrodynamics in the nearshore zone, the average bottom shear stress, $\tau_b$, is generally taken to be of the form

$$\overline{\tau_b} = \rho \, \frac{f}{8} \, \overline{u_b |u_b|} \qquad (2.23)$$

where f is a Darcy-Weisbach friction factor and $u_b$ is the total instantaneous scalar velocity at the bottom (Longuet-Higgins (1970a)). This relation is known as a quadratic friction law. The components of shear stress in the x and y directions can be given quite generally by (Liu and Dalrymple (1978))

$$\overline{\tau_{bx}} = \frac{\rho f}{16\pi} \int_0^{2\pi} (U + u_m \cos \theta \cos \sigma t) \cdot |\vec{u_b}| \, d(\sigma t) \qquad (2.24)$$

$$\overline{\tau_{by}} = \frac{\rho f}{16\pi} \int_0^{2\pi} (V + u_m \sin \theta \cos \sigma t) \cdot |\vec{u_b}| \, d(\sigma t) \qquad (2.25)$$

where $u_m$ is the maximum wave orbital velocity given by

$$u_m = \frac{\pi H}{2 \sinh kh} \qquad (2.26)$$

and $\overrightarrow{u_b}$ is the vector velocity at the bottom. The nonlinear model of Ebersole and Dalrymple (1979) retains these forms, where the integration is approximated by a 16 term Simpson's rule summation.

The linear model retains the form originally used by Birkemeier and Dalrymple (1976). For this form, the assumption that friction is primarily due to the influence of the wave orbital velocity is used. Making a small mean-current assumption, LeBlond and Tang (1974) show that the bottom stress is anisotropic, with

$$\overline{\tau_{bx}} = \frac{\rho f}{2\pi} u_m U \qquad (2.27)$$

$$\overline{\tau_{by}} = \frac{\rho f}{4\pi} u_m V \quad , \qquad (2.28)$$

with U, V, $u_m$, and f as previously defined. A derivation of these equations is given in Birkemeier and Dalrymple (1976), Appendix A.

## 2.6 Wave Refraction and Shoaling Including Wave-Current Interation

The equations which govern both wave refraction and shoaling as a result of wave-current interaction used in the model are those of Noda et al. (1974). The advantage of Noda's method is that it can predict the wave angles and wave heights at certain points rather than along a wave ray. This procedure lends itself well to use in the finite difference model because calculations are performed at points which lie in the center of rectangular grid elements which are part of a larger grid mesh.

Starting with a progressive linear gravity wave, the free surface can be written as,

$$\eta(x,y,t) = a(x,y,t)\cos\{\phi(x,y,t)\}$$

where a is the wave amplitude and $\phi$ is a phase function. A wave number vector can be defined as

$$\vec{k} = \nabla\phi \tag{2.29}$$

and a wave scalar frequency can be defined as

$$\bar{\sigma} = -\frac{\partial\phi}{\partial t} \tag{2.30}$$

Using the mathematical property that the curl of a gradient is identically zero, it is shown that

$$\nabla \times \nabla\phi = 0$$

which implies that

$$\nabla \times \vec{k} = 0$$

This equality states that the wave number vector is irrotational. Assuming $\phi(x,y,t)$ is continuous, then

$$\frac{\partial}{\partial t}(\nabla\phi) = \nabla\frac{\partial\phi}{\partial t} \quad .$$

On substituting Eqs. (2.29) and (2.30) into the above expression, it is found that

$$\frac{\partial\vec{k}}{\partial t} + \nabla\bar{\sigma} = 0 \tag{2.31}$$

which is the classical conservation of waves equation.

For the case of a wave propagating on a current with velocity $\vec{u} = u\vec{i} + v\vec{j}$, it can be shown that the scalar frequency with respect to a stationary reference frame is

$$\bar{\sigma} = \sigma + k \cdot \vec{U} \quad .$$

The wave frequency with respect to a moving reference frame is given by the dispersion relation,

$$\sigma^2 = gk \tanh kh \quad . \tag{2.32}$$

If it is also assumed that the wave number field is constant in time then, from Eq. (2.31),

$$\nabla(\sigma + \vec{k} \cdot \vec{U}) = 0$$

or

$$\sigma + \vec{k} \cdot \vec{U} = \text{constant} \quad . \tag{2.33}$$

This constant can be evaluated for the case where $\vec{U} = 0$ in which case $\sigma = \frac{2\pi}{T}$ where T is the wave period. Eq. (2.33) then becomes

$$\sigma + \vec{k} \cdot \vec{U} = \frac{2\pi}{T} \quad . \tag{2.34}$$

Using the coordinate system shown in Figure 1 and expanding Eqs. (2.29) and (2.34) into Cartesian coordinates and using the dispersion relation, the equations which govern wave refraction through wave-current interaction are given by

$$\cos\theta \left\{\frac{\partial\theta}{\partial x} - \frac{1}{k}\frac{\partial k}{\partial y}\right\} + \sin\theta \left\{\frac{\partial\theta}{\partial y} + \frac{1}{k}\frac{\partial k}{\partial x}\right\} = 0 \tag{2.35}$$

$$\{gk \tanh(kh)\}^{1/2} + Uk \cos\theta + Vk \sin\theta = \frac{2\pi}{T} \tag{2.36}$$

where $\theta$, k, h, U and V are all functions that may vary in both the x and y directions.

The shoaling of waves is also affected by the interaction of waves and currents. The effect on the waves is determined by solving the energy equation. Dividing Eq. (2.14) by E and expanding in Cartesian coordinates, we get

$$\frac{1}{E}\frac{\partial E}{\partial t} + (U + C_g \cos\theta)\frac{1}{E}\frac{\partial E}{\partial x} + (V + C_g \sin\theta)\frac{1}{E}\frac{\partial E}{\partial y}$$

$$+ \frac{\partial}{\partial x}(U + C_g \cos\theta) + \frac{\partial}{\partial y}(V + C_g \sin\theta)$$

$$+ \frac{1}{E}\{S_{xx}\frac{\partial U}{\partial x} + S_{xy}\frac{\partial U}{\partial y} + S_{yy}\frac{\partial V}{\partial y} + S_{xy}\frac{\partial V}{\partial y}\} = \frac{\varepsilon}{E} \quad .$$

Using this result, carrying out the differentiation, and letting a quantity Q be defined as

$$Q = \frac{1}{E}\{S_{xx}\frac{\partial U}{\partial x} + S_{xy}\frac{\partial U}{\partial y} + S_{xy}\frac{\partial V}{\partial x} + S_{yy}\frac{\partial V}{\partial x}\}$$

the energy equation becomes,

$$\frac{2}{H}\frac{\partial H}{\partial t} + (U + C_g \cos\theta)\frac{2}{H}\frac{\partial H}{\partial x} + (V + C_g \sin\theta)\frac{2}{H}\frac{\partial H}{\partial y} + \frac{\partial U}{\partial x} + \frac{\partial V}{\partial y}$$

$$- C_g \sin\theta\frac{\partial\theta}{\partial x} + \cos\theta\frac{\partial C_g}{\partial x} + C_g \cos\theta\frac{\partial\theta}{\partial y} + \sin\theta\frac{\partial C_g}{\partial y} + Q = \frac{\varepsilon}{E} \quad . \tag{2.37}$$

For all applications of the model the wave height H is assumed constant in time, so $\frac{\partial H}{\partial t} = 0$. From linear wave theory the group velocity $C_g$ is given by

$$C_g = \frac{C}{2} \{1 + \frac{2kh}{\sinh(2kh)}\}$$

where

$$C = \{\frac{g}{k} \tanh(kh)\}^{1/2}$$

is the wave speed or celerity, k is the wave number, and h is the water depth.

## 2.7 Wave Breaking Criteria

Since Eq. (2.37) is applicable only in determining the wave heights of nonbreaking waves, some method is needed to determine the point of breaking and the wave heights after breaking. Though a number of formulas for doing this have been developed, there is not as yet one which is universally applicable or accepted. The choice of a breaking criteria, although somewhat arbitrary, must be made with care since it determines the width of the surf zone and thus controls the set-up. The simplest breaking criteria is that predicted by solitary wave theory.

$$(\frac{H}{D})_b = \text{constant} = .78 \tag{2.38}$$

where the subscript, b, denotes the value at breaking. There is, however, considerable evidence (Weggel, 1972) that this is an oversimplification.

Noda *et al*. (1974) used a modified version of the Miche formula

$$(\frac{H}{L})_b = .12 \tanh (\frac{D}{L})_b \tag{2.39}$$

both to predict the point of breaking and the decay of the wave after breaking. This was done by calculating both a wave height from Eq. (2.37) and a breaking height from Eq. (2.39). When the point was reached where the wave height was equal to or greater than the breaking height, the wave was considered to have broken and the wave height from Eq. (2.39) was used. Eq. (2.39) is used in both models to determine broken wave heights.

## 2.8 Lateral Mixing

The non-linear model of Ebersole and Dalrymple (1979) includes the effect of the lateral shear stress terms

$$\frac{-D}{\rho}\frac{\partial\overline{\tau_\ell}}{\partial y} \quad , \quad \frac{-D}{\rho}\frac{\partial\overline{\tau_\ell}}{\partial x}$$

in the x and y momentum equations (2.12) and (2.13) respectively. The need for these terms is pointed out by Longuet-Higgins (1970a) in his treatment of the longshore currents due to obliquely incident waves on a plane beach. Neglecting the effects of lateral shear stresses led to prediction of a longshore current distribution with a discontinuity at the breaker line and no current outside the surf zone. However, physical observation in both the laboratory and field indicate that mean longshore flows are present beyond the breaker line. Longuet-Higgins (1970b) presented a formulation which included the effect of lateral mixing as the means for handling the effect of lateral shear; the shear stresses are thus based on turbulent Reynolds stresses proportional to the local gradient of the mean velocity. The resulting velocity distributions have no discontinuity at the breaker line, and the peak velocities are shifted shoreward of the breaker line. Figure 2-2 shows a comparison of a theoretical velocity profile to one without lateral mixing included.

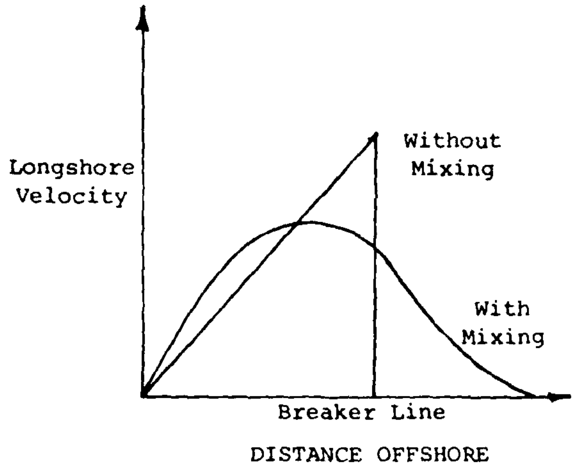


Figure 2-2 Longuet-Higgins' Analytical Solution for Oblique Wave Attack on a Plane Beach

Following the derivation of Longuet-Higgins (1970b), the lateral shear stress is written as

$$\tau_\ell = -\rho(\varepsilon_y \frac{\partial U}{\partial y} + \varepsilon_x \frac{\partial V}{\partial x}) \qquad (2.40)$$

Longuet-Higgins argued that the mixing coefficient $\varepsilon_x$ must tend to zero as the shoreline was approached since the turbulent eddies responsible for mixing cannot be of a scale greater than the distance to shore. He assumed that $\varepsilon_x$ is proportional to the distance offshore, x, multiplied by some velocity scale which he chose to be $\sqrt{gh}$, the speed of a wave in shallow water where h is the local water depth. Therefore, $\varepsilon_x$ can be written as

$$\varepsilon_x = Nx\sqrt{gh}$$

where N is a dimensionless constant whose limits Longuet-Higgins gave as

$$0 \leq N \leq 0.016 \quad .$$

In this model the coefficient, $\varepsilon_x$, was allowed to vary linearly with x to some value around the breaker line. From this point seaward the coefficient remained at this constant value. The reason for this approximation is that physically there must be some limit on the scale of these eddies. This limit is at present not known. The coefficient, $\varepsilon_y$, was chosen to be constant. The values of N and $\varepsilon_y$ are chosen during the calibration of the model.

### 2.9 Wave Height Decay

In all applications of the circulation model to date, calculation of wave parameters has been confined to a region within several wavelengths of the shore. Over this distance, wave energy decay due to interaction with the bottom is not likely to be significant, except possibly in the case of waves propagating over a soft mud bottom (Dalrymple and Liu (1978)), which is not treated here. However, the circulation model could reasonably be used to model propagation over much longer offshore extents of shallow coastal waters. At some point, the accumulated effects of bottom interaction would result in wave height reductions of a significant degree. In order to accurately model the amount of wave energy available for driving currents and maintaining mean water level variations, it is necessary to include the effects of various dissipation mechanisms in the equation for calculating wave height (2.37).

Ebersole and Dalrymple (1979) included in the nonlinear computer model, but did not describe, the option to calculate wave energy dissipation due to viscous shear in the bottom boundary layer, and due to the effect of "pumping" of water through the permeable sand bottom due to wave induced pressure gradients at the water-bottom interface. At present, the option of calculating wave energy decay due to both mechanisms is included in both the linear and nonlinear model.

The application of wave damping to the nearshore circulation model has been described by McDougal (1979), who included the energy dissipation rate $\varepsilon$ in Eq. (2.14) in a sediment transport model based on the linear wave-current interaction model. The derivation of $\varepsilon$ is based on Liu (1973). Let $\varepsilon$ be given by

$$\varepsilon = \varepsilon_p + \varepsilon_f \tag{2.41}$$

where $\varepsilon_p$ is the dissipation rate due to the permeability of the bottom, and $\varepsilon_f$ is the dissipation rate due to bottom friction. The two effects are treated separately.

Liu (1973) solved the linear problem for waves over a porous bed of infinite depth. If the wave amplitude $a(x,y,t) = \frac{H}{2}(x,y,t)$ is assumed to be a slowly varying function of the form

$$a(x,y,t) = a_o e^{-\alpha t} \quad ,$$

Liu's solution leads to the following form for $\alpha$;

$$\alpha = \frac{kg}{2\left|\cosh kh + (\frac{\sigma}{Q}) \sinh kh\right|^2} \left(\frac{\nu}{K_p} \frac{1}{|Q|^2} + \sqrt{\frac{\nu}{2\sigma}} \frac{k}{\sigma}\left|\frac{i\sigma}{Q} - 1\right|^2\right) \tag{2.42}$$

where Q is given by

$$Q = \frac{i\sigma}{P_o} - \frac{\nu}{K_p} \tag{2.43}$$

and

$K_p$ = bed permeability ≈ $10^{-10}$ $M^2$

$P_o$ = bed porosity ≈ 0.6

$\nu$ = kinematic viscosity ≈

For these values of $K_p$, $P_o$, and $\nu$, the viscosity term in Q is dominant, and $\alpha$ may be reduced to the form

$$\alpha = \frac{gk}{2 \cosh^2 kh} \frac{k_p}{\nu} \tag{2.44}$$

The dissipation rate $\alpha$ is related to $\varepsilon_p$ by

$$\varepsilon_p = \frac{\partial E}{\partial t} = - 2\alpha E$$

giving

$$\varepsilon_p = - \frac{gkE}{\cosh^2 kh} \frac{K_p}{\nu} \tag{2.45}$$

The rate of energy dissipation due to bottom friction, $\varepsilon_f$, is given by

$$\varepsilon_f = \overline{(\vec{\tau}_b \cdot \vec{U}) A_b} \tag{2.46}$$

where $A_b$ is the bed surface area.

Substituting for $\vec{\tau}_b$ and $\vec{U}$ using results derived in the absence of a mean current, we obtain the form

$$\varepsilon_f = - \frac{\rho f}{6\pi} (u_m)^3$$

where $u_m$ is the maximum wave induced velocity at the bottom, given by (2.26).

After some manipulation, we obtain the form

$$\varepsilon_f = -\frac{k}{6\pi}\,\frac{\sigma\, f\, H}{(\cosh^3 kh - \cosh kh)} \cdot E \qquad (2.47)$$

The total energy dissipation including the effects of the porous bottom and friction is given by

$$\varepsilon = \varepsilon_p + \varepsilon_f$$

$$= -\left\{\frac{g\,k}{\cosh^2 kh}\;\frac{K_p}{\nu} + \frac{\sigma\, k\, f\, H}{6\pi(\cosh^3 kh - \cosh kh)}\right\} \cdot E \qquad (2.48)$$

The option of including these effects is available in both forms of the numerical model presented here.

## 3. AN OVERVIEW OF THE LINEAR AND NONLINEAR MODELS

While both of the numerical models described in Chapter III are based on the theory outlined in the previous section, each model contains a somewhat different subset of the overall development. In this section, we review the differences and similarities between the models before going on to their numerical formulation.

The intent of both of the models is to solve for the mean values U, V, and $\bar{\eta}$ at each grid point by solving the time and depth averaged equations of continuity (2.11) and momentum (2.12-13). Each model utilizes the refraction scheme of Noda et al. (1974), as represented by (2.35-37), to solve for wave angle and wave height. The model of Birkemeier and Dalrymple (1976) treats linearized forms of Eqs. (2.12-13), obtained by dropping the convective acceleration terms

$$\frac{\partial}{\partial x}(U^2D) \quad ; \quad \frac{\partial}{\partial y}(UVD)$$

from the x-momentum equation, and the terms

$$\frac{\partial}{\partial x}(UVD) \quad ; \quad \frac{\partial}{\partial y}(V^2D)$$

from the y-momentum equation. The model of Ebersole and Dalrymple (1979) retains the full nonlinear form of the momentum equations, leading to the principle theoretical difference between the models as well as explaining the distinction expressed by their names. The mathematical differences in the governing equations also lead to the requirement of significantly different numerical schemes, discussed in Chapter III.

The momentum equations contain various forcing terms which are formulated as stresses or stress gradients; these include radiation, surface and bottom stresses and a lateral stress representing the effect of turbulent mixing. The models treat radiation stresses and surface wind stresses identically. The linear model treats bottom stress according to a "weak current" formulation developed by LeBlond and Tang (1974), based on the assumption that the stress develops principally in response to the wave orbital motion. The nonlinear model uses a more exact bottom stress formulation, making no assumption as to the relative magnitude of wave orbital and mean current velocities. This distinction between the models is more historical than essential; the linear model can be updated to include the more exact relation given by Eqs. (2.24) and (2.25). This modification has been used by Allender et al. (1981) in a version of the linear model described here. A further possibility would be to represent the bottom friction using a "large-current" formulation developed by Liu and Dalrymple (1978); this extension has not been investigated.

The remaining distinction between the models stems from the neglect of the "lateral mixing" terms Eqs. (2.12-13)

$$\frac{-D}{\rho}\frac{\partial \overline{T_{\ell}}}{\partial y} \quad ; \quad \frac{-D}{\rho}\frac{\partial \overline{T_{\ell}}}{\partial x}$$

in the linear model, and their inclusion in the nonlinear model. This difference is again historical rather than essential; these terms could be included in a modified version of the linear model, although their inclusion would require more effort than the bottom friction modification discussed above. No investigation of the effect of including lateral mixing in the linear model has been made to date.

Chapter III

# FORMULATION OF THE NUMERICAL MODELS

## 1. INTRODUCTION

In the previous chapter a mathematical formulation of the governing equations and associated boundary conditions for the problem of nearshore wave-induced circulation has been outlined. In this chapter, the numerical formulations of the mathematical model are reviewed, corresponding to the work of Birkemeier and Dalrymple (1976) and Ebersole and Dalrymple (1979).

The two models reviewed shall be referred to as the "linear model" and the "nonlinear model." The models contain significant differences as well as significant similarities in their numerical formulation as well as in their underlying mathematical formulation. Differences in the models will be discussed below following a review of the overall structure common to both models.

Both models reviewed here are finite-difference approximations to a set of three first order hyperbolic differential equations consisting of the continuity equation (2.11) and the x and y direction momentum equations (2.12, 2.13), with associated unknowns $U(x,y,t)$, $V(x,y,t)$ and $\bar{\eta}(x,y,t)$. The quantities of wave height $H(x,y,t)$ and wave angle $\theta(x,y,t)$ are solved for using the refraction scheme Eq. (2.35) and the wave energy equation (2.37). The models as developed contain the flexibility to handle unsteady response to time varying incident wave conditions; however, we will be concerned exclusively with representing the response to a constant wave climate. In this guise, the models represent iterative schemes to determine the response to a steady state exciting force, and updated unknowns may be regarded as iterated values rather than advanced-in-time values.

Listings of the computer programs for the linear and nonlinear models are given in Appendix I together with some notes on running the programs.

## 2. THE GRID SCHEME AND LOCATION OF THE UNKNOWN QUANTITIES

The first step in constructing a finite difference model lies in choosing a network of discrete grids overlaying the physical domain of interest. The grid used by the present models is that of Noda et al. (1974), as illustrated in Figure 3-1. The physical domain is divided into regular grids of longshore extent $\Delta y$ and offshore extent $\Delta x$. The topography is assumed to be periodic in the longshore $y$ direction with a length $\lambda$ given by

$$\lambda = (N - 1) \cdot \Delta y$$

Various requirements affecting the choice of grid are:

1. The grid must extend offshore far enough to remove the offshore region of the domain from the influence of currents driven by the surf zone, and to allow for the specification of a uniform longshore depth which will not significantly alter the wave refraction results in the nearshore.

2. The grid mesh must be fine enough to resolve the surf zone in a reasonable manner.

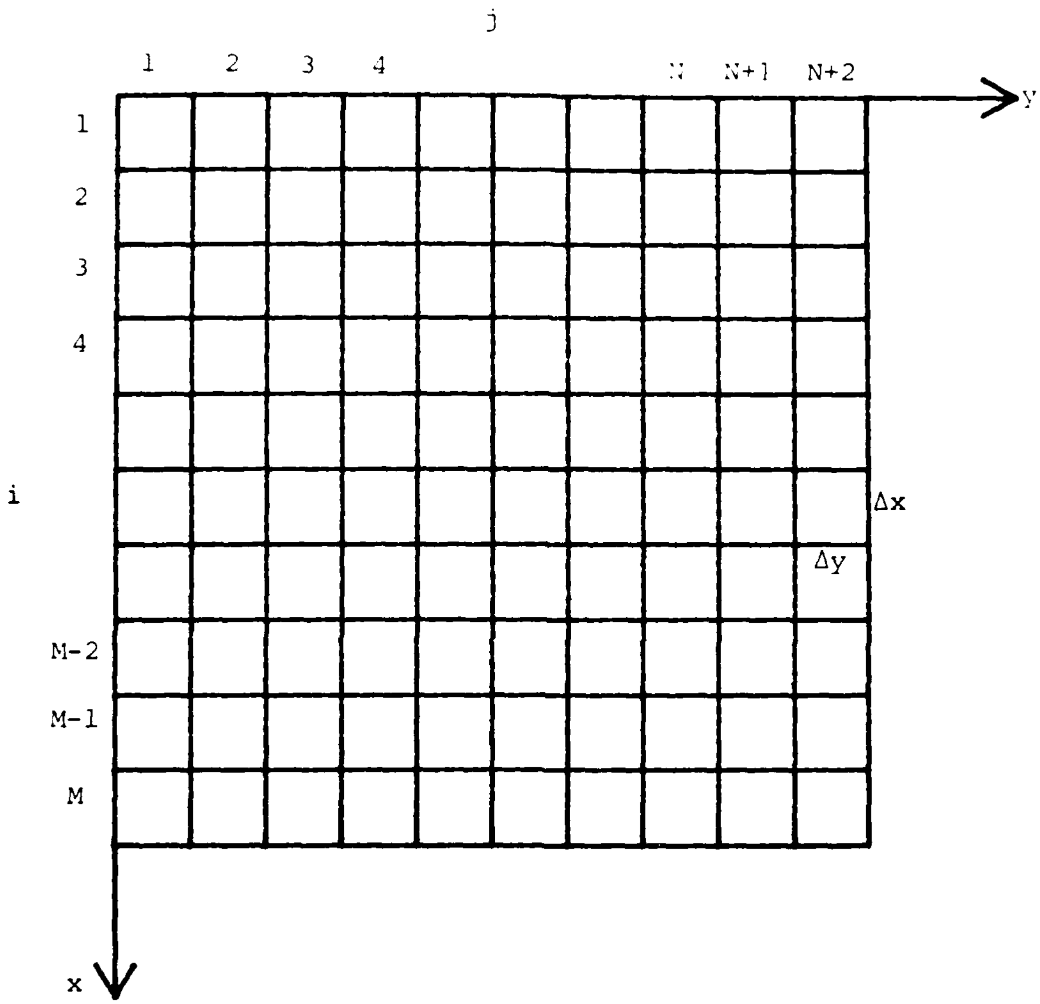


Figure 3-1. Grid Scheme [After Noda et. al. (1974)]

3. In the event that a single physical feature isolated in the longshore direction is to be modelled, the longshore extent of the grid must be sufficiently large to isolate the physical system from the effect of images created by the longshore periodicity requirement.

In the event that large, non-periodic physical features creating significant current patterns seaward of the breaker line are present, requirements (1) and (3) lead to the choice of a large grid, whereas requirement (2) can lead to choice of quite small offshore grid spacings on steep beaches. The resulting grid will often contain a large number of elements, leading to the requirement of large amounts of computer time to solve the complex set of governing equations.

The fixed and variable quantities are defined in relation to the grid structure as shown in Figure 3-2. The quantity $A_{i,j}$ is defined at the grid center and represents any of the set of quantities

$$A_{i,j} = \{H, \theta, k, \bar{\eta}, S, D, \tau_b, \tau_s\}_{i,j} \tag{3.1}$$

Velocities U and V are given at grid sides. This formulation relates naturally to the conservation law scheme of relating changes of a quantity in a bounded region to the fluxes of that quantity across the bounding surface, and is therefore physically correct in an heuristic sense, as well as possessing whatever degree of numerical accuracy consistent with the chosen difference schemes.

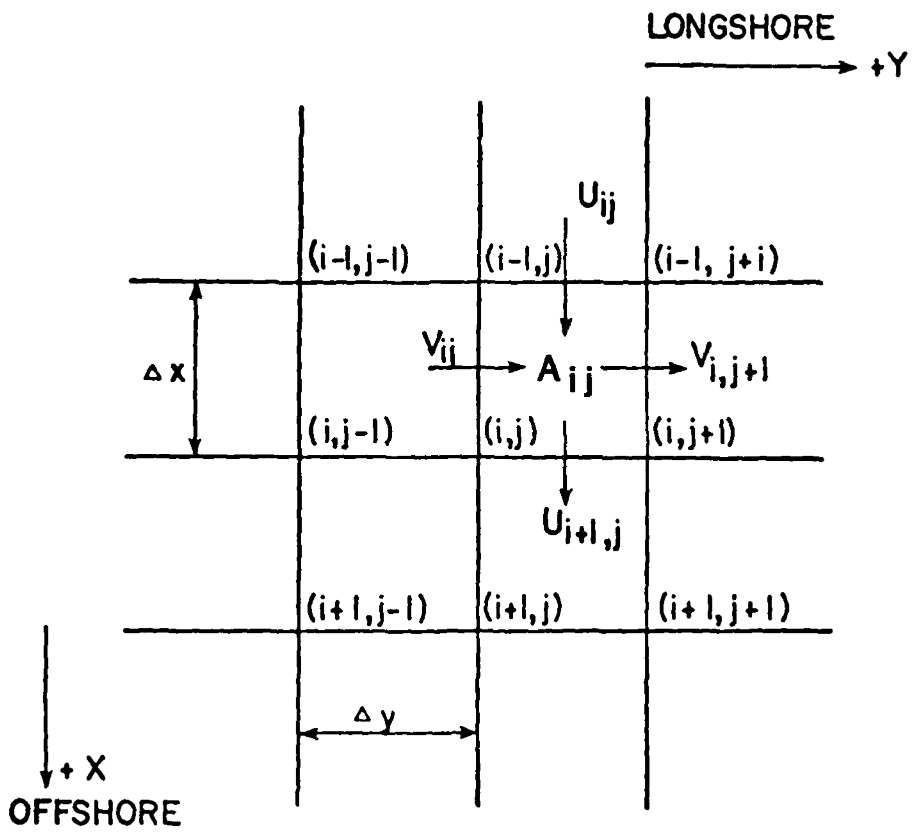


Figure 3-2. Velocity Components for Grid Block (i,j). All Other Variables (D, $S_{xx}$, $S_{xy}$, H, etc.) Are Determined at Grid Center.

3. BOUNDARY CONDITIONS

In order to formulate the numerical models, a scheme was established which incorporated the lateral periodicity requirements mentioned above and the no-flow requirements at the shore and the offshore grid row, as mentioned in Chapter II.

The user defined depth grid is established for the M by N portion of the total grid shown in Figure 3.1, with the requirement that

$$D_{i,N} = D_{i,1} \tag{3.2}$$

to satisfy the periodicity requirement. The grid N then extended to the N + 1 and the N + 2 columns according to

$$\begin{aligned} D_{i,N+1} &= D_{i,2} \\ D_{i,N+2} &= D_{i,3} \quad . \end{aligned} \tag{3.3}$$

Similar periodicity requirements are met by all calculated quantities (the $A_{ij}$ in Eq. (3.1)). The models calculate values of the $A_{ij}$ quantities from the j = 2 row to the j = N row. Periodicity is then established by setting

$$\begin{aligned} A_{i,1} &= A_{i,N} \\ A_{i,N+1} &= A_{i,2} \\ A_{i,N+2} &= A_{i,3} \end{aligned} \tag{3.4}$$

The velocities U and V are treated somewhat differently in that the calculations are performed from the $j = 3$ to the $j = N+1$ grid rows, with periodicity established accordingly.

At the offshore grid row ($i = M$), a no-flow condition is applied for U and V. This condition serves to bound the calculated velocities during initial start-up of the model; however, the condition is artificial in that the offshore side of the modelled area becomes a solid vertical boundary. This treatment leads to potential seiching in the model. The presence of a seiching mode in the model calculations has been discussed thoroughly by Birkemeier and Dalrymple (1971) and Ebersole and Dalrymple (1979), who have shown that the period of seiching can be accurately predicted by the shallow water formulas for known topographies. For example, for a basin of triangular cross-section, Wilson (1966) predicts the period of the first mode oscillation by

$$T = \frac{3.28L}{\sqrt{gh_{max}}} \tag{3.5}$$

where

$T$ = period of oscillation in the basin

$L$ = length of the basin = $(M - 1) \cdot \Delta x$

$h_{max}$ = maximum still water depth in the basin.

Similarly, a no flow condition for the shore-normal velocity U is applied at the onshore grid row, whose position remains fixed during a model run. The linear model originally described by Birkemeier and Dalrymple (1976) included a provision for flooding shoreward dry grids in order to model the effect of wave set-up; model results have been seen to be somewhat insensitive to the correction provided by this provision. Flooding is not included in the nonlinear model of Ebersole and Dalrymple or in the present version of the linear model.

In addition to the lateral boundary conditions, the system of hyperbolic equations requires initial conditions for a complete solution. The models are started from a state of rest with no wave field present. In order to reduce the effect of seiching, the wave height H at the offshore grid is brought up to its full value gradually according to

$$H = H_o \tanh\left(\frac{2t}{T}\right) \quad , \tag{3.6}$$

where

t = model time

T = arbitrary fixed time period.

Wave height is typically allowed to build up for 400 model iterations. It is also noted that, in principal, the seiching effect could be removed by setting $\bar{\eta}$ to zero at the offshore boundary, rather than U.

## 4. FINITE DIFFERENCE OPERATORS AND NOTATIONS

The derivations of the numerical models given by Birkemeier and Dalrymple (1976) and Ebersole and Dalrymple (1979) differ significantly in notation. For this reason, a standardized notation is presented here. We retain as far as possible the terminology of Ebersole and Dalrymple (1979) in describing both the linear and nonlinear models.

The numerical formulations require both averaging and differencing operations. Let F(x,y,t) be an arbitrary function varying in space and time. The average of the function over one grid spacing is given by

$$\overline{F(x,y,t)}^{\,x} \equiv \frac{1}{2}\left\{F(x + \frac{\Delta x}{2}, y,t) + F(x - \frac{\Delta x}{2}, y,t)\right\} \tag{3.7}$$

for an average in the x-direction. Successive averaging is given by

$$\overline{F(x,y,t)}^{xy} \equiv \overline{\overline{F(x,y,t)}^{x}}^{y} \qquad (3.8)$$

First derivatives can be given in terms of forward and backward differences over a single grid space, or as central differences over two grid spaces. We define the forward and backward difference operators, respectively, as

$$\delta_x\{F(x,y,t)\} = \frac{1}{\Delta x}\{F(x+\Delta x,y,t) - F(x,y,t)\} \qquad (3.9)$$

$$\delta_{\bar{x}}\{F(x,y,t)\} = \frac{1}{\Delta x}\{F(x,y,t) - F(x-\Delta x,y,t)\} \qquad (3.10)$$

and the central difference operator as

$$\delta_{\hat{x}}\{F(x,y,t)\} = \frac{1}{2\Delta x}\{F(x+\Delta x,y,t) - F(x-\Delta x,y,t)\} \qquad (3.11)$$

We also define an auxilary operator which represents the central difference at a grid center based on values at the grid sides

$$\delta_{\tilde{x}}\{F(x,y,t)\} = \frac{1}{\Delta x}\ F(x+\frac{\Delta x}{2},y,t) - F(x-\frac{\Delta x}{2},y,t)\} \qquad (3.12)$$

It is easily shown by direct substitution that the $\delta_{\tilde{x}}$ operator is related to $\delta_{\hat{x}}$ through the relation

$$\delta_{\tilde{x}}\{\overline{F(x,y,t)}^{x}\} = \delta_{\hat{x}}\{F(x,y,t)\} \qquad (3.13)$$

The nonlinear model makes extensive use of the $\delta_{\tilde{x}}$ operator, while the linear model is formulated more conventionally in terms of the standard forward and backward differences given by Eqs. (3.9) and (3.10).

## 5. FINITE DIFFERENCE FORMS OF THE GOVERNING EQUATIONS - LINEAR MODEL

Before applying the finite difference scheme to the linear formulation, we rewrite the equations here for clarity. The equations of continuity and x- and y-momentum are given respectively by

$$\frac{\partial \bar{\eta}}{\partial t} = - \frac{\partial}{\partial x} (UD) - \frac{\partial}{\partial y} (VD) \tag{3.14}$$

$$\frac{\partial U}{\partial t} = - g \frac{\partial \bar{\eta}}{\partial x} - \frac{1}{\rho D} \left\{ \frac{\partial S_{xx}}{\partial x} + \frac{\partial S_{xy}}{\partial y} - \overline{\tau_{sx}} + \overline{\tau_{bx}} \right\} \tag{3.15}$$

$$\frac{\partial V}{\partial t} = - g \frac{\partial \bar{\eta}}{\partial y} - \frac{1}{\rho D} \left\{ \frac{\partial S_{xy}}{\partial x} + \frac{\partial S_{yy}}{\partial y} - \overline{\tau_{sy}} + \overline{\tau_{by}} \right\} \tag{3.16}$$

In deriving this set of equations, we have tacitly assumed that variations of $\bar{\eta}$ with respect to time are small in comparison to variations in U and V. As we are striving for a steady state solution, the model results should not be sensitive to this assumption. Care should be taken, however, in removing time derivatives of D in cases where time dependent results are desired.

In keeping with standard techniques for treating first order linear hyperbolic equations, difference equations are formulated using a forward time-forward space (FTFS) scheme for the continuity equation (3.14), and forward time-backward space (FTBS) formulation for the momentum equations (3.15) and (3.16). Recalling that depths and set-up are known at grid centers, while velocities are given at grid boundaries, equations (3.14) - (3.16) are written in finite difference form as:

$$\delta_t\{\bar{\eta}\} = - \delta_x\{U\bar{D}^{\,x}\} - \delta_y\{V\bar{D}^{\,y}\} \tag{3.17}$$

$$\delta_t\{U\} = - g\ \delta_{\bar{x}}\ \{\eta\} - \frac{1}{\rho \bar{D}^{\,x}} \left\{ \delta_{\bar{x}}\{S_{xx}\} + \delta_{\hat{y}}\{\overline{S_{xy}}\}^{x} \right.$$

$$\left. - \overline{\tau_{sx}}^{\,x} + \overline{\tau_{bx}}^{\,x} \right\} \tag{3.18}$$

$$\delta_t\{V\} = - g\delta_{\bar{y}}\{\bar{\eta}\} - \frac{1}{\rho \bar{D}^{y}} \left\{ \delta_{\hat{x}}\{\overline{S_{xy}}\}^{y} + \delta_{\bar{y}}\{S_{yy}\} - \overline{\tau_{sy}}^{y} + \overline{\tau_{by}}^{y} \right\} \qquad (3.19)$$

Note that $\delta_t(F)$ yields the forward difference

$$\delta_t(F) = \frac{F^{k+1} - F^{k}}{\Delta t} \qquad (3.20)$$

where k and k+1 are successive time levels. Expanded forms of the equations (3.17) - (3.19) can be found in Birkemeier and Dalrymple (1976). At each iteration, the values of U and V are updated to time level k+1 using $\bar{\eta}$ and forcing terms evaluated at time level k. Then $\bar{\eta}$ is updated using the newly evaluated values of U and V at time level k+1. The method thus requires only one time level of storage for each of the unknown quantities.

Difference forms of the type used here have been discussed extensively by a number of authors (see, for example, Roache (1976)). The explicit method is subject to certain stability conditions. The problem of obtaining stability criteria for equations with non-constant coefficients is in general unsolved to date; however, we can make a reasonable guess based on constant-coefficient forms of the governing equations. If we drop the forcing terms, assume $D \simeq h$, and hold h constant, we obtain

$$\frac{\partial\bar{\eta}}{\partial t} = - h \left\{\frac{\partial U}{\partial x} + \frac{\partial V}{\partial y}\right\}$$

$$\frac{\partial U}{\partial t} = - g \frac{\partial\bar{\eta}}{\partial x} \qquad (3.21)$$

$$\frac{\partial V}{\partial t} = - g \frac{\partial\bar{\eta}}{\partial y}$$

Cross-differentiating to eliminate U and V, we obtain the second-order hyperbolic equation for $\bar{\eta}$:

$$\frac{\partial^2 \bar{\eta}}{\partial t^2} = gh \left\{ \frac{\partial^2 \bar{\eta}}{\partial x^2} + \frac{\partial^2 \bar{\eta}}{\partial y^2} \right\} \tag{3.22}$$

The stability criterion corresponding to this reduced equation is given by the Courant condition:

$$\Delta t \leq \frac{\Delta x}{\sqrt{2gh}} \quad , \tag{3.23}$$

assuming that $\Delta y = \Delta x$. Generalizing to the full model, the stability criterion (3.23) can be extended to include the effect of rectangular grids and the advection of disturbances by the mean currents.

$$\Delta t \leq \frac{\sqrt{(\Delta x)^2 + (\Delta y)^2}}{\sqrt{2gh} + |\vec{U}|} \tag{3.24}$$

The stability criterion basically states that time steps in the model may not be so large as to allow long wave disturbances to pass completely through a grid in one iteration. Violation of the criterion leads to rapidly growing instability of the numerical solution. In practice, time steps on the order of 0.25 times the maximum $\Delta t$ are used.

## 6. FINITE DIFFERENCE FORMS OF THE GOVERNING EQUATIONS - NONLINEAR MODEL

The set of nonlinear momentum equations (2.12) - (2.13), together with the continuity equation (2.11), require a more careful development in difference form than the previously described linear model. Nonlinear formulations are in a practical sense subject to a number of instability mechanisms which are not strictly related to stability criteria for the corresponding linear formulations, as discussed by Roache (1976).

The nonlinear model has been formulated using a method which has been applied successfully to geophysical and tidal models by Lilly (1965) and Blumberg (1977). Using the difference and average operators defined in section 4, the equations (2.11-13) are rewritten as

Continuity:

$$\delta_{\tilde{t}}\{\overline{\eta}^{t}\} + \delta_{\tilde{x}}\{\overline{D}^{x}U\} + \delta_{\tilde{y}}\{\overline{D}^{y}V\} = 0 \tag{3.25}$$

X-Momentum

$$\delta_{\tilde{t}}\{\overline{\overline{D}^{x}U}^{t}\} + \delta_{\tilde{x}}\{\overline{\overline{D}^{x}U}^{x}\ \overline{U}^{x}\} + \delta_{\tilde{y}}\{\overline{\overline{D}^{y}V}^{x}\ \overline{U}^{y}\} =$$

$$= -g\,\overline{D}^{x}\,\delta_{x}\{\overline{\eta}\} + \frac{1}{\rho}\{\overline{\tau_{sx}}^{x} - \overline{\tau_{bx}}^{x} - \delta_{\tilde{y}}\{\overline{S_{xy}}^{xy}\} -$$

$$- \delta_{\tilde{x}}\{S_{xx}\}\} + \overline{D}^{x}\,\delta_{\tilde{y}}\{\varepsilon_{y}\delta_{\tilde{y}}\{U\} + \overline{\varepsilon_{x}}^{xy}\,\delta_{\tilde{x}}\{V\}\} \tag{3.26}$$

Y-Momentum

$$\delta_{\tilde{t}}\{\overline{\overline{D}^{y}V}^{t}\} + \delta_{\tilde{x}}\{\overline{\overline{D}^{x}U}^{y}\,\overline{V}^{y}\} + \delta_{\tilde{y}}\{\overline{\overline{D}^{y}V}^{y}\,\overline{V}^{y}\} =$$

$$- g\,\overline{D}^{y}\,\delta_{y}\{\overline{\eta}\} + \frac{1}{\rho}\left\{\overline{\overline{\tau_{sy}}}^{y} - \overline{\overline{\tau_{by}}}^{y} - \delta_{\tilde{y}}\{S_{yy}\}\right.$$

$$\left. - \delta_{\tilde{x}}\{\overline{S_{xy}}^{xy}\}\right\} + \overline{D}^{y}\,\delta_{\tilde{x}}\{\varepsilon_{y}\delta_{\tilde{y}}\{U\} + \overline{\varepsilon_{x}}^{xy}\,\delta_{\tilde{x}}\{V\}\} \tag{3.27}$$

The formula for lateral mixing given by Eq. (2.46) has been substituted into Eqs. (3.26-27). Note that, following Eq. (3.13), the central difference on the time averaged wate set-up in Eq. (3.25) leads to

$$\delta_{\bar{t}}\{\overline{\eta}^{\,t}\} = \delta_{\bar{t}}\{\overline{\eta}\} = \frac{\overline{\eta}^{k+1}_{i,j} - \overline{\eta}^{k-1}_{i,j}}{2\Delta t} \tag{3.28}$$

The governing equations in this case then contain function values at three times levels, given by k+1, k, and k-1. The equations (3.25-27) can be found written out with respect to the i,j grid in Ebersole and Dalrymple (1979). These three equations can also be written in the following abbreviated form,

$$\overline{\eta}^{k+1}_{i,j} = \overline{\eta}^{k-1}_{i,j} + 2\Delta t\ F_1 \tag{3.29}$$

$$U^{k+1}_{i,j} = A\ U^{k-1}_{i,j} + 2\Delta t\ F_2 \tag{3.30}$$

$$V^{k+1}_{i,j} = B\ V^{k-1}_{i,j} + 2\Delta t\ F_3 \tag{3.31}$$

where A and B are functions of the depth alone and $F_1$, $F_2$, and $F_3$ are functions of all the variables in the problem. The quantities $F_1$, $F_2$, and $F_3$ contain quantities evaluated at time level k and k-1.

The method of solution for Eqs. (3.29-31) is based on a leapfrog scheme, and thus requires the storage of three time levels of values for all the calculated variables. In order to select the model, a single step is taken based on a forward difference formulation similar to that described in conjunction with the linear model. The forward difference formulation can be indicated schematically by

$$\overline{\eta}^{k+1}_{i,j} = \overline{\eta}^{k}_{i,j} + \Delta t\ F_1 \tag{3.32}$$

$$U^{k+1}_{i,j} = C\ U^{k}_{i,j} + \Delta t\ F_4 \tag{3.33}$$

$$V^{k+1}_{i,j} = D\ V^{k}_{i,j} + \Delta t\ F_5 \quad . \tag{3.34}$$

The computational method is schematized in Figure 3-3.

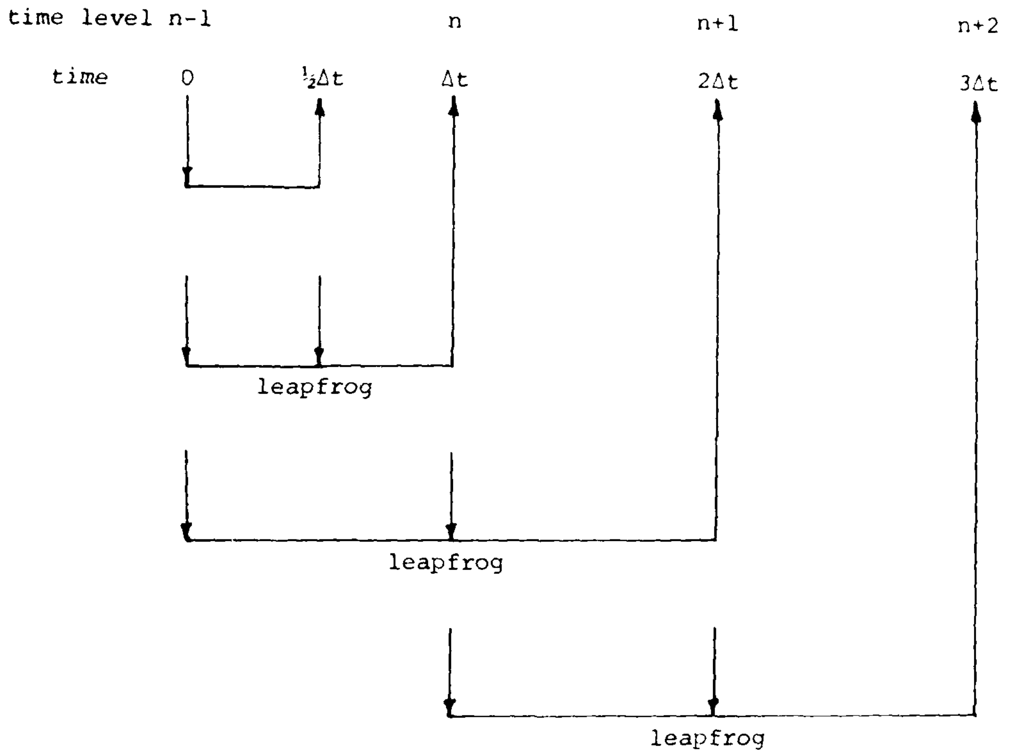


Figure 3-3. General Leapfrog Solution Scheme

The stability criterion for the present scheme was assumed to be given by Eq. (3.24), which has physical if not mathematical significance in the present situation. In practice, as is the case of the linear model, it was necessary to reduce the maximum allowable time step to a value significantly below the one predicted by the stability criterion.

The nonlinear model was also subject to a second computational stability problem. In general, computational schemes for first order equations which are centered in space and time (CSCT) exhibit forms of unstable behavior. In particular, in the context of the first order parabolic diffusion equation, such explicit CSCT schemes can be shown to be unconditionally unstable. In the present case, as the model approached a steady state, the solution diverged into two disjoint solutions; one associated with the even time steps and the other the odd steps. These solutions oscillated with growing amplitudes about the steady state solution. In Roache (1976), the author referred to this as time splitting.

To alleviate the problem, a leapfrog-backward correction scheme, Kurihara (1965), was initiated every tenth time step. The scheme is shown below as,

$$h^* = h^{k-1} + 2\Delta t\ G^k \tag{3.35}$$

$$h^{k+1} = h^k + \Delta t\ G^* \tag{3.36}$$

where h may be U, V or $\bar{\eta}$. Equation (3.35) is simply the leapfrog calculation done by the Eqs. (3.29-31) where * denotes the new or "interim" time level. Using the new values U, V, $\bar{\eta}$ at time *, the functions G*, like the functions $F_1$, $F_2$, and $F_3$ from Eqs. (3.29-31) are calculated and used in Eq. (3.36) which is merely a backwards difference in time to the level k.

This scheme was chosen because it damps the computational mode of the solution while leaving the physical mode relatively unaffected. For a more in-depth discussion the reader is referred to the work by Kurihara. With this correction scheme included, which essentially "ties" the solutions together every tenth iteration, the model proceeded to reach a steady state without any further time-splitting instability.

## 7. THE NUMERICAL SCHEME FOR REFRACTION AND THE WAVE HEIGHT FIELD

The equations governing wave refraction, wave height, and wave number are given by Eqs. (2.35), (2,37), and (2.36) respectively. The method of solving these equations for the unknown $\theta_{i,j}$, $H_{i,j}$ and $k_{i,j}$ is identical in both the linear and nonlinear models. The method was given originally by Noda et al. (1974).

If Eq. (2.36) is differentiated with respect to x to get $\frac{\partial k}{\partial x}$ and with respect to y to get $\frac{\partial k}{\partial y}$, these quantities can be substituted into Eq. (2.35), which can then be written in the following form:

$$A \frac{\partial \theta}{\partial x} = B \frac{\partial \theta}{\partial y} = C \tag{3.37}$$

where A, B and C are functions of the quantities sin θ, cos θ, k, h, u and v. By taking a forward difference in x to approximate $\frac{\partial \theta}{\partial x}$ and a backwards difference in y to approximate $\frac{\partial \theta}{\partial y}$, Eq. (3.37) becomes:

$$\theta_{i,j} = D + E\, \theta_{i,j-1} - F\, \theta_{i+1,j} \tag{3.38}$$

where D, E and F are now functions of the quantities sin $\theta_{i,j}$, cos $\theta_{i,j}$, $k_{i,j}$, $h_{i,j}$, $u_{i,j}$, $v_{i,j}$. To evaluate sin $\theta_{i,j}$ and cos $\theta_{i,j}$ Noda used a first order Taylor series expansion to the four neighboring grids (i+1,j), (i-1,j), (i,j+1) and (i,j-1), summed the results and took an average value.

The theta field $\theta_{i,j}$ is solved for in the following way. Snell's Law is used to approximate the angles at the offshore row. Working shoreward Eq. (3.38) is solved for in a row-by-row relaxation until the angles converge to their correct values with wave-current interaction included. After each updated value of theta, a new wave number must be solved for.

Eq. (2.36) can be written as

$$E(k) \equiv \{gk \tanh(kh)\}^{1/2} + uk\cos\theta + vk\sin\theta - \frac{2\pi}{T} = 0 \quad . \tag{3.39}$$

To solve for the wave number, k, after each updated angle is found, the Newton-Raphson Method, or "method of tangents", is used. This method states that

$$k_{new} = k_{old} - \frac{E(k_{old})}{E'(k_{old})}$$

Differentiating Eq. (3.39), $k_{new}$ is iteratively solved for until $|k_{new} - k_{old}| \leq .001|k_{new}|$ .

The wave height field is calculated in much the same way as the wave angle field. Multiplying Eq. (2.37) by $\frac{H}{2}$ and letting $\frac{\partial H}{\partial t} = 0$, the energy equation can now be written in the form

$$A \frac{\partial H}{\partial x} + B \frac{\partial H}{\partial y} = C\ H \tag{3.40}$$

where A, B and C are functions of u, v cos θ, sin θ, $C_g$, Δx, Δy and the radiation stresses. Taking a forward difference in x to approximate $\frac{\partial H}{\partial x}$ and a backward difference in y to approximate $\frac{\partial H}{\partial y}$ and solving for $H_{i,j}$, it can be shown that

$$H_{i,j} = D\ H_{i,j-1} - E\ H_{i+1,j}$$

where D and E are functions of the same quantities as A, B and C. Again the offshore row of wave heights are obtained from shoaling and refraction due to Snell's Law and the wave height field is determined by relaxing row by row in the shoreward direction. On each row a solution for the wave height is reached when $|H_{new} - H_{old}| \leq .01\ H_{new}$. After each updated value of $H_{i,j}$, a breaking wave height is also calculated from the breaking criteria given by the Miche formula

$$\left(\frac{H}{L}\right)_b = .12 \tanh(kh)_b \quad .$$

If the calculated $H_{i,j}$ is larger than the allowable breaking height, the height $H_{i,j}$ was set equal to the breaking height.

# CHAPTER IV

# CALIBRATION OF THE NEARSHORE CIRCULATION MODELS

In order to make the circulation model more generally applicable to prediction of field conditions, both versions of the model were calibrated using field data. The calibrations consisted of determining a monochromatic deepwater wave condition and a uniform wind condition, and then running the models using the field conditions and measured bathymetry. Adjustable coefficients were then tuned to obtain the best possible qualitative and quantitative fit between the currents predicted by the model and those measured in the field.

In this chapter, the field data set used for calibration is described. Results for the circulation models are then shown for a range of coefficient values.

## 1. FIELD DATA USED FOR CALIBRATION

Field data used during calibration of the nearshore circulation models was obtained from the results of the Nearshore Sediment Transport Study (NSTS) experiment conducted at Torrey Pines beach, near La Jolla, Ca., (see Figure 4-1) in November - December 1978. The results of this study were chosen as being applicable to calibration of the models for several reasons. Torrey Pines beach is a long, straight beach with fairly uniform and parallel offshore contours. The field bathymetry was thus easily adapted into the model's scheme of longshore periodicity.

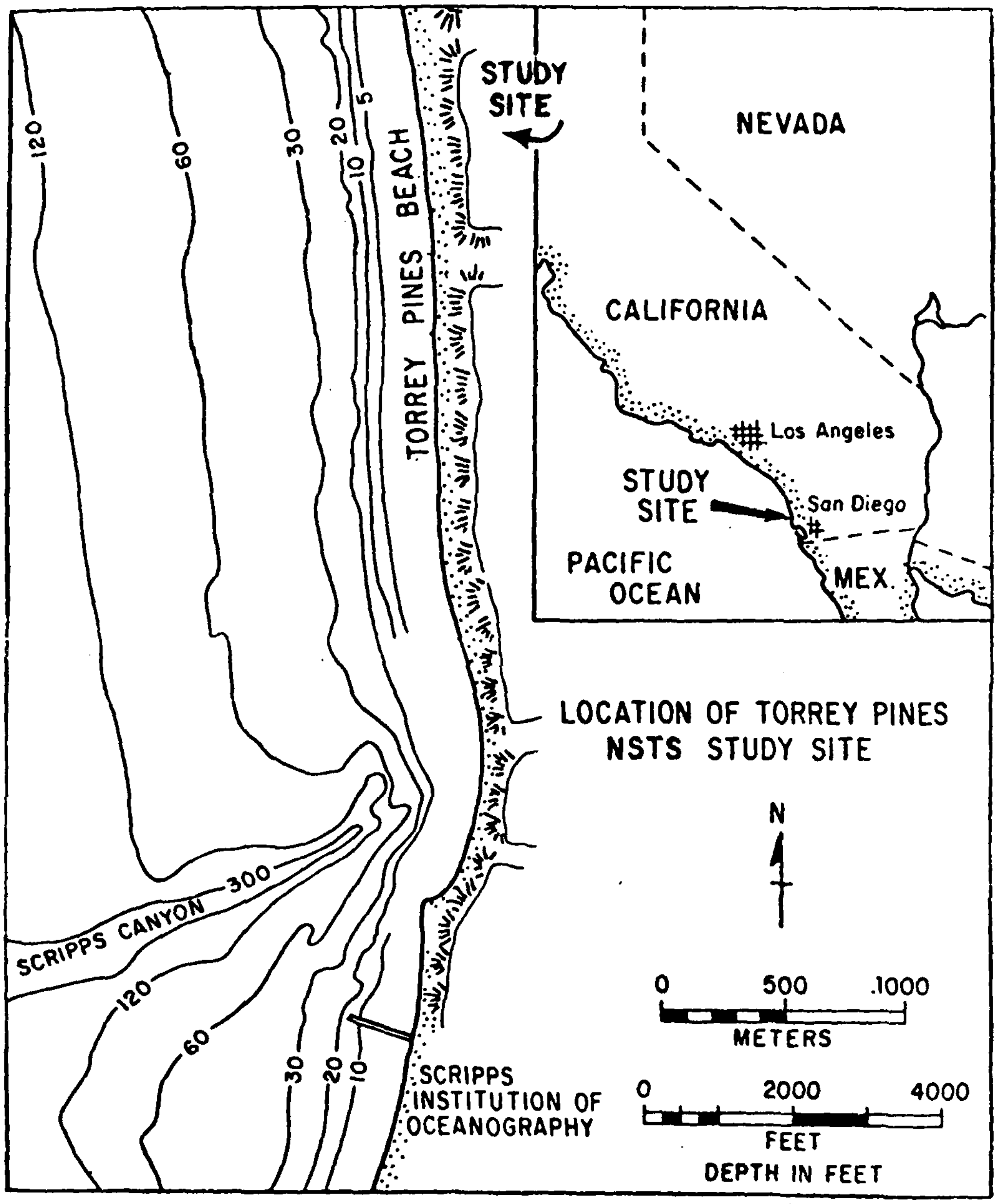


Figure 4-1. Location of NSTS Torrey Pines Experiment. (From Gable, 1979)

The experiment itself produced a detailed picture of nearshore currents and waves, with up to 22 current meters, 10 pressure gages, and 7 wave staffs being operated simultaneously. Thus the resolution needed to accurately fit the model predictions was present in the field data. Gable (1979) gives a detailed description of the site, instrumentation, and conduct of the NSTS experiment. The arrangement of fixed instruments used in the experiment is shown in Figure 4-2. Angles and distances used in this report will be with respect to the baseline (0 offshore distance) in Figure 4-2. Two separate bathymetry maps are shown in Figures 4-3 and 4-4. It is noted that the survey of Nov. 9, 1978 indicates the presence of a shallow channel oriented almost perpendicular to the baseline at about 40 m left of the main range (0 m alongshore). This feature is not present in the Nov. 18, 1978 survey, which, on the whole, exhibits greater random fluctuation in the location of the contours. Both the channel in the Nov. 9 bathymetry data and the unevenness in the Nov. 18 data appear to be transient features, as will be discussed below.

### 1.1 Choice of Field Data for Calibration

Several requirements were chosen in order to determine a valid set of field data for comparison to the numerical model. First, the numerical models in their basic state are designed to be run with a monochromatic deepwater wave condition. It was therefore required that the wave field for the chosen data be narrow banded both in a frequency and directional sense. The presence of a second wave component at a different direction than the primary component introduces a forcing mechanism

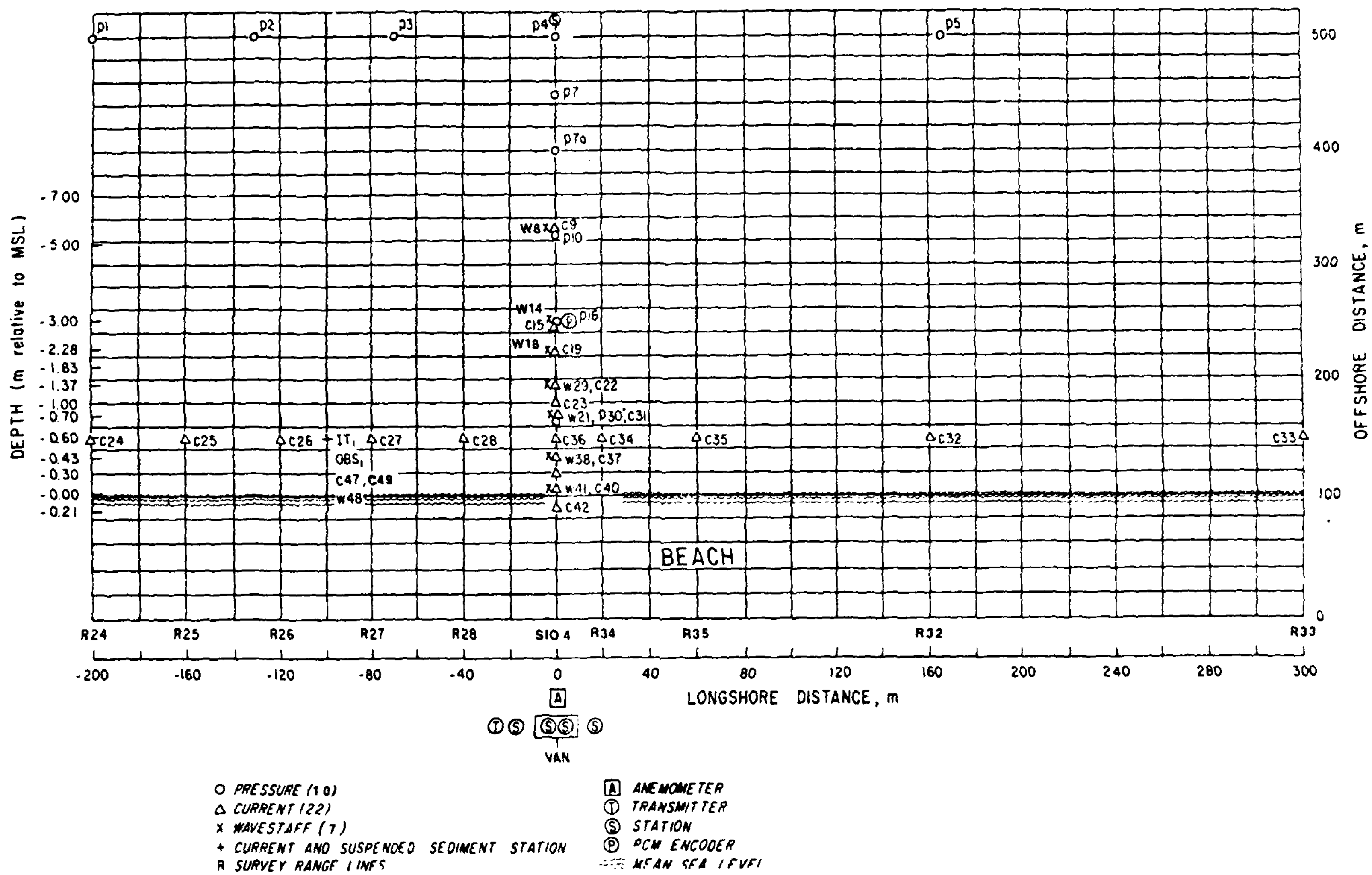


Figure 4-2. Instrumentation for NSTS Torrey Pines Experiment.
([illegible])

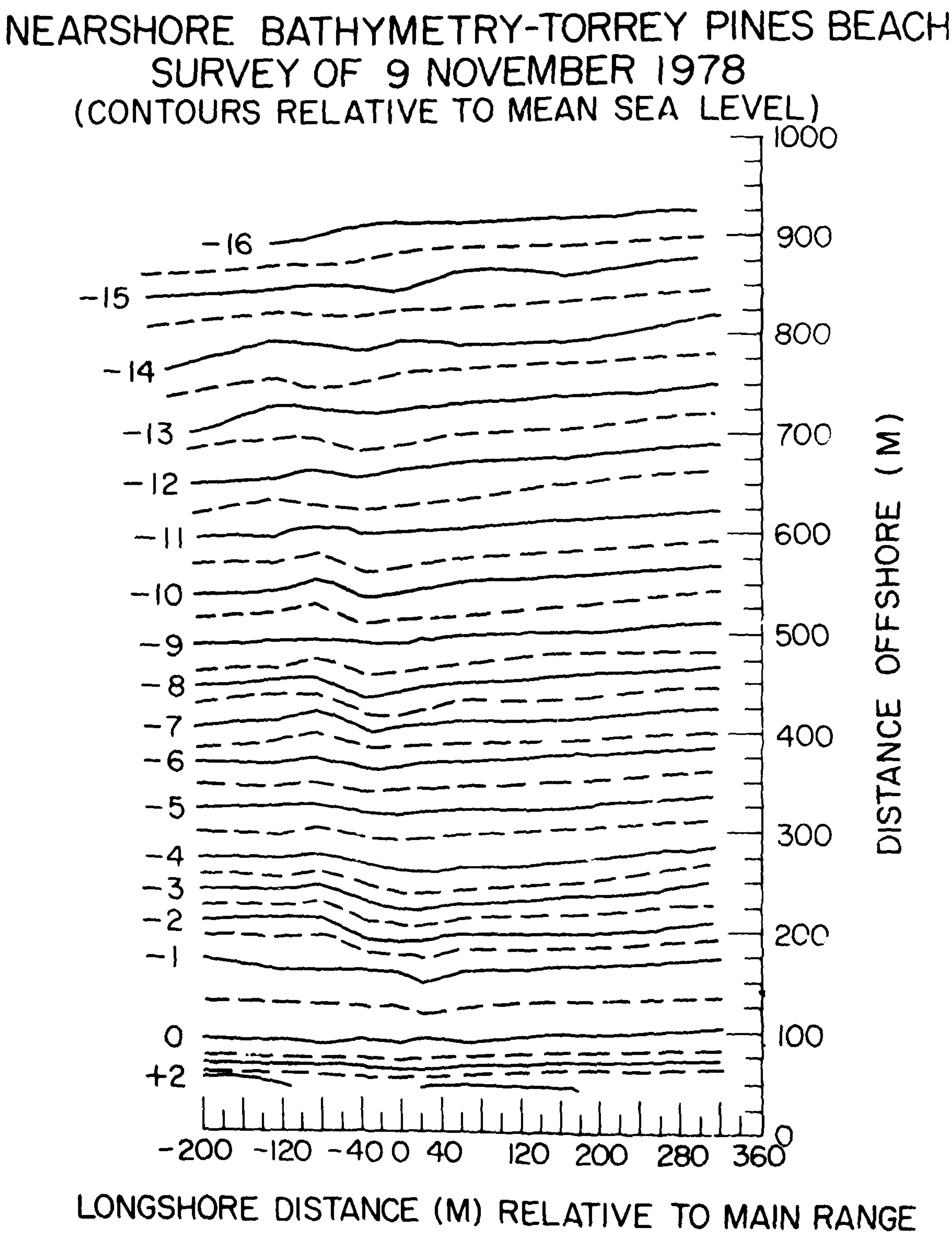


Figure 4-3. Nearshore Bathymetry, Nov. 9, 1978
(from Gable 1979)

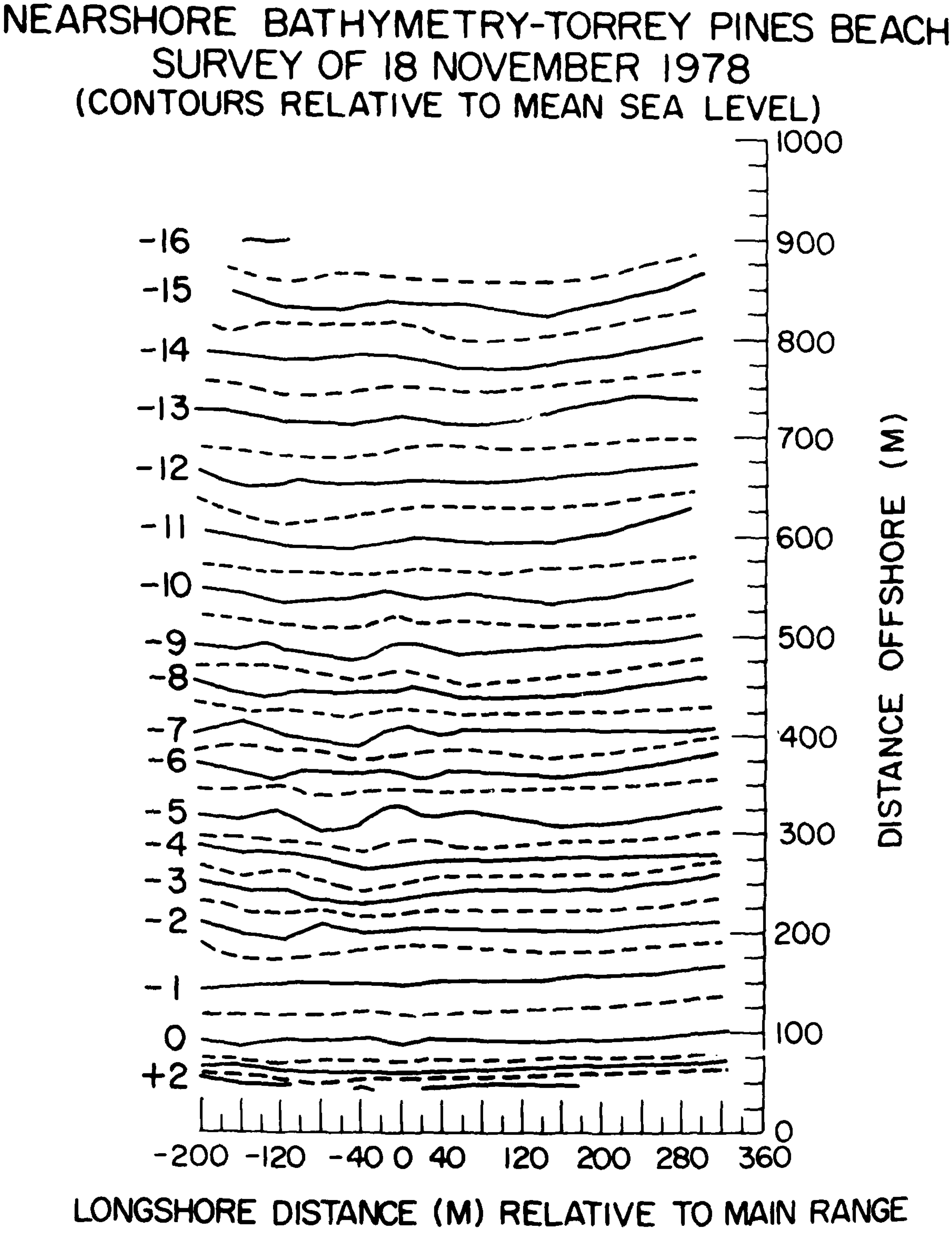


Figure 4-4. Nearshore Bathymetry, Nov. 18, 1978
(from Gable 1979)

which would tend to produce rip cells on a plane beach, as shown by Dalrymple (1975). Just such a case was treated by a simplified refraction model in Ebersole and Dalrymple (1979), but the capability to handle the condition has not been retained in the final model versions since the refraction scheme used does not model the interaction of different waves. In addition, the use of a 17 minute average of the field measured currents in order to obtain fairly steady conditions precluded the modelling of essentially transient circulation phenomenon.

Secondly, since it was desired to calculate a steady state wave and current field, it was required that wave and wind conditions be nearly steady over the interval of averaged field measurements. This required either a quiet or unidirectional wind field as well as fairly steady wave direction, height and period.

The field data set available from the NSTS results was roughly screened on the basis of the beach observations given in Gable (1979). In particular, observation of long crested waves indicated the presence of narrow banded directional spectra. It was found that the NSTS data presented a problem, in that almost all data sets exhibited at least some degree of bi-directionality, with waves approaching from both the north and south. The data chosen for initial calibration has a somewhat smaller wave component from the north than other records, but is still suspect as a valid calibration standard.

Data Set Number 1

The NSTS data tapes divide the current and pressure records into 17 minute segments. The first data set chosen for use in cailbration, and subsequently used for the majority of calibration runs, was taken from the second 17 minute segment of the test of Nov. 10, 1978. The 17 minute segments were further subdivided into four 4.25 minute segments, and averaged current fields were plotted for each 4.25 minute segment. Two representative plots for the first data set are shown in Figure 4-5a and b.

Based on an average of the 4.25 minute average velocity profiles, an average 17 minute velocity profile was constructed for data values on the main range (offshore array of meters) and is shown in Figure 4-6. The resulting velocity profile indicates a longshore current of about 8 cm/sec magnitude offshore of the surf zone. This current is too far outside the breaker line to be surf driven, and may be due to the presence of a tidal or seasonal current. The effect of this current on the model results is discussed below.

The monochromatic deepwater wave conditions determined for data set No. 1 were as follows:

| | | | |
|---|---|---|---|
| Wave period | $T$ | : | 14.52 seconds |
| Wave height | $H_o$ | : | 0.62 meters |
| Wave angle | $A$ | : | $165.7^o$ measured clockwise from +x (offshore direction). |

The uniform wind conditions were:

| | | | |
|---|---|---|---|
| Wind speed | $W$ | : | 7.2 meters/second |
| Wind angle | $\alpha$ | : | $294.5^o$ measured clockwise from -x (onshore) direction. |

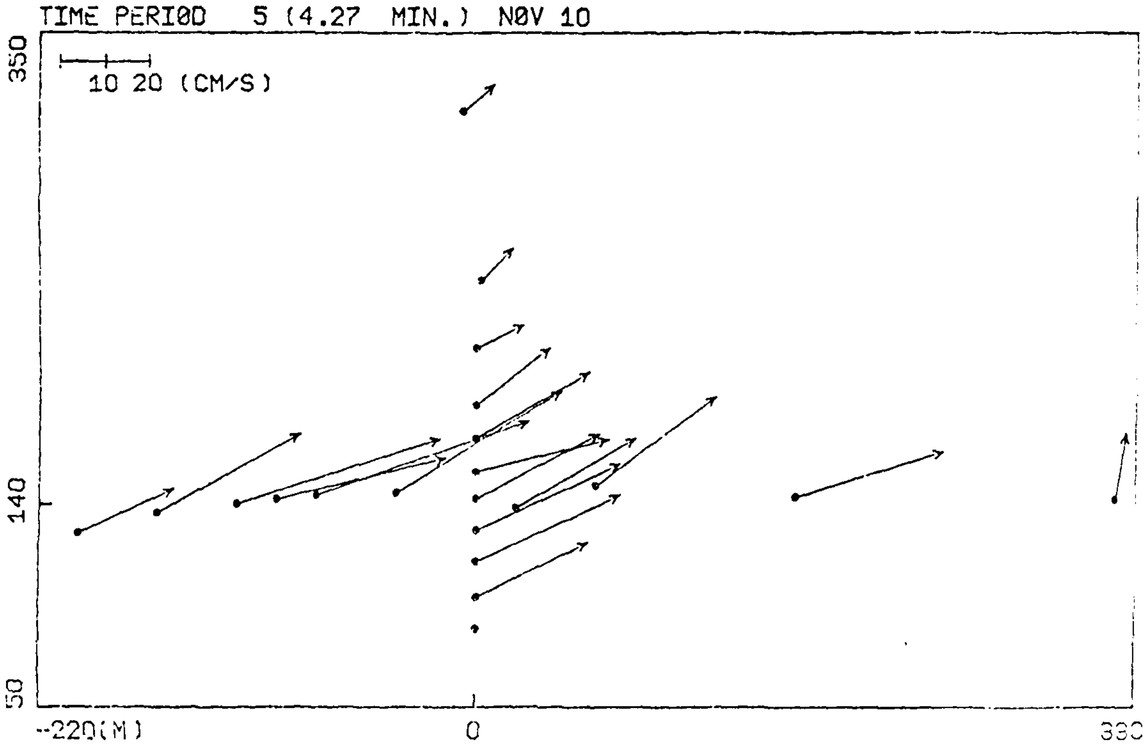


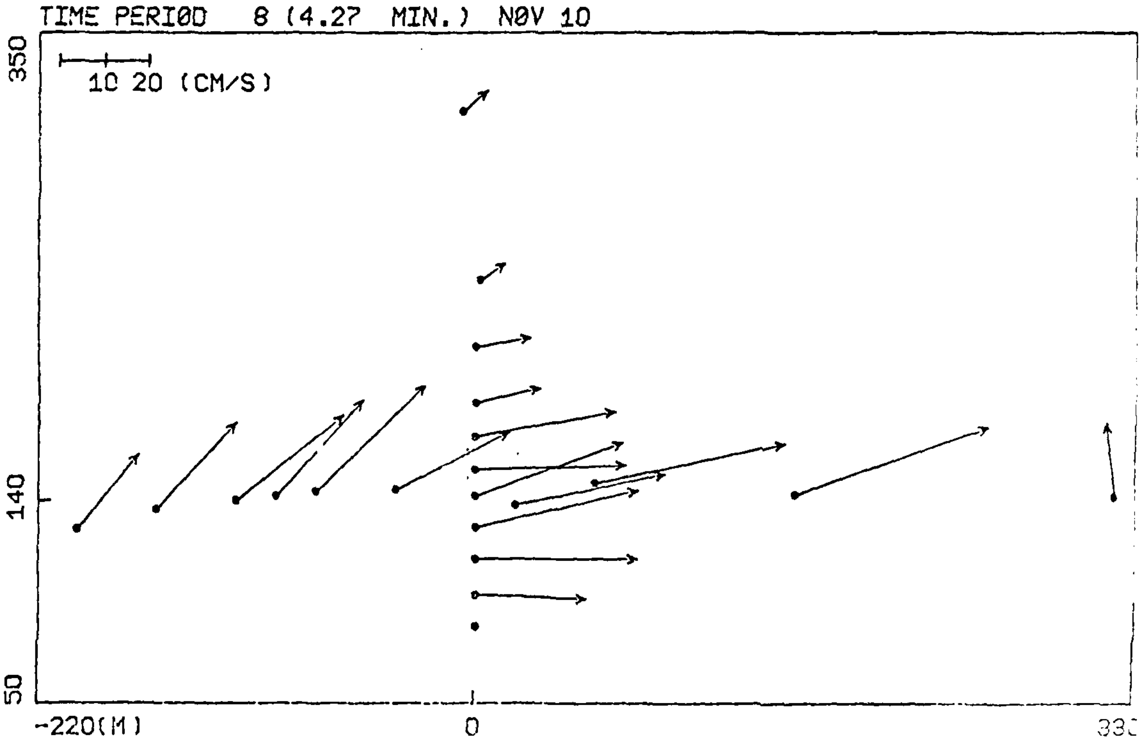


Figure 4-5. 4.27 Minute Average Current Vectors, Nov. 10, 1978.

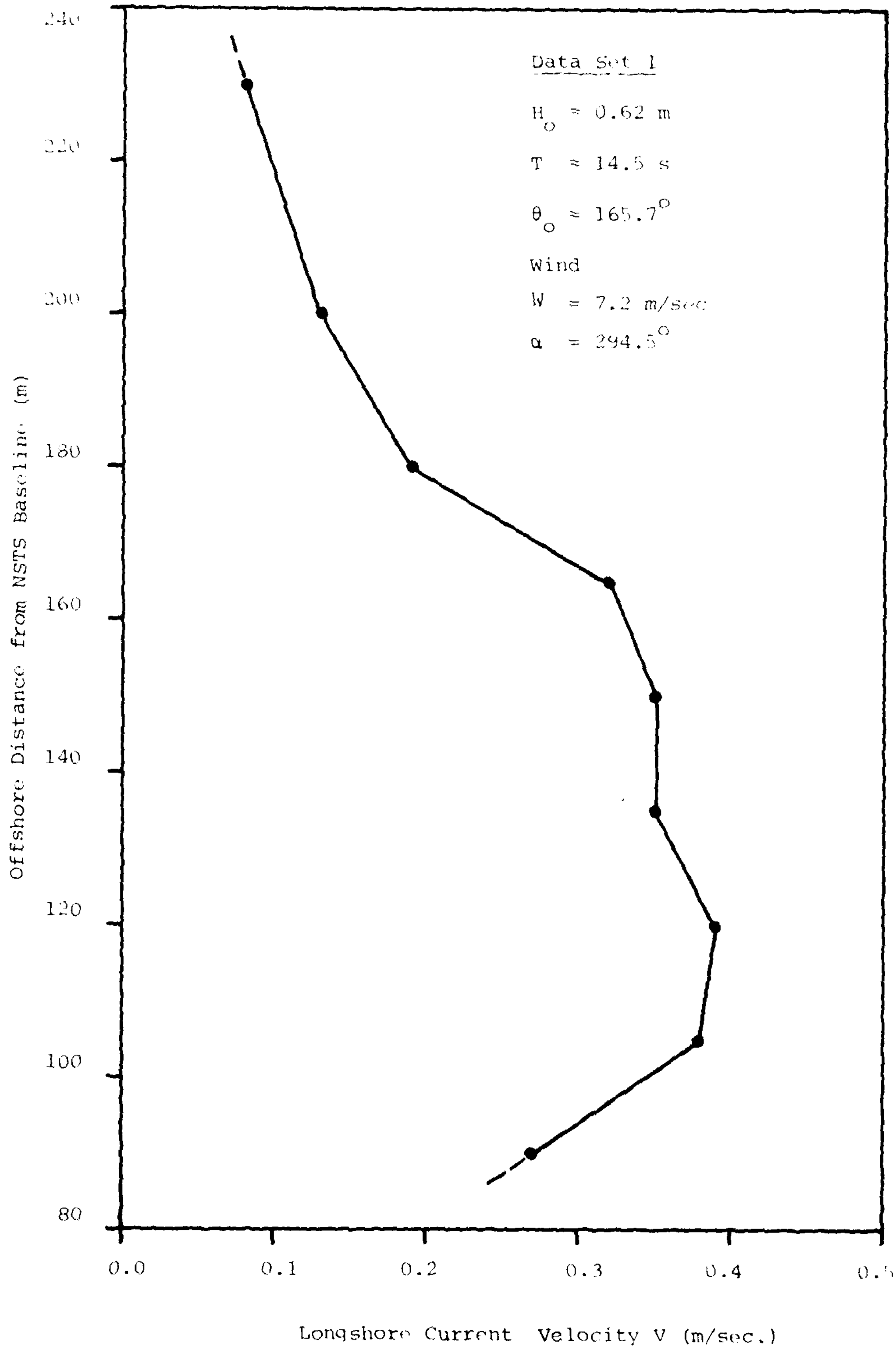


Figure 4.6 Average Field Velocity Profile
Data Set 1.

## Data Set Number 2

Data Set Number 1 represented the only strongly unidirectional, narrow banded wave spectrum contained in the Torrey Pines data. The remaining data sets, even in the absence of locally generated short wind waves, exhibited at least a strong tendency towards bidirectionality, with spectral peaks nearly symmetrically placed about the shore-normal axis. Since it is anticipated that measured wave fields in general would seldom exhibit the narrow banded, unidirectionality required as input into the model, a data set was constructed based on averaging over the parameters of the measured wave field in order to test the response of the model using a "best guess" for the desired input parameters.

The data chosen for this test was from the eighth 17-minute time period of the November 15 data. Wave energy was contained in two directional peaks in a narrow frequency band (Figure 4-7). Using directional spectra supplied by Pawka (1980), the data set was constructed by summing the mean energy density over all frequencies in the dominant spectral peak. The wave angle was chosen as the average of the dominant angle at each frequency weighted by the energy densities. The peak energy containing frequency was taken as the dominant frequency. The resulting data set follows:

| | | | |
|---|---|---|---|
| Wave Period | $T$ | : | 14.71 seconds |
| Wave Height | $H_o$ | : | 0.43 meters |
| Wave Angle | $A$ | : | 168° measured clockwise from +x (offshore direction) |

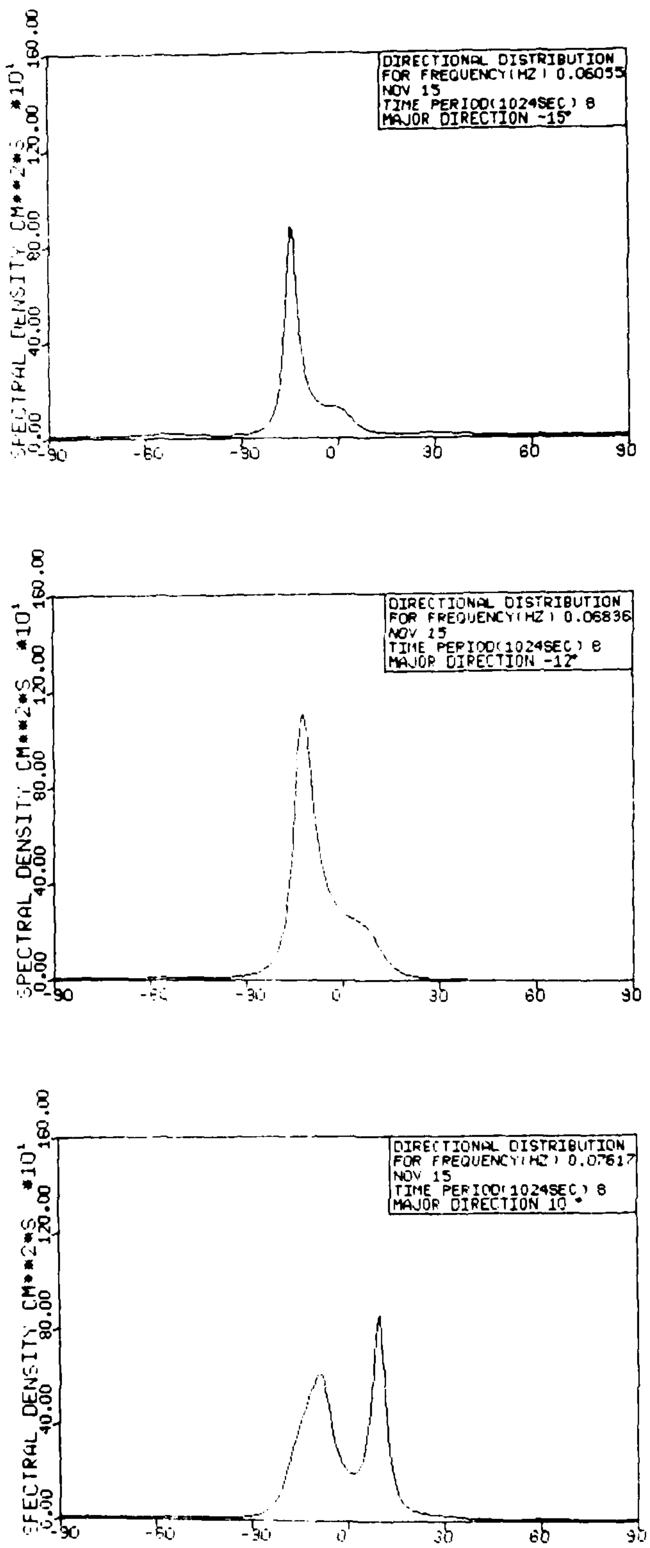


Figure 4-7. Directional Distribution of Wave Energy at Peak Frequencies, Nov. 15, 1978 (supplied by S. Pawka, 1980)

There was no significant steady wind component.

| | | | |
|---|---|---|---|
| Wind speed | W | : | 0.0 meters/second |
| Wind angle | $\alpha$ | : | not applicable. |

The resulting data set has an indeterminant connection with the measured field data, and at best the model could be expected to exhibit results in qualitative agreement with the field data.

Figure 4-8 shows a plot of average longshore current over the 17 minute period of data collection. Individual plots (not shown) of 4.25 minute averages show a great deal of scatter in peak velocities and shape of the profile, indicating some unsteadiness in the current field, as would be expected due to the bi-directional wave field.

## 2. CALIBRATION OF THE MODELS

Both the linear and nonlinear models have a bottom friction factor f and the Van Dorn coefficients $K_1$ and $K_2$ as adjustable parameters. In addition, the nonlinear model has adjustable coefficients of lateral eddy mixing in both the longshore and offshore directions.

The Van Dorn wind stress formulation used in the models is intended to represent the transfer of momentum from a wind field to the water column, leading to a wind-induced longshore current for wind stress applied in the long shore direction, and wind set up for wind blowing towards shore. Wind set up cannot currently be accurately calibrated in the present models due to the artificial barrier at the offshore grid row; no additional water can

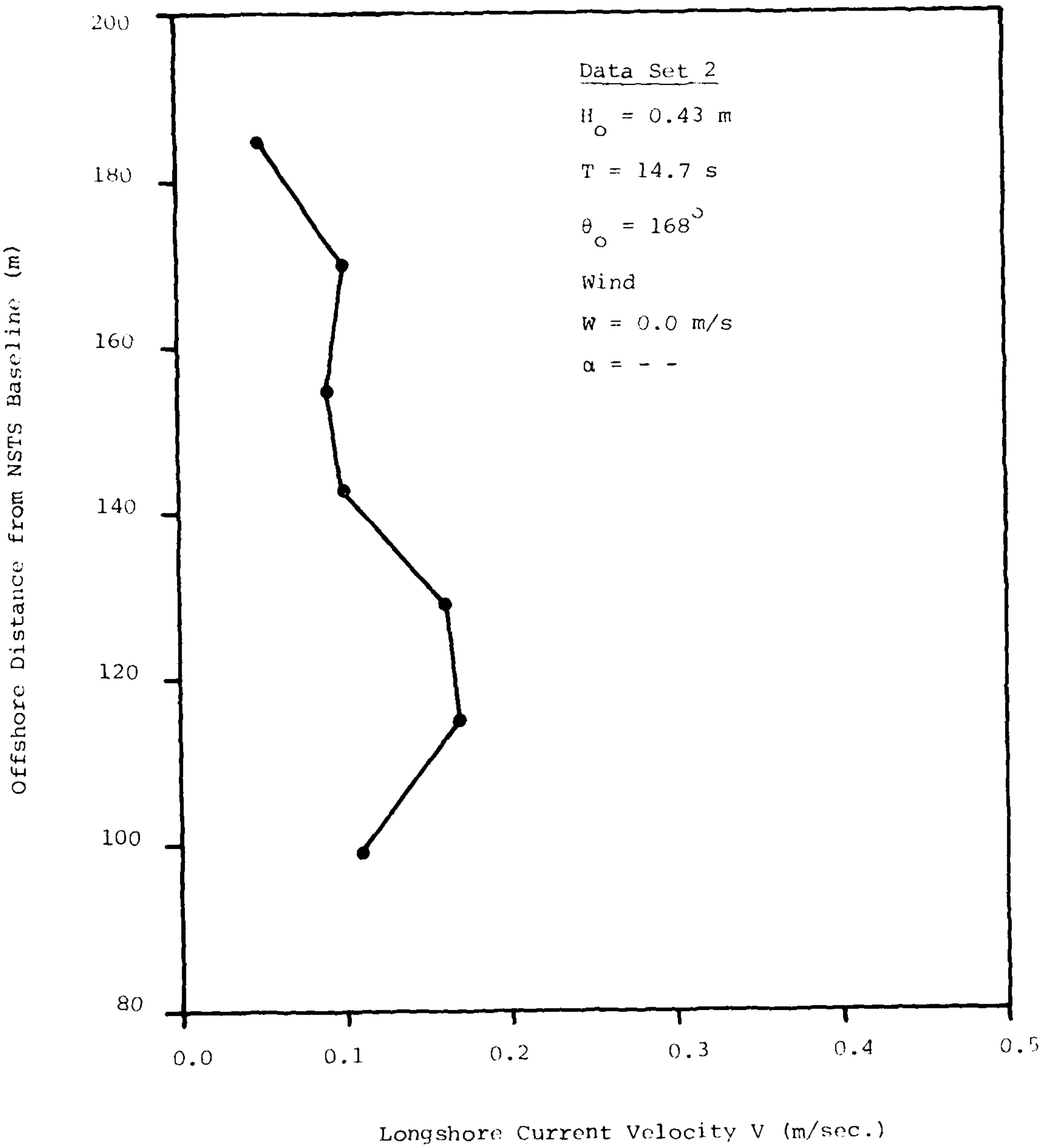


Figure 4-8 Average Field Velocity Profile
Data Set 2

enter the model after the start of the run with a given depth grid. The parameters used in the Van Dorn formula have been tested in previous large scale models (Pearce, 1972), and have been found to be satisfactory.

With the elimination of the wind stress coefficients, only the bottom friction coefficient, f, remained to be calibrated in the linear model. The procedure used was to choose a value of f for both models based on a comparison of field data with the linear model. The value of f chosen was then used in the nonlinear model as a first approximation, and values of the eddy mixing coefficients were adjusted to again obtain a best fit between the results of the nonlinear model and the field data. It should be noted, however, that there is no a priori reason that both models should behave optimally with the same value of f.

## 2.1 Linear Model Calibration

Runs of the linear model were conducted using the deepwater wave conditions of Data Set 1 and the measured bathymetry of Nov. 9, 1978. For all values of f chosen, rip currents formed near the shallow channel seen in the Nov. 9 bathymetry. These rip currents were not apparent in the Nov. 10 currents (Figure 4-5), where they would affect the main range velocity profile. An example of the current field calculated using the Nov. 9 bathymetry is shown in Figure (4-9). The value of f for the run shown was 0.01.

It was tentatively concluded at this point that the shallow channel seen in the Nov. 9 data was a transient feature and was not present on Nov. 10, juding from the uniformity of the measured currents. It was decided to run a model using a bathymetry based on a longshore average of the Nov. 9 bathymetry

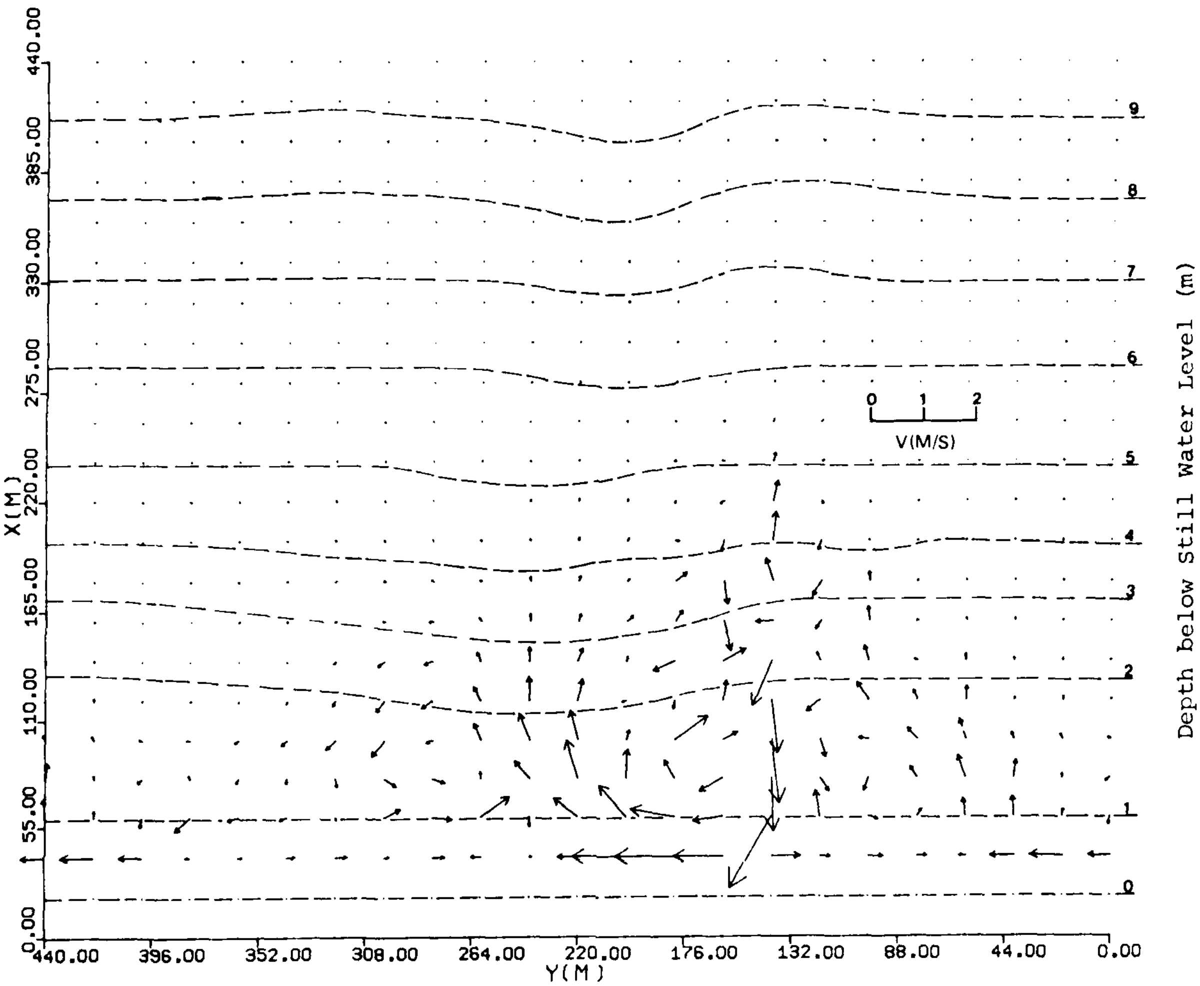


Figure 4-9 Currents Induced in Field Using Nov. 9 Bathymetry Nonlinear Model: Data Set 1.

data. The longshore extent of the beach was arbitrarily chosen as 200 meters. The profile is shown in Figure 4-10.

Using the longshore averaged bathymetry, model runs were conducted for a range of f values. Velocity profiles for values of f of 0.01, 0.015 and 0.02 are shown in Figure 4-11, in comparison to the current distribution measured in the field. In addition, a "corrected" field current distribution constructed by subtracting the 0.08 m/sec offshore current is shown as the dashed line.

Figure 4-11 shows that, by using a value of f equal to 0.015, the linear model closely predicts the maximum velocities and the general velocity distribution in the surf zone. The longshore current predicted by the model dies off more quickly offshore due to the absence of lateral mixing effects in the linear model.

## 2.2 Nonlinear Model Calibration

The nonlinear model was run using Data Set 1 and the value of $f = 0.015$ obtained from the linear model calibration. Three sets of mixing coefficients $\varepsilon_x$ (or N) and $\varepsilon_y$ were used (see Equation (2.40)).

| N | $\varepsilon_y$ | |
|---|---|---|
| 0.000 | 0.00 | no mixing |
| 0.0025 | 0.25 | |
| 0.005 | 0.50 | |

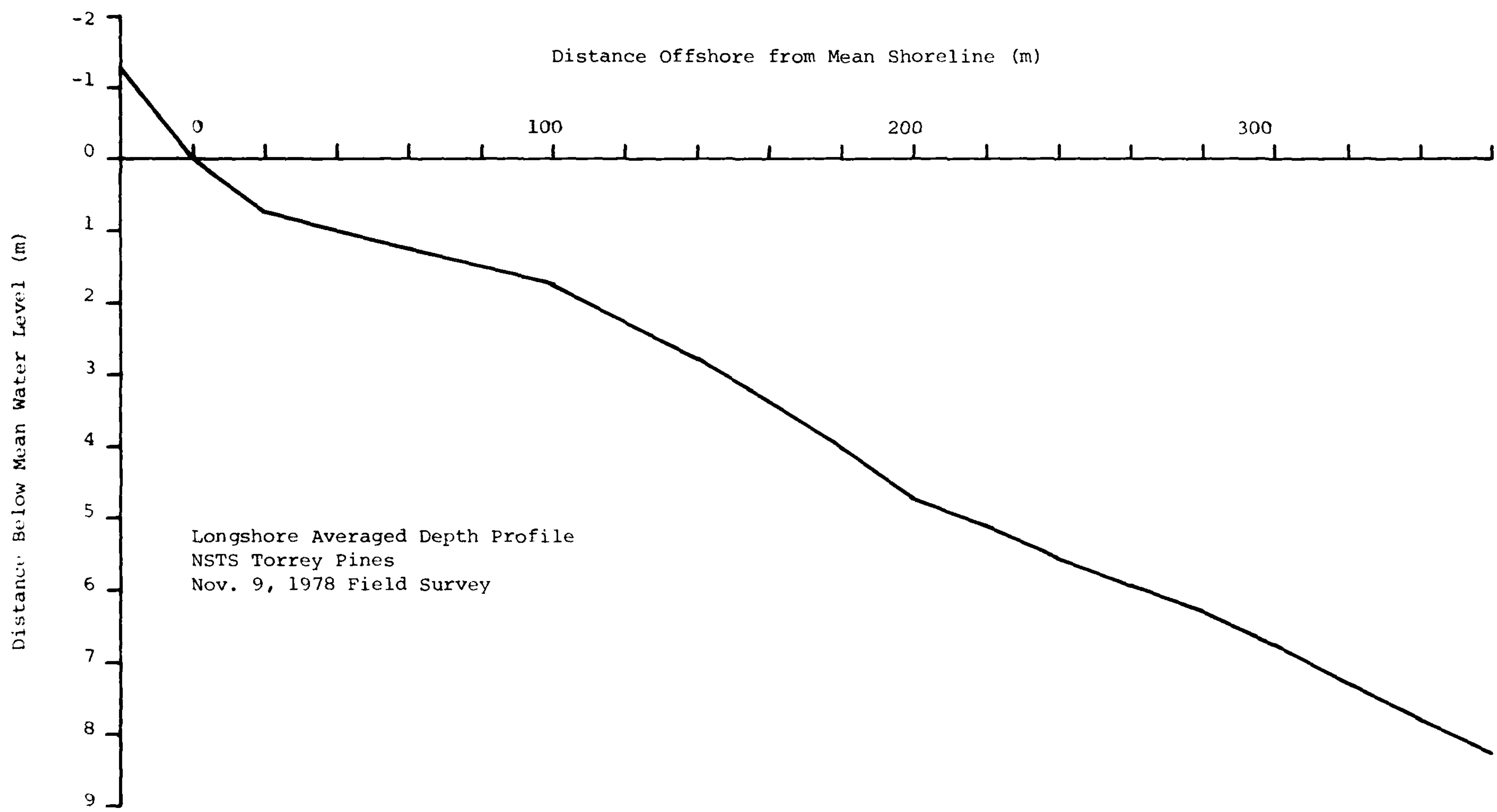


Figure 4-19 Longshore Average Depth Profile, Torrey Pines, November 9, 1978.

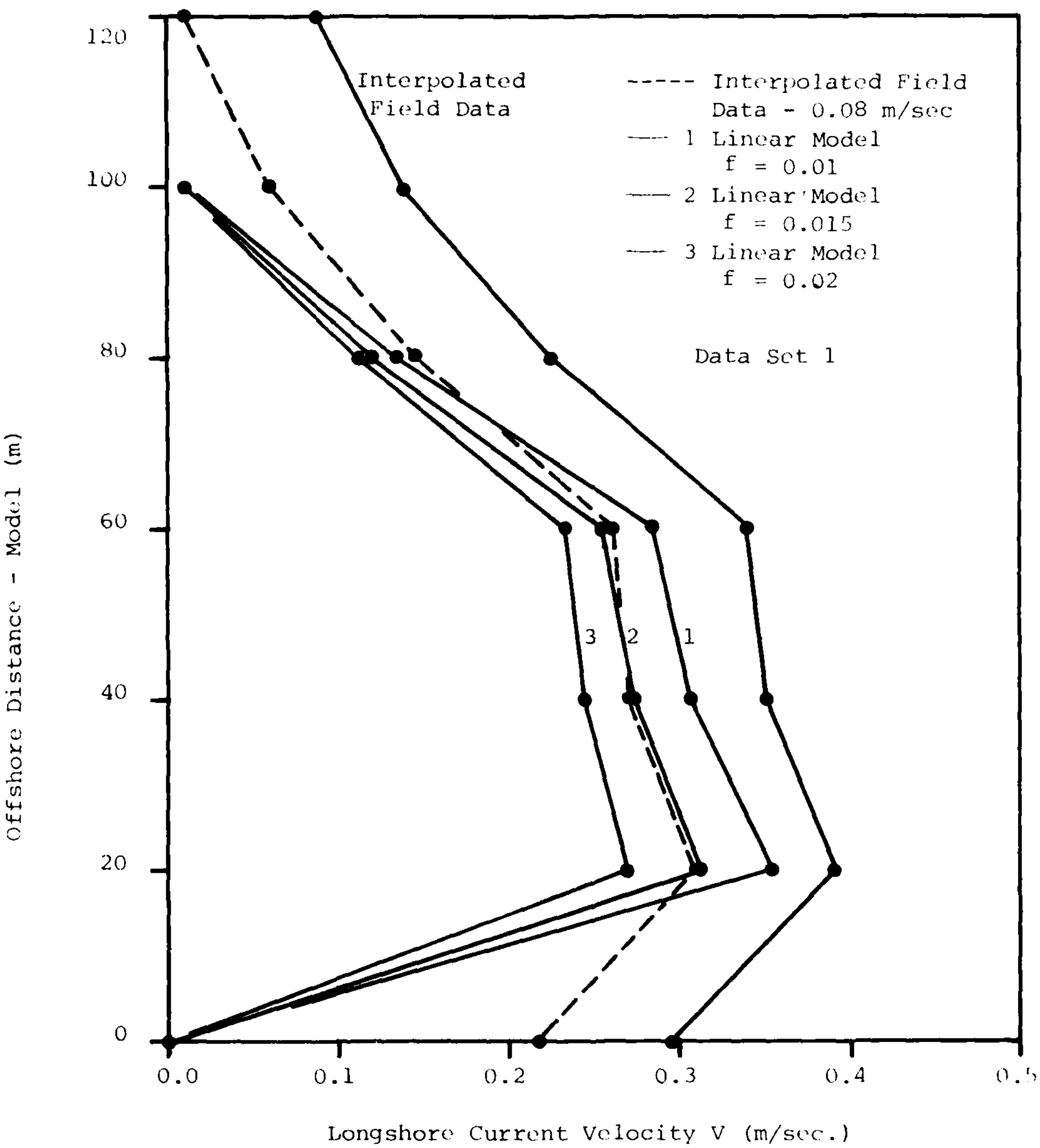


Figure 4-11 Variation of Longshore Current with Friction Factor in the Linear Model.

Results for $f = 0.015$ are shown in Figure 4-12. It was found that the inclusion of mixing satisfactorily extended the velocity profile in the offshore direction, but in both cases, including mixing, the current magnitudes in the surf zone were underpredicted. The model was therefore retested using a smaller value for the friction coefficient, $f = 0.01$. Results are shown in Figure 4-13. The smaller value of f is seen to correct for the underprediction of longshore current. Coefficient values for the nonlinear model were chosed based on the second set of results,

$$f = 0.01$$

$$N = 0.0025$$

$$\varepsilon_y = 0.25 \quad .$$

## 2.3 Response of Both Models Using Data Set 2

The linear and nonlinear models were run using Data Set 2 and the calibrated coefficients obtained above. Results for the linear model are shown in Figure 4-14. Nonlinear model results were similar to the linear model results. Both models were seen to overpredict the maximum longshore current in comparison to the averaged field data, and to underpredict the offshore extent of the longshore current. It is likely that a better fit to the field data could be obtained by artificially increasing the lateral mixing in the nonlinear model. However, the field data represents the average of a complex flow pattern, where the effect of mixing in the averaged data is induced by large scale phenomenon not likely to be found in the steady current fields induced by a unidirectional wave field. Since it is likely that the magnitude of artificial mixing would vary greatly as a function of

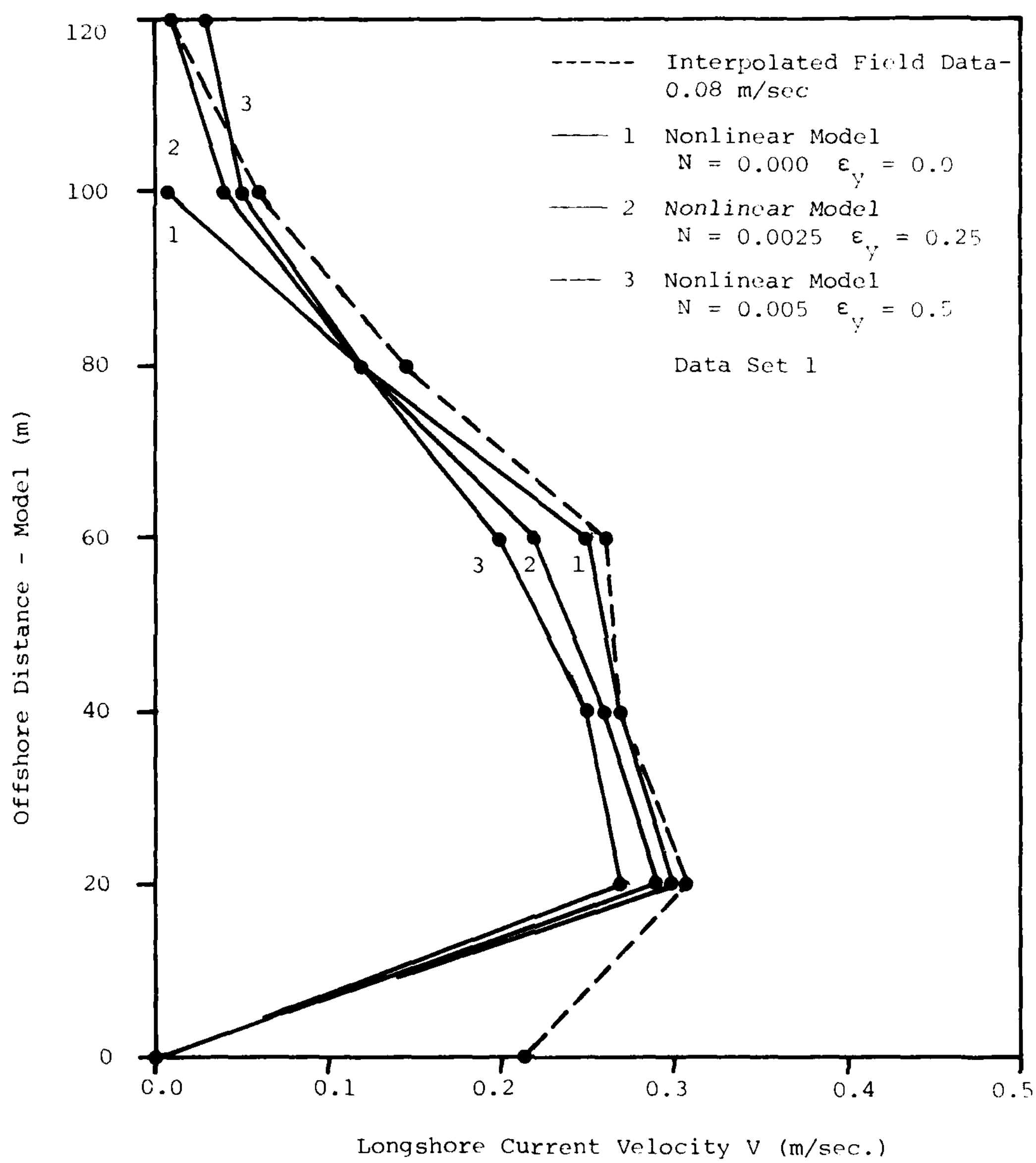


Figure 4-12 Variation of Longshore Current with Lateral Mixing in the Nonlinear Model. f = 0.015

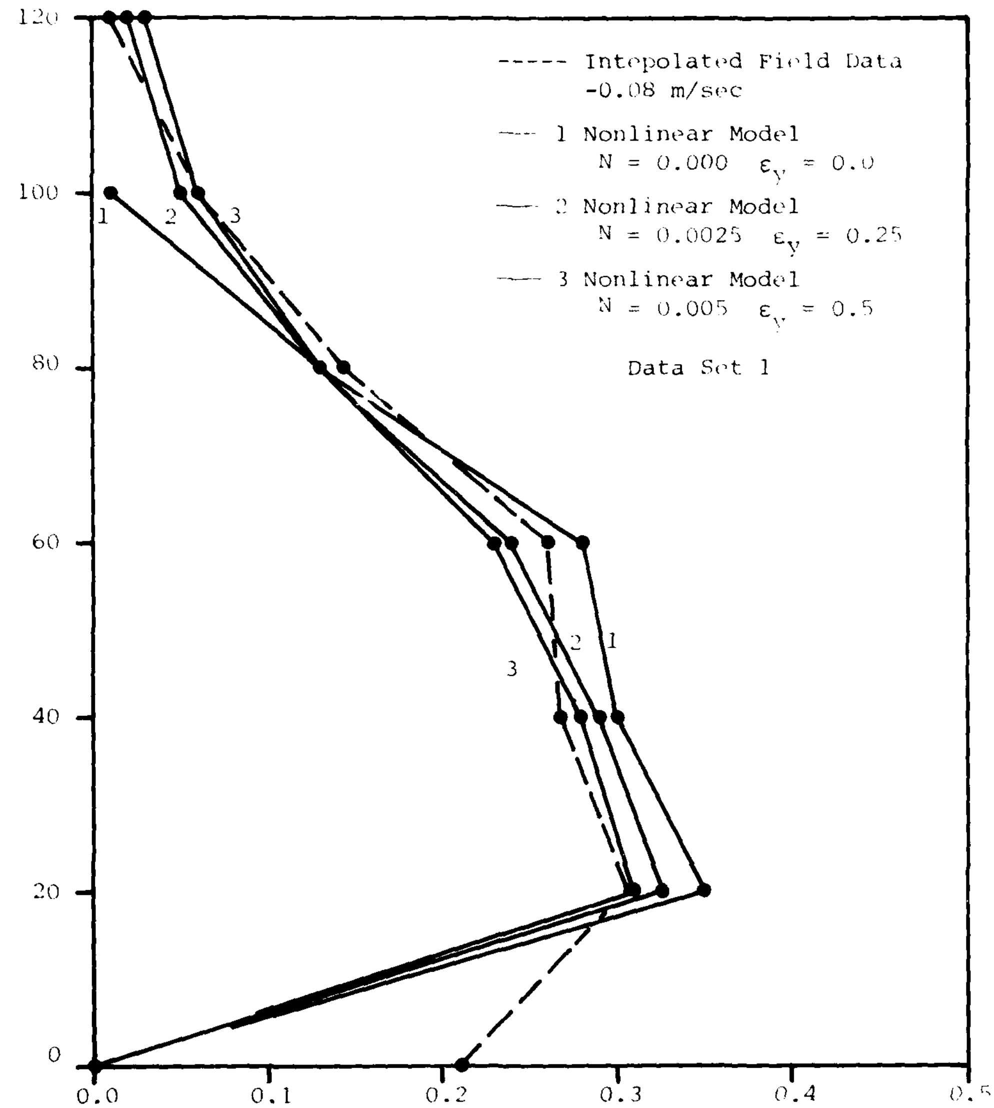


Figure 4-12 Variation of Longshore Current with Lateral Mixing in the Nonlinear Model.
f = 0.010

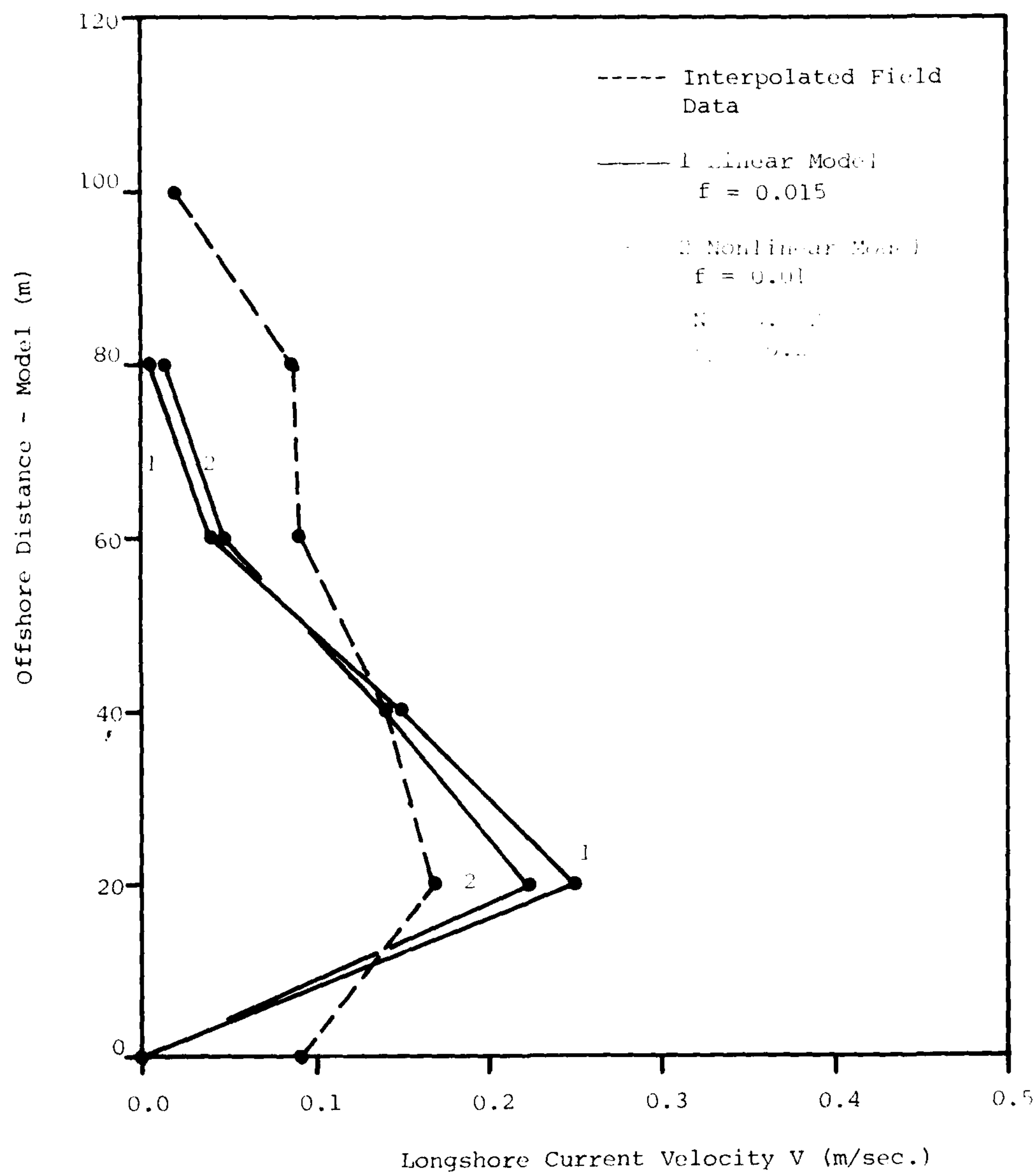


Figure 4-14 Longshore Current in the Linear and Nonlinear Models. Data Set 2

wave directionality and spatial complexity, it would be unjustified to alter the parameters of the model to fit a single case. It may become possible at some future date to estimate mixing parameters based on the characteristics of the random wave field.

A plot of the velocity vectors for data set 2 obtained using the calibrated model and the November 18 bathymetry is shown in Figure 4-15. As in the November 10 case, the circulation pattern is seen to be sensitive to the bottom variations. This result is probably due to the low values obtained for the friction coefficient f.

## 3. DISCUSSION OF THE CALIBRATED COEFFICIENTS

The value of the friction factor f obtained in this study differs significantly from the value used in previous work and retained by Allender et al. (1981). Based on a bottom shear stress relation given by Eqs. (2.27-2.28), Birkemeier and Dalrymple (1976) chose a value of $C_f = 0.01$, which corresponds to a choice of $f = 0.08$. This value of f is carried over into the results discussed in the next chapter. However, model calibration has indicated that the value of f is more of the order 0.01-0.02, with values of 0.015 and 0.01 chosen for the linear and nonlinear models respectively. It is felt that this alteration in choice of the friction factor requires some discussion.

Many formulae exist to calculate the bottom friction factor under waves, the most successful being those of Jonsson (1966) and Kajiura (1968). Writing Kajiura's formula in a form given by Dalrymple and Lozano (1978), we obtain

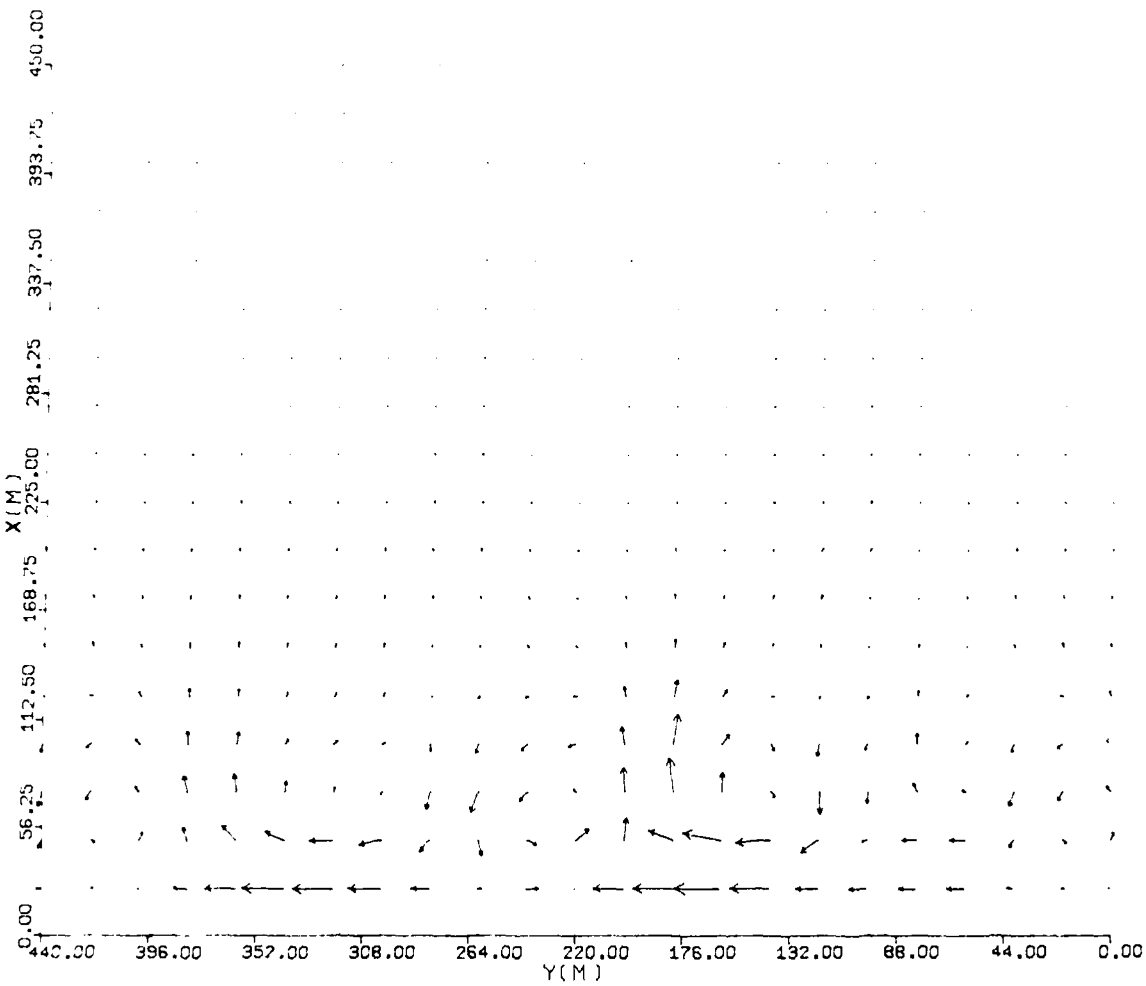


Figure 4-15. Currents Induced on Nov. 18, 1978 Bathymetry Using Data Set 2: Nonlinear Model.

$$C_f = \frac{f}{8} = 1.41 \left\{\frac{4\pi d}{T(gh_b\kappa^2)^{1/2}}\right\}^{2/3}$$

where d is the median sand grain dimeter and $\kappa$ is the breaking index. The value of f at the breaker line represents a reasonable choice for an average value over the surf zone region. For Torrey Pines Beach, d is approximately given by

$$d \sim d_{50} = 0.27 \text{ mm}$$

For the field data used, $h_b$ is taken as approximately 1.5 m. This yields a value of

$$C_f = .0025 \text{ or } f = 0.02$$

The values of f obtained during calibration are thus of the correct order of magnitude for flows over a planar bed with no ripples. However, the real physical bottom being studied should exhibit a higher roughness, with length scales based on ripple geometry rather than the sand grain diameter, indicating that the initially chosen value of $C_f = 0.01$ is probably more correct on physical grounds.

In this regard, we note the questionable practice of using distinctly bi-directional wave data to generate monochromatic input wave conditions for calibration purposes. The calibration obtained here possible constitutes a valid site specific calibration for the Torrey Pines beach, since it was found to be possible to predict net longshore flows resulting from wave fields with several components. In a practical sense, few data sets exist which are strictly useful for calibration purposes.

The values of the offshore mixing coefficient N chosen in this study are approximately one order of magnitude smaller than the corresponding value suggested by Bowen and Inman (1974), who investigated a group of dye dispersion studies performed by various investigators. Some indication that a larger value of N may be desirable is given by Figure (4-9): however, the validity of the field bathymetry is suspect in this case. It should be noted that the model exhibits a certain degree of numerical diffusion when large grid spacings are used, indicating that the value of N chosen should be less than the corresponding physically realistic value in any case.

## Chapter V

## EXAMPLES OF NUMERICAL RESULTS USING THE NEARSHORE CIRCULATION MODELS

### 1. INTRODUCTION

Various results of calculations using the linear and nonlinear models have been described in detail in Birkemeier and Dalrymple (1976) and Ebersole and Dalrymple (1979). Results pertaining to the questions of model stability and convergence have been mentioned in the previous chapters, with special attention to the seiching mode of oscillation generated at model start-up. In this chapter, results of model calculations in specific situations will be discussed, with emphasis on comparison to analytic models, and to bottom topographies which reproduce earlier efforts.

In addition to the general facilities for user-defined input, each of the models described in the two previous studies contained specialized facilities for the purpose of illustrating specific situations not covered by the basic model structures. These special cases are discussed here for completeness, although in most cases the final model versions may not retain the corresponding capability.

### 2. SPECIFIC APPLICATIONS OF THE LINEAR AND NONLINEAR MODELS

In this section, we review results presented by Birkemeier and Dalrymple (1976) and Ebersole and Dalrymple (1979). In addition, we present results for an additional form of generalized topography.

## 2.1 Plane Beach Applications

Historically, the first application of the averaged momentum flux formulation presented in Chapter II to nearshore dynamics was made in an attempt to explain the phenomenon of wave set-up and longshore wave-induced currents in the surf zone. In the simplest formulation, the equation lead to a linear longshore current profile as shown in Figure 2-2 (Longuet-Higgins, 1970a). The addition of a turbulent stress term representing the effect of lateral mixing leads to a smoothed profile which is more representative of observed current distributions, as discussed by Longuet-Higgins (1970b). In the development in Chapter II, a lateral mixing model in the x and y directions was outlined based on the model used by Longuet-Higgins. Here, we review results calculated both with and without the lateral mixing effects.

Birkemeier and Dalrymple (1976) presented results for set-up resulting from normally incident waves on a plane slope, as shown in Figure 5-1 in comparison with the latoratory measurements of Bowen _et al_. (1968). Since, for this case, no currents are generated, the distinction between the linear and nonlinear models are inapplicable. The model is seen to accurately reproduce aspects of the solution based on linear incident waves, including the sharp drop in the mean water level just outside of the breaker line. It is noted that this drop can be eliminated, and a more realistic solution obtained, by the use of radiation stress terms derived from cnoidal wave theory (James 1974)). This possible refinement has not been included in the models.

Birkemeier and Dalrymple also investigated the dynamic set-up resulting from a time varying incident wave height given by

$$H_o = H_s + A \sin \left(2\pi n \frac{\Delta t}{T_g}\right) \qquad (5.1)$$

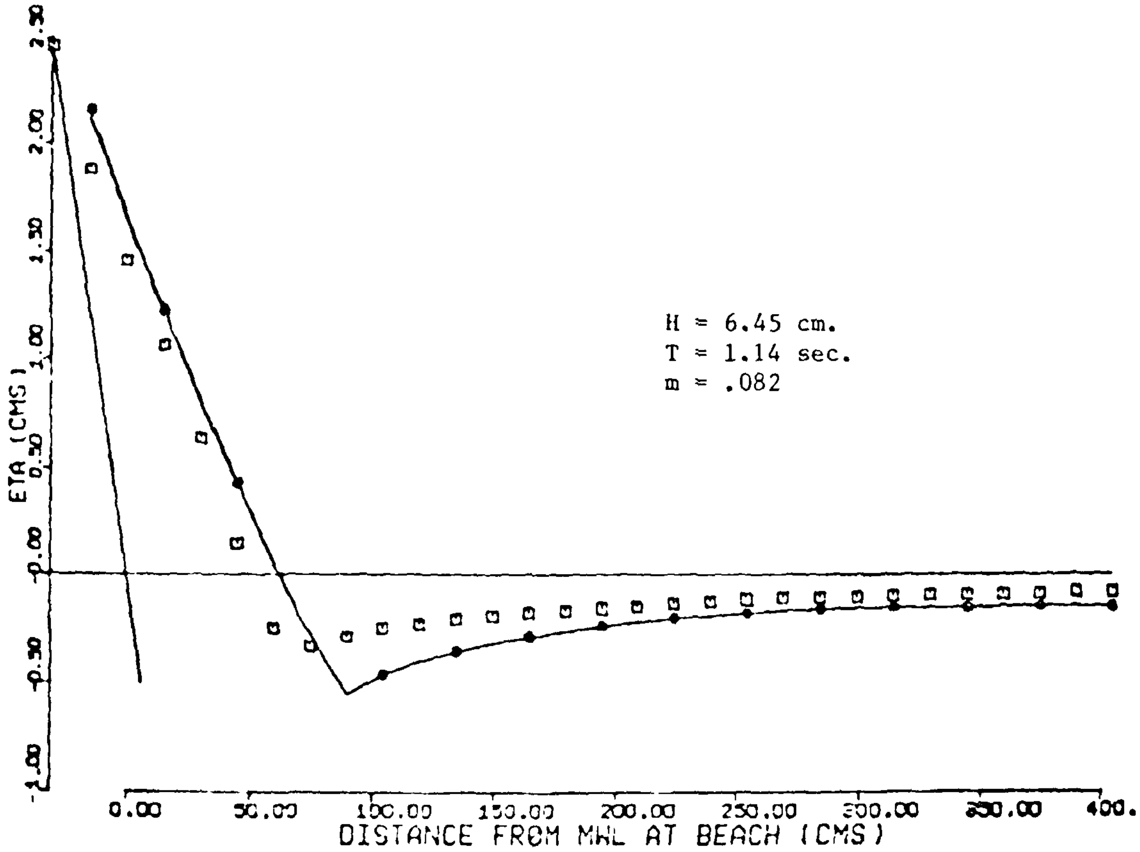


Figure 5-1. Set-up on a Plane Beach

□ - Bowen et. al. (1968) experiment
. - Linear Model

where

$H_s$ = starting wave height

A = amplitude of variation

n = iteration index

$T_g$ = group period.

Results for dynamic set-up in comparison to incident wave height are shown in Figure 5-2. As an example of the seiching response of the model, a case was also run where the group period corresponded to the seiche period of the model as given by Eq. (3.5). Figure 5-3 indicates the resulting instability in the set-up which represents the growth of the seiche.

In the previous example, a model seiche appeared as a forced response to the applied wave-induced stress. Figure 5-4 indicates a more typical result of a seiching response to the transient model start-up. In this case, the oscillation is a free motion which gradually dies away due to the effect of bottom friction (as well as numerical dispersion). As mentioned in section 3.4, this type of response can be reduced by a gradual build-up of the incident wave height.

Results for a longshore current on a plane beach are shown in Figure 5-5, for the linear model and no lateral mixing, and in Figure 5-6, for the nonlinear model with mixing. The two solutions clearly represent the behavior predicted by the theoretical solutions, with the exception that the sharp decay in velocity at the breaker line predicted by the solution with no mixing is spread over several grid spaces in the linear model due to the use of finite grid squares. This effect can be reduced by the use of a finer grid spacing.

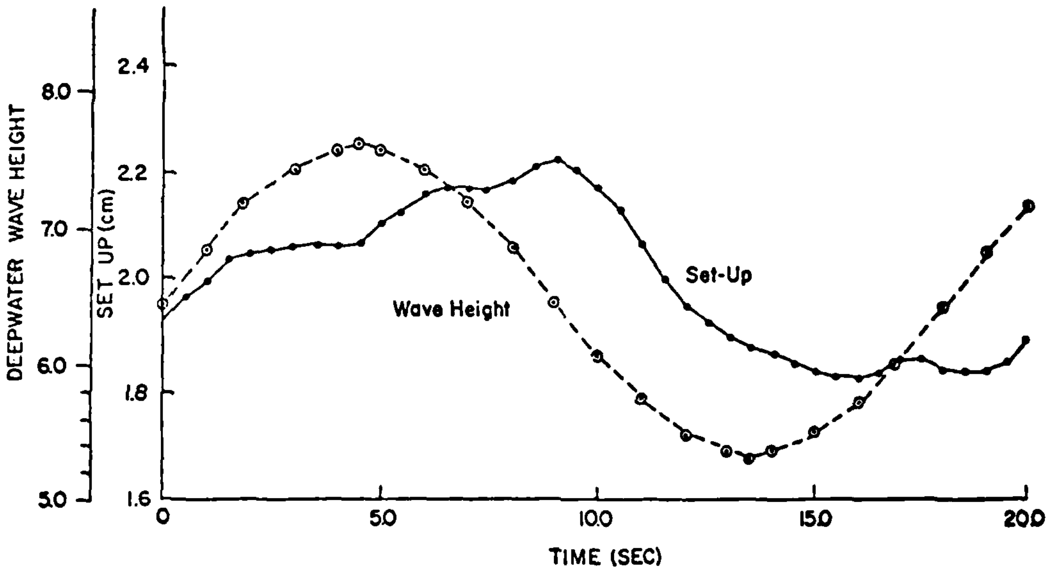


Figure 5-2. Set-up at Shoreline due to a Wave Group with 18 second period. Linear Model

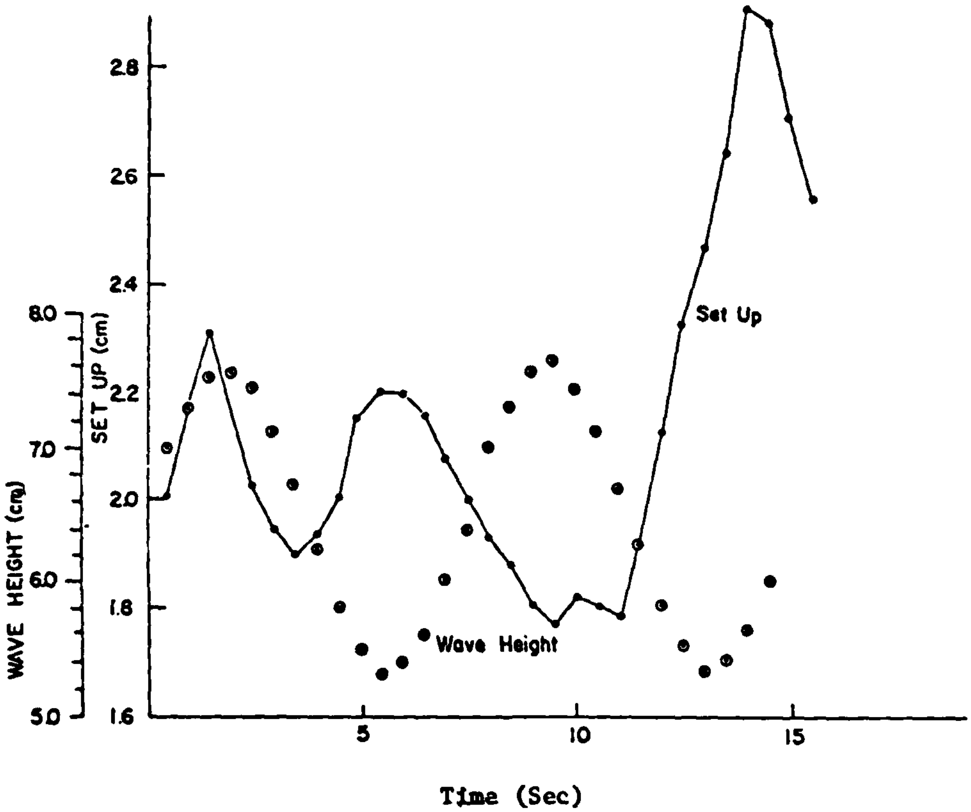


Figure 5-3. Resonance of Wave Channel Due to Forcing at Seiche Period

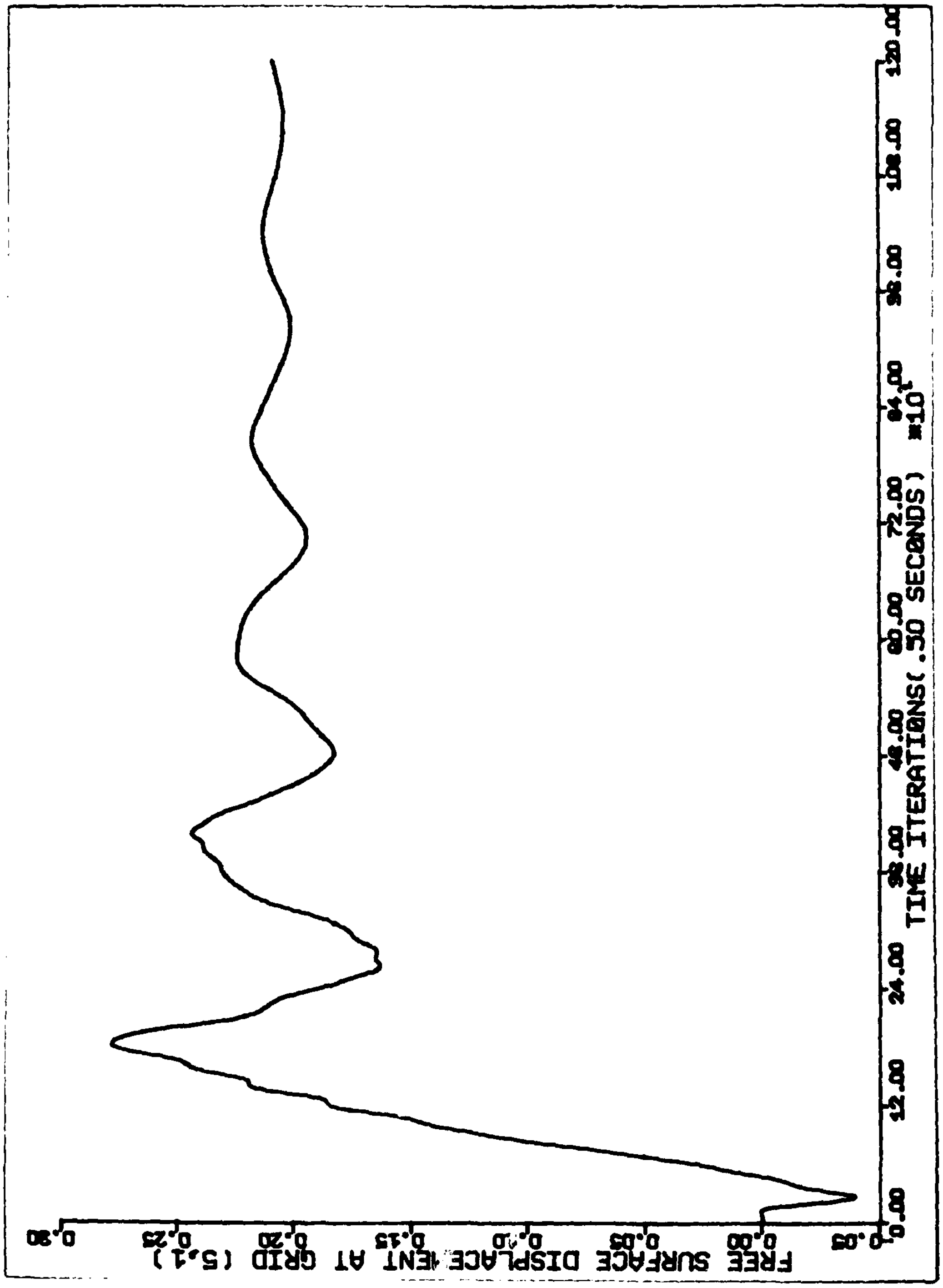


Figure 5-4. Inshore Mean Free Surface Displacement Versus Time for the Non-Linear Model Application to a Plane Beach

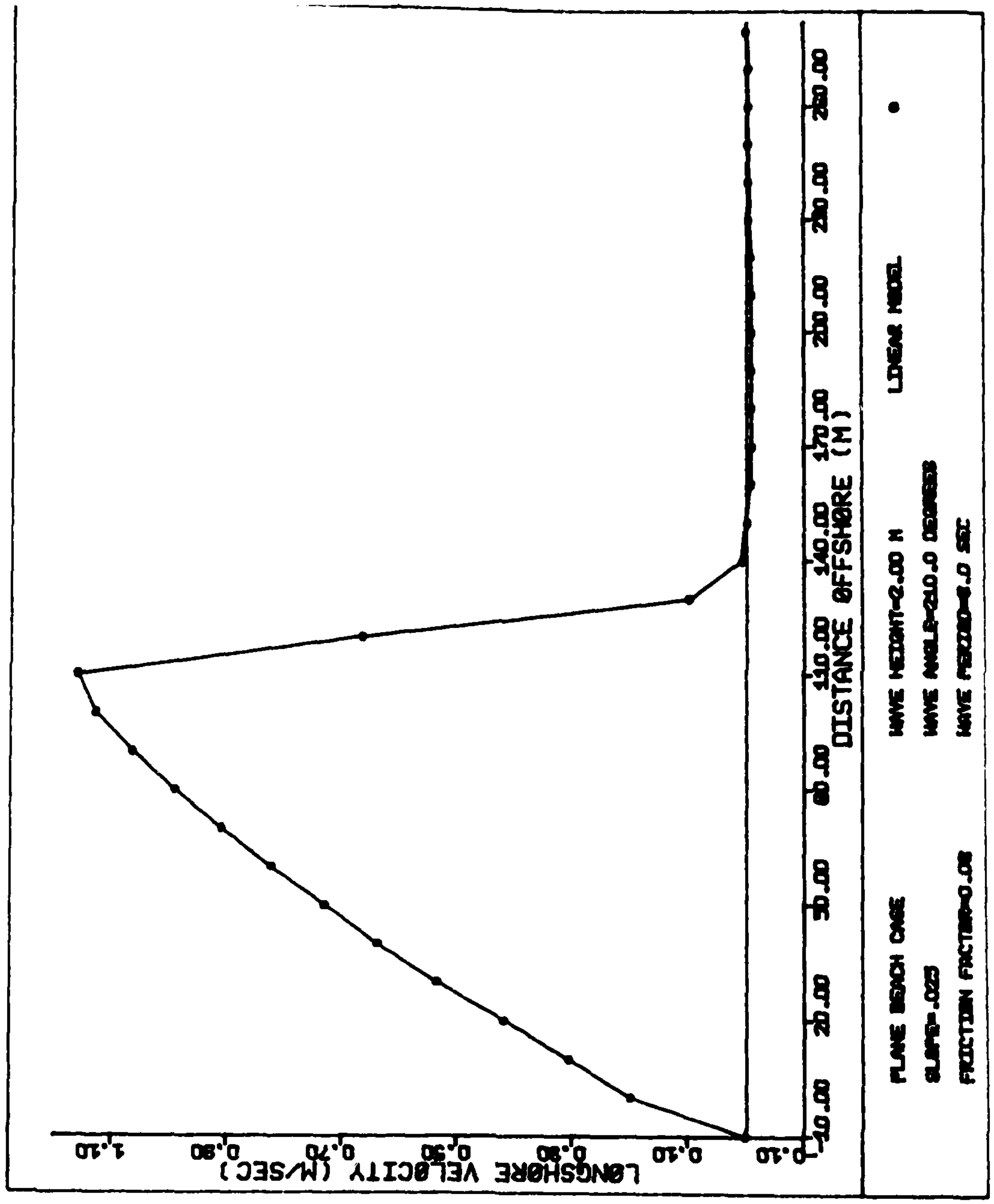


Figure 5-5. Longshore Current Profile for Plane Beach
Linear Model

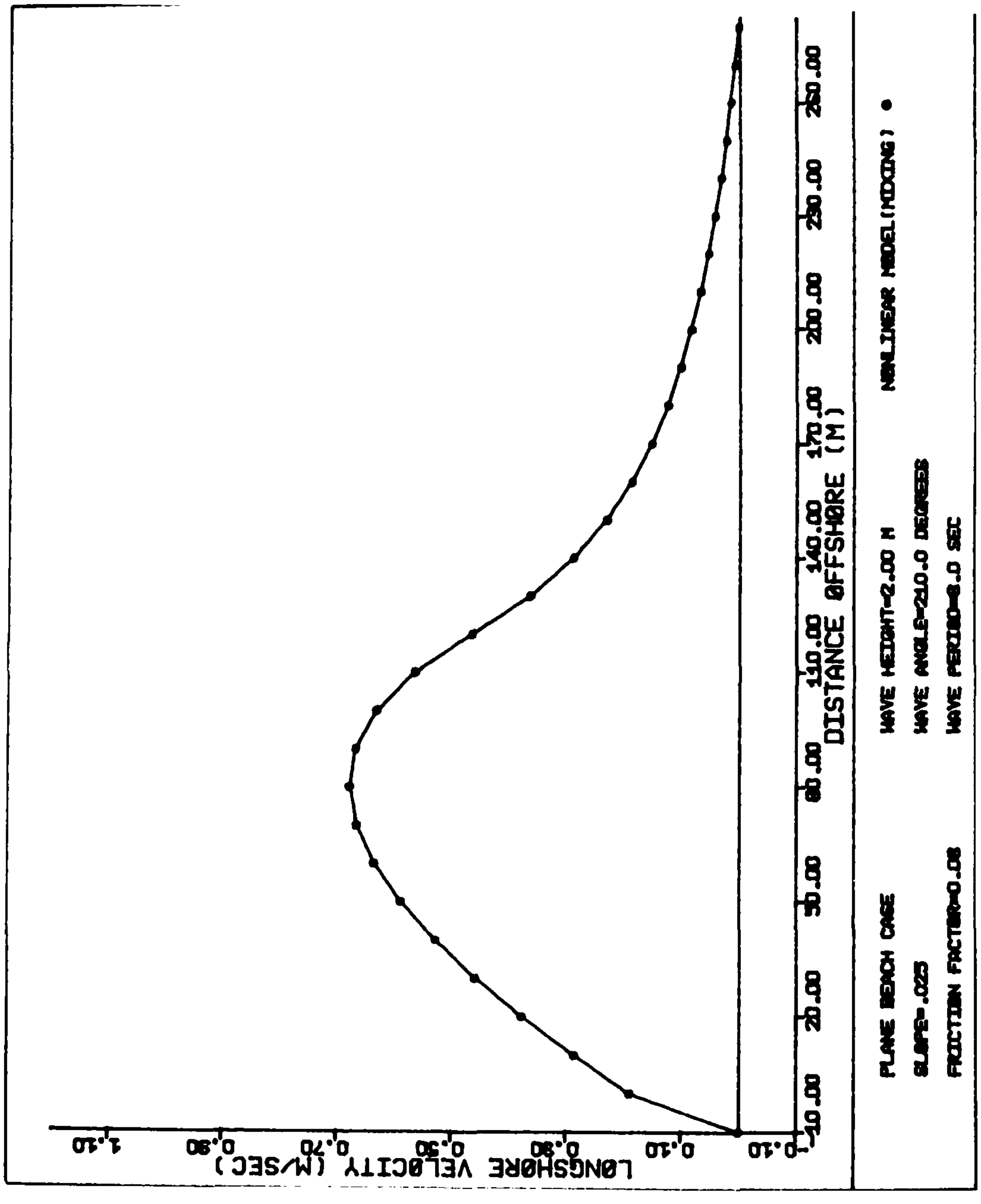


Figure 5-6. Longshore Current Profile for Plane Beach including Lateral Mixing Nonlinear Model

The applications discussed here indicate that the model accurately reproduces the available analytic solutions for simplified physical situations.

2.2 Barred Profile Applications

In nature, beaches are often fronted by continuous or fragmented longshore bars. In order to model this situation, the nonlinear model was run using a barred profile (Figure 5-7) for the same wave conditions used to generate the plane beach results described above. For this case, the model was run neglecting the effect of lateral mixing, and including the effect; results are shown in Figures 5-8 and 5-9 respectively. The solution without lateral mixing demonstrates the major discrepancy found between theoretical solution and field data for the special case. As the model wave passes the crest of the offshore bar, it stops breaking since it responds instantaneously to the local bottom. In the absence of lateral mixing, no currents are generated in the trough between shore and bar. This result is in disagreement with field observation as shown recently by Allender et al. (1981) as well as other investigators. The inclusion of lateral mixing effects partially alleviates this discrepancy.

Two factors may contribute to the observations that currents in natural surf zones tend to be strongest in the trough between bar and shore. First, fragmented bars tend naturally to induce two dimensional flow patterns characterized by rip currents flowing seaward at the gaps in the bar system. These currents are driven by longshore variations in the set-up resulting from interaction between the incident waves and the non-uniform topography.

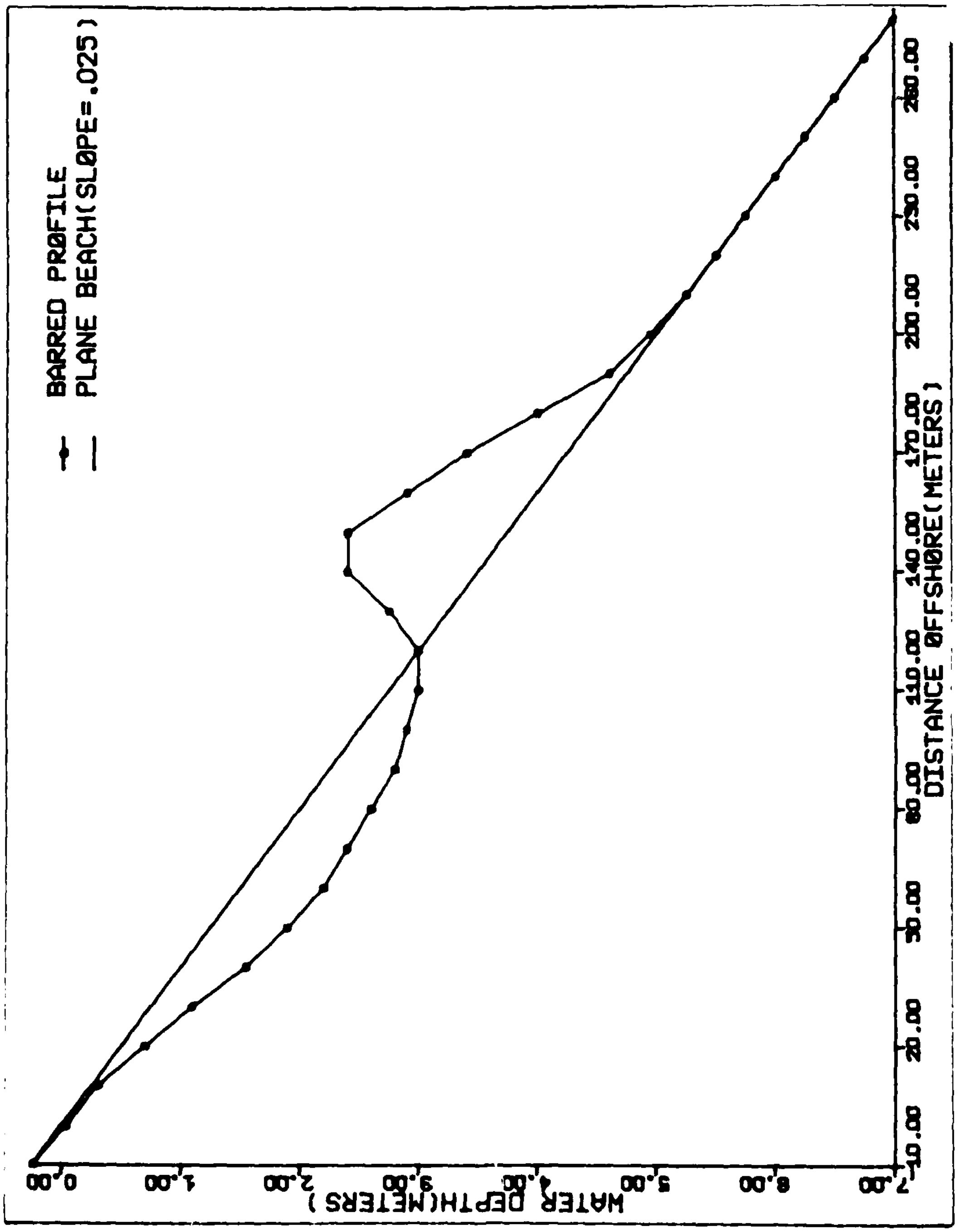


Figure 5-7. Barred Profile used for Results in Figures 5-8, 5-9.

AD-A118 518 DELAWARE UNIV NEWARK DEPT OF CIVIL ENGINEERING F/G 8/3
NUMERICAL MODELING OF THE NEARSHORE REGION.(U)
JUN 82 J T KIRBY, R A DALRYMPLE N00014-81-K-0297
UNCLASSIFIED CE-82-24 NL

2 OF 2
AD A
118518

END
DATE
FILMED
10-82
DTIC

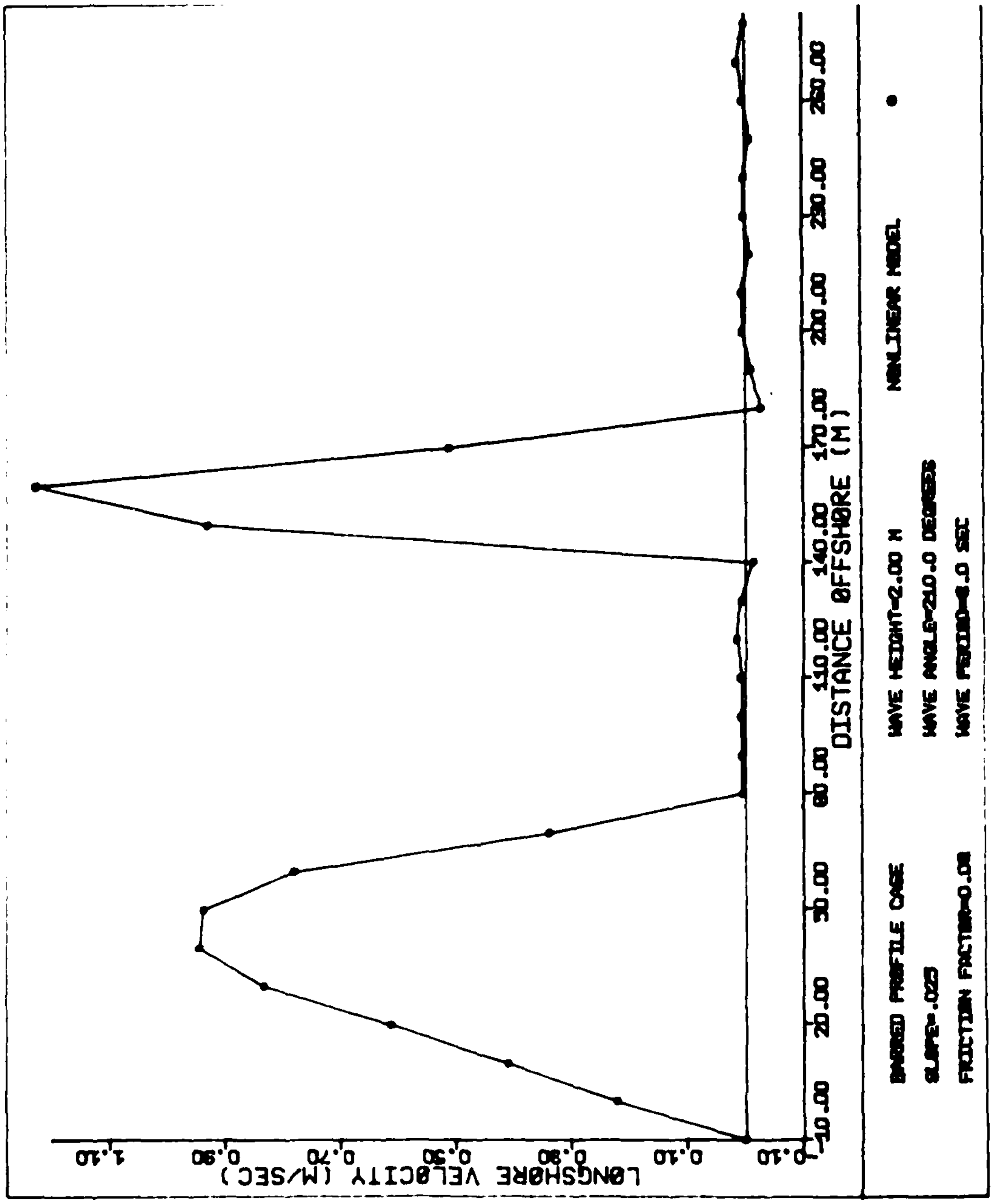


Figure 5-8. Longshore Current for Barred Profile
Nonlinear Model, No Lateral Mixing

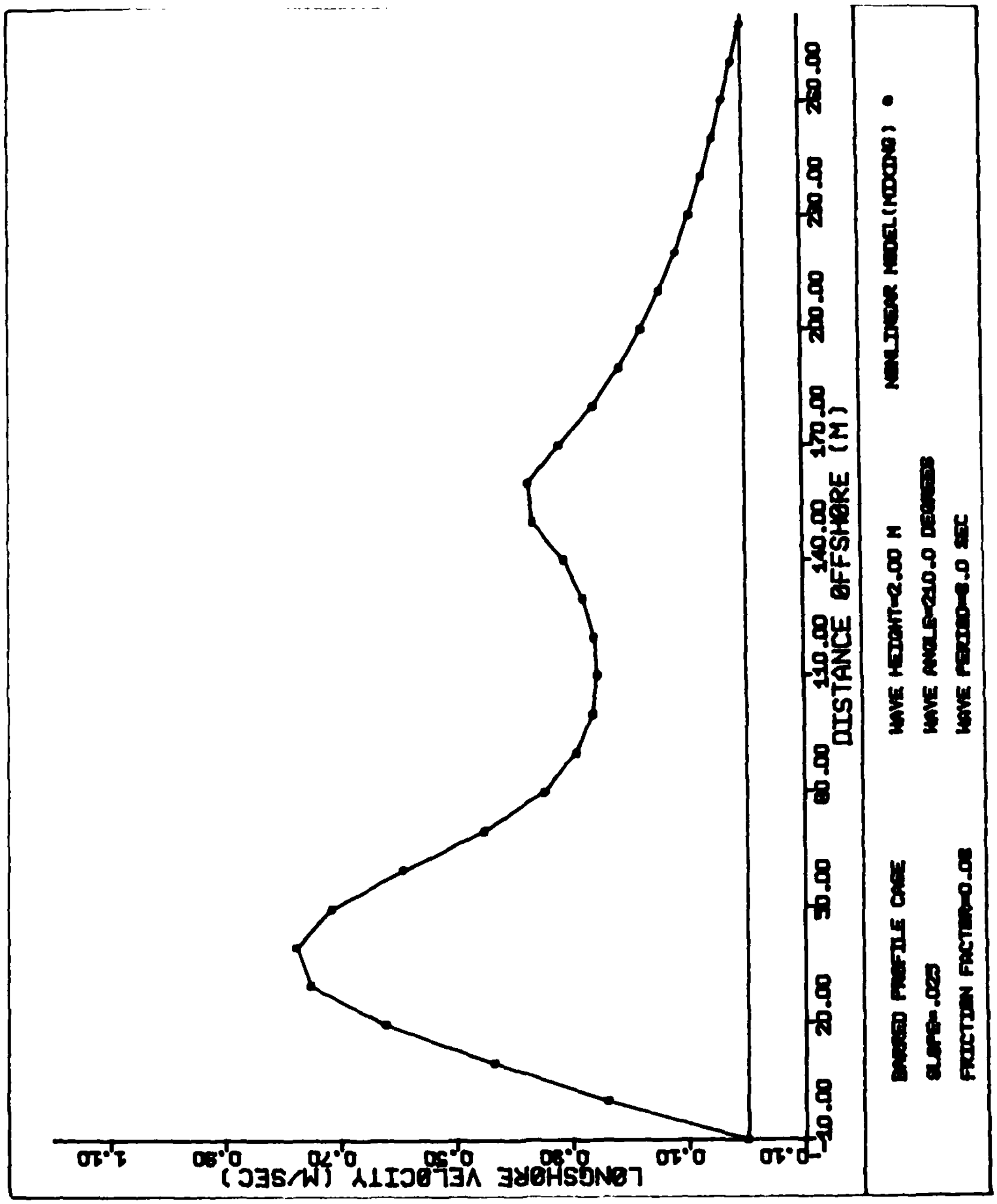


Figure 5-9. Longshore Current for Barred Profile
Nonlinear Model, Lateral Mixing Included

In these situations, currents flowing along the beach are driven by gradients in the mean water surface; the flow is naturally higher in the trough, where hydraulic resistance is lower. This mechanism for rip current maintenance has been discussed by Dalrymple (1978). It is possible that this mechanism will always bias the currents observed on real beaches.

The second possibility perhaps lies in the standard treatment of surf zone wave height as a function only of the local depth. The process of wave breaking initiates a turbulent flow pattern which is certain to have some time dependence, at least in its decay. A model for spilling breakers including this effect has been discussed by Longuet-Higgins and Turner (1974). It is possible, then, that an accurate picture of currents on a barred profile would require the inclusion of a continuation of wave energy decay in a time dependent manner past the point where the wave stops shoaling. Wave energy decay models have been used successfully by Divoky, LeMehaute and Lin (1970) in a study of wave height decay in the surf zone, and by Miller and Barcilon (1978) in a study of rip currents. However, present models do not allow for the cessation of breaking, which is required if the process of wave breaking and reformation is to be successfully treated.

## 2.3 Applications to the Laboratory Wave Basin

In order to model currents in a laboratory wave basin, the linear model described here was modified to include no flow boundary conditions at the longshore boundaries. (This option is not included in the present model.) Model tests were conducted to numerically approximate the experimental set-up and analytic theory of Dalrymple et al. (1977). In the physical experiment, a plane beach was established at an angle of 15° to a flap-type wavemaker. Waves approached the beach over a flat bottom until they reached the front of the beach slope, where refraction effects began. Three cases were tested experimentally and theoretically; here, we restrict our attention to the case where the surf zone is bounded laterally by walls extending to infinity in the offshore direction. Experimentally determined streamlines are shown in Figure (5-10), in comparison to the analytic solution. In the numerical model, the physical situation was altered by extending impermeable walls in a direction normal to the beach; the waves, however, are allowed to propagate freely according to refraction governed by an infinite beach. The numerical model corresponded to the conditions used to develop the analytic solution. Velocity vectors calculated by the linear model are shown in Figure (5-11), in mirror image to the geometry in Figure (5-10). Longshore current velocities calculated by the linear model are compared to experimental values in Figure (5-12). The model is seen to underpredict currents in comparison to the analytic and experimental results.

## 2.4 Periodic Bottom Topography

In a study of rip currents caused by submerged on-offshore channels, Noda (1970) developed an equation for the depth which produces a channel oriented at an angle to the beach. The present models were tested using Noda's periodic bottom, given by

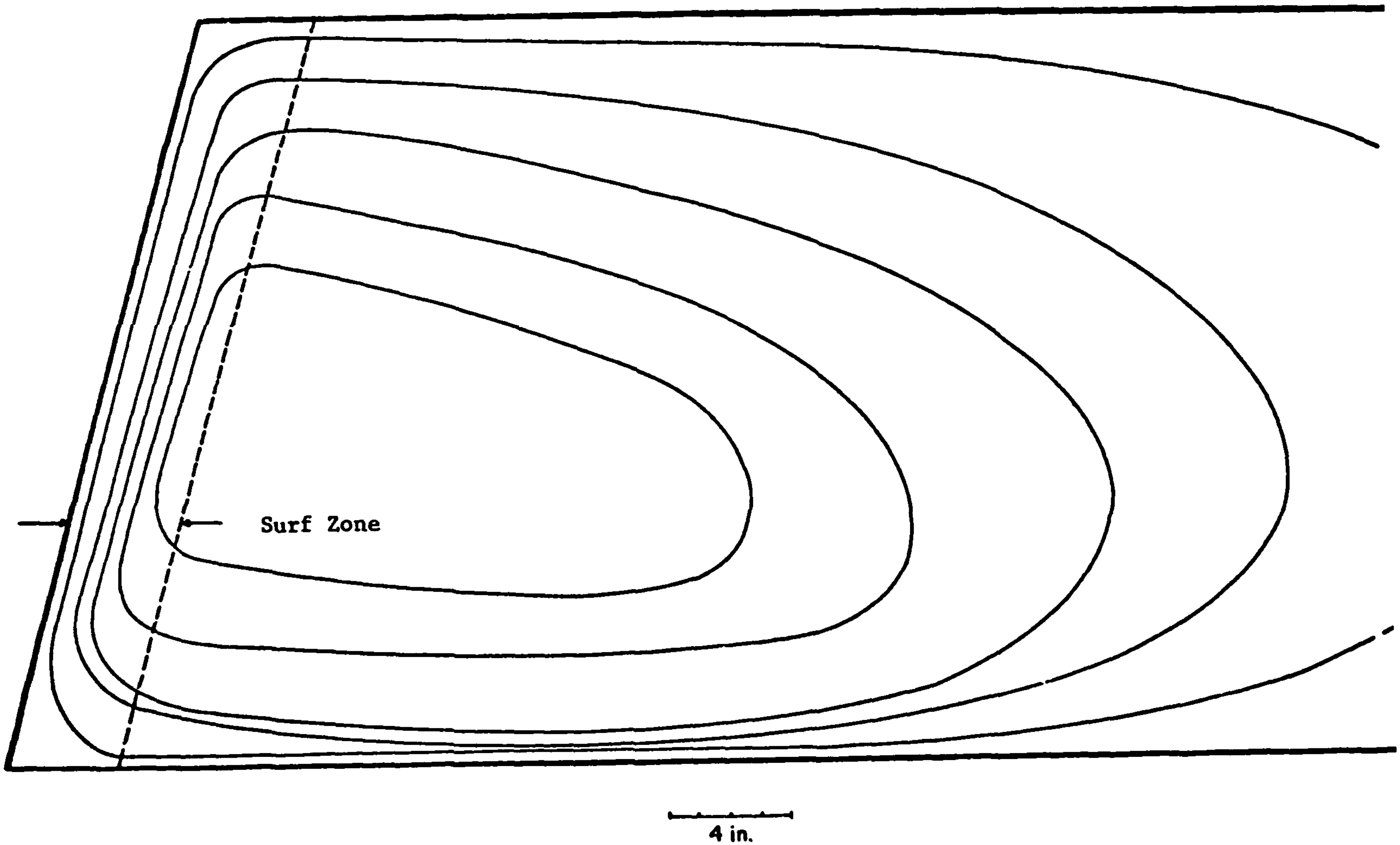


Figure 5-10. Experimental Strealines in the Wave Basin [From Dalrymple et al. (1977)].

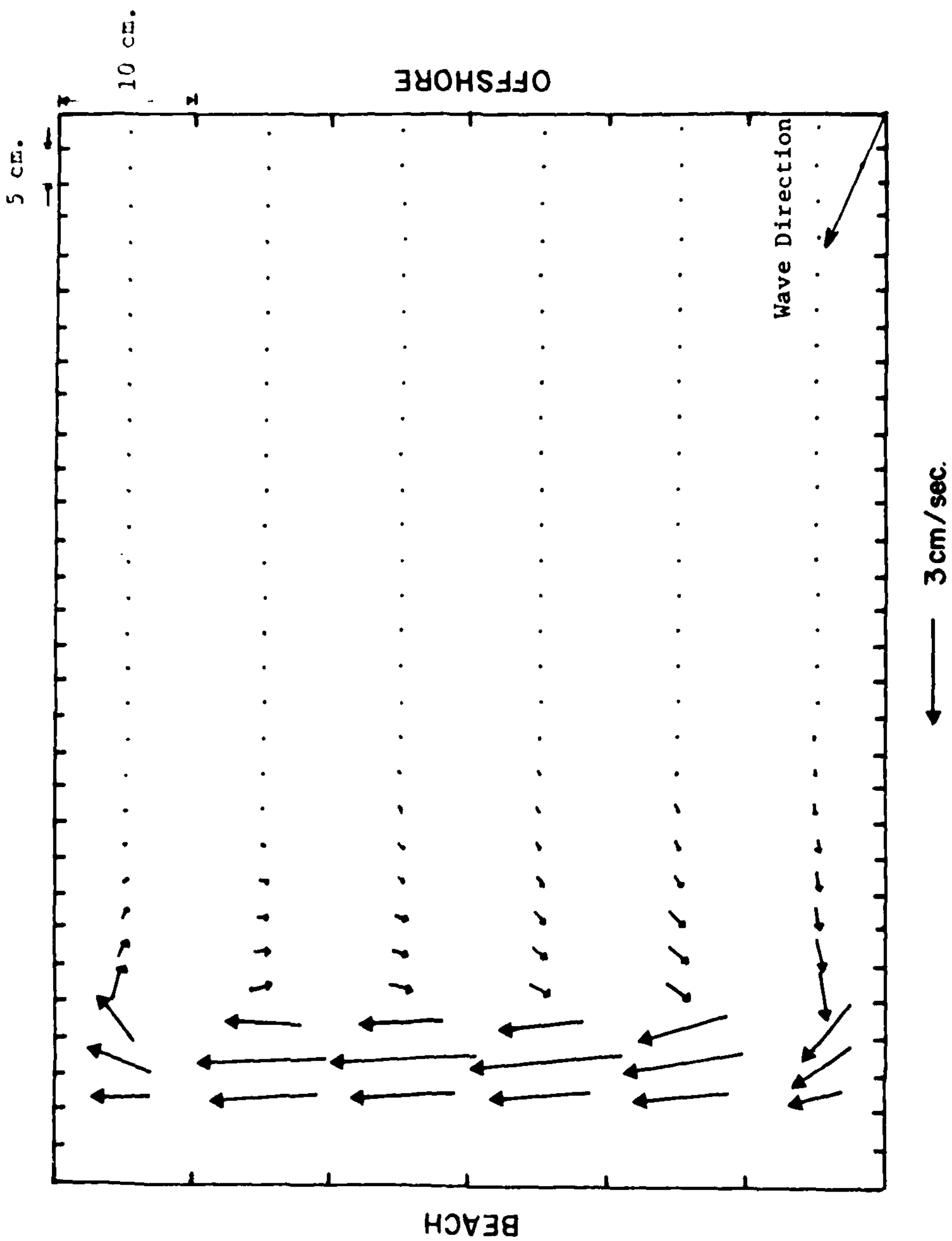


Figure 5-11. Calculated Velocity Vectors for Closed Basin Corresponding to Experimental Results of Figure 5-10

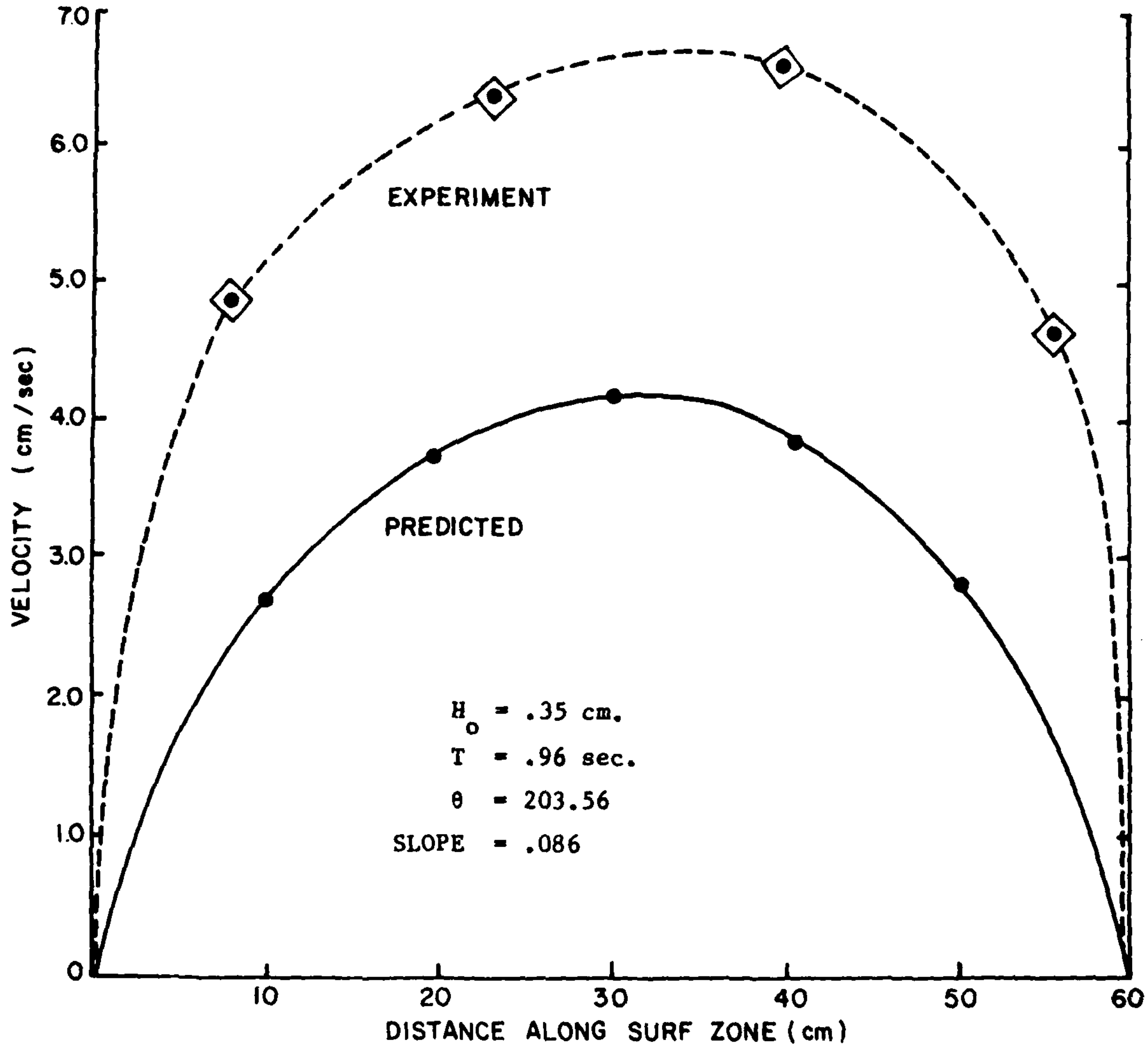


Figure 5-12. Predicted and Measured Longshore Velocities for the Closed Basin Test Case. Linear Model.

$$D_{i,j} = \begin{cases} -m(4 - i)\Delta x & i = 1,2,3,4 \\ m\Delta x\{1+A \exp[- 3(\frac{x}{20})^{1/3}]\sin^{10} \frac{\pi}{\lambda} (y-x \tan \beta)\} & i > 4 \end{cases}$$

where $x$, $y$ are coordinates of grid $(i,j)$

$m$ = average beach slope = 0.025

$\lambda$ = length of periodicity = 70 m

$A$ = amplitude of bottom variation = 20

$\beta$ = angle of rip channel to beach normal = 30°

The test contours are shown in Figure 5-13. The bottom topography was intended to model a field case studied by Sonu (1972). Current vectors calculated using the linear model are shown in Figure 5-14; current magnitude agree well with the field data reported in Noda et al. (1974), and are higher than the currents calculated in Noda et al.'s model, in which only 50% of the calculated current is used in determining the wave number due to numerical instability problems.

The Noda profile was also tested using the nonlinear model with lateral mixing (Figure 5-15). The effect of the extra terms modelled is to largely drop out the rip current clearly seen in the linear model results. Similar results have been obtained by Liu (1982), using a finite element approach, but the absence of a rip current under the given conditions is clearly at odds with the field data of Sonu (1972).

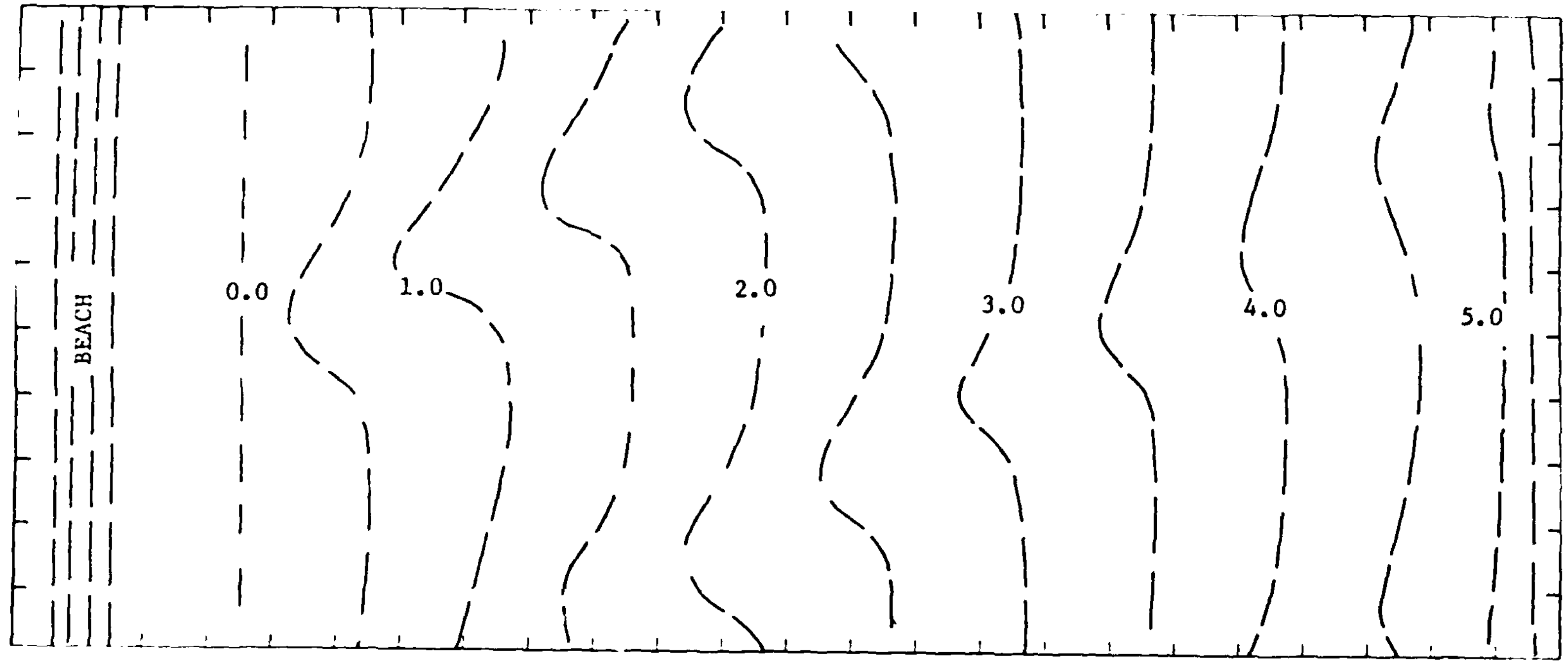


Figure 5-13. Depth Contours for the Periodic Bottom Due to Noda (1973).

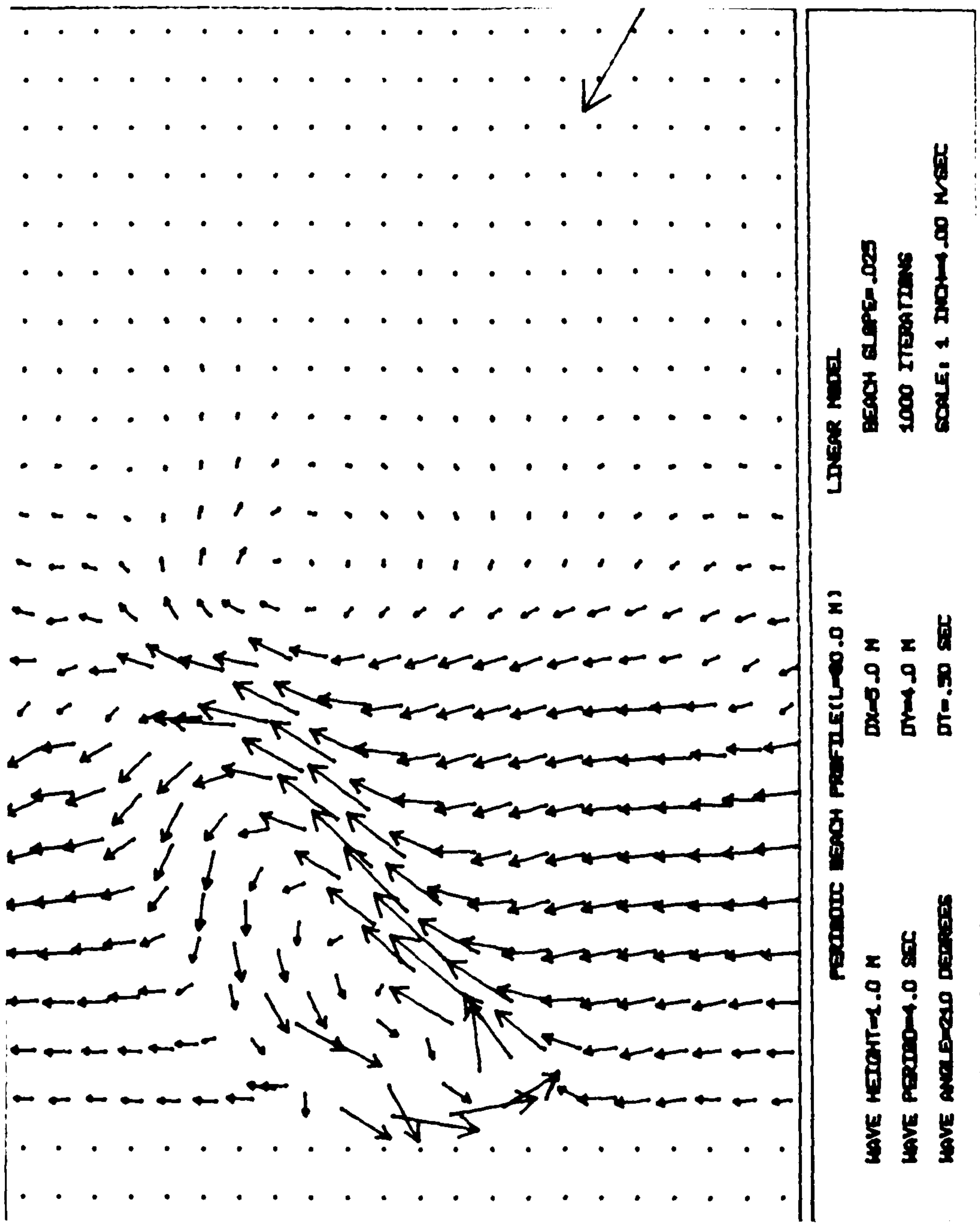


Figure 5-14. Current Vector Plot for Bottom Topography of Noda. Linear Model, No Lateral Mixing.

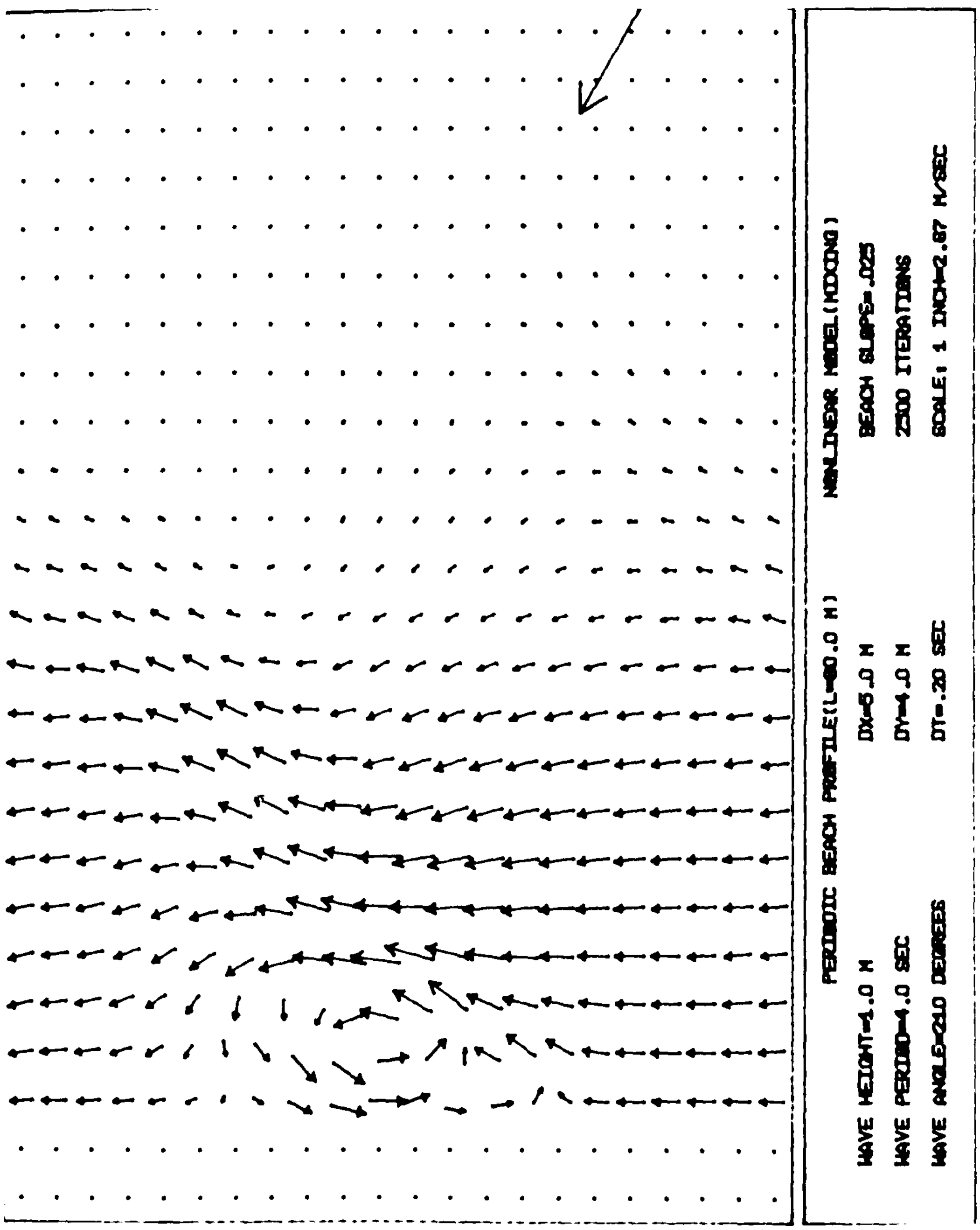


Figure 5-15. Current Vector Plot for Bottom Topography of Noda. Nonlinear Model, Lateral Mixing Included.

A second periodic topography has been investigated for the present study. It is well established that the presence of a nearly shore-normal channel deeper than the surrounding beach slope will tend to induce a rip current, with flow directed offshore in the channel. For the present case, a longshore-periodic perturbation consisting of a localized bulge, or relatively shallow region, has been added to an otherwise planar beach profile. The bottom is given by the relation

$$D_{i,j} = \begin{cases} -\, m\,(2 - i)\,\Delta x & i = 1 \\ m(i\Delta x)\left(1 - 0.9\cos^6\left\{\frac{j}{(N-1)}\,\pi\right\}\exp(-0.015\, i\Delta x)\right) & i > 1 \end{cases}$$

where

$m$ = average beach slope = 0.02

$i,j$ = grid coordinates

$(N-1)\Delta y$ = longshore periodicity

Results using both models are shown in Figures 5-16 and 5-17. The effect of the inclusion of convective acceleration terms in the nonlinear model is not apparent in the results, which may be a result of the counter-balancing effect of lateral mixing. The lateral mixing effect can be seen in the shoremost grid row. The overall effect modelled here can be explained most simply in terms of a longshore imbalance in the steady state set-up. As the bulge concentrates wave energy by refraction, a region of relatively high breaking waves is created. As water is pumped on shore by the gradient of the onshore radiation stress, a localized region of high set-up is created; this region in turn pumps the onshore-flowing water alongshore into the regions of low set-up. The waves over the region of the bulge then must continuously pump water onshore in an attempt to fill the surf zone up to the

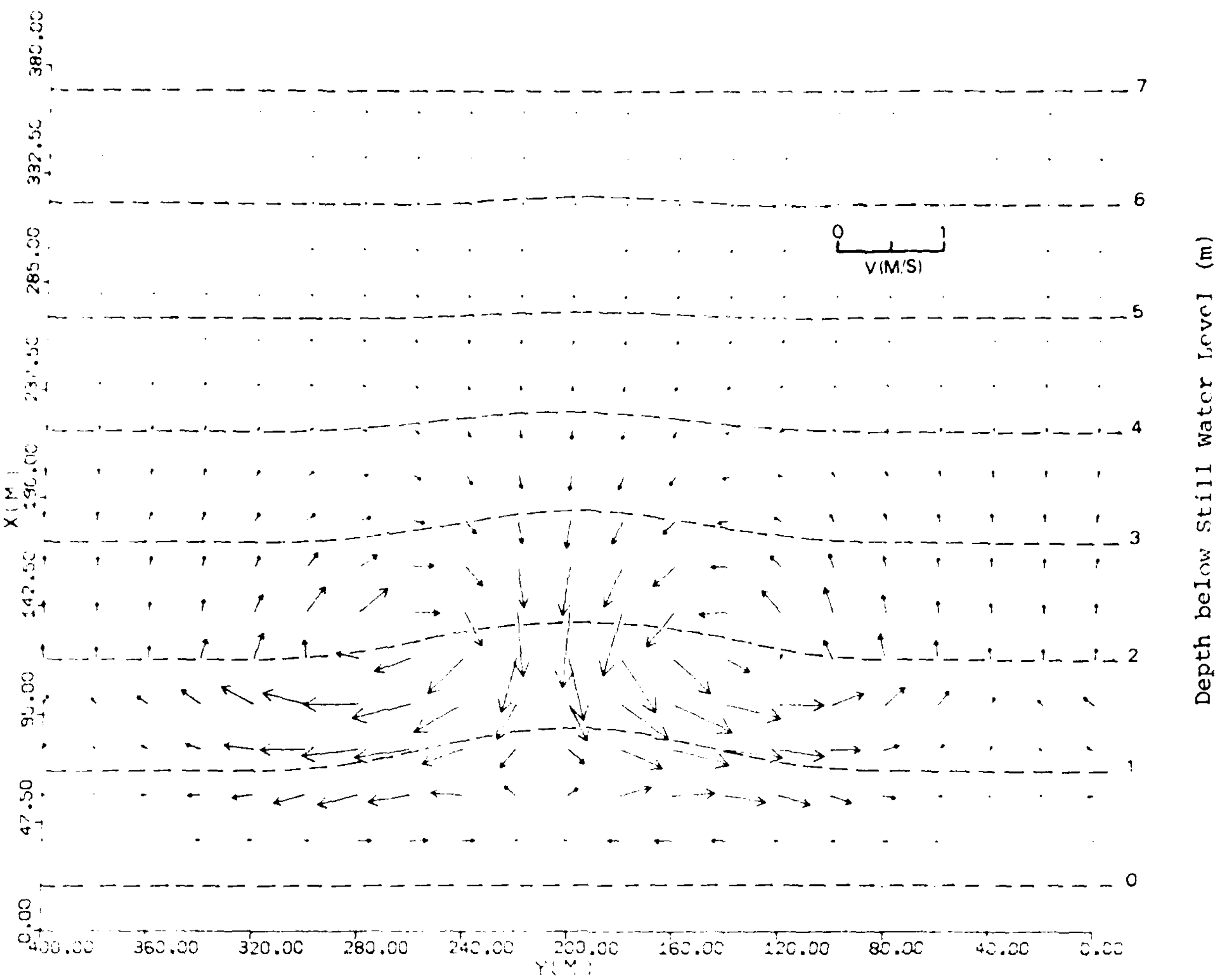


Figure 5-16. Currents Induced by Bulge on a Plane Beach Linear Model: $T = 10.0$ s, $H_o = 1.0$ m, $\theta_o = 180^{o}$.

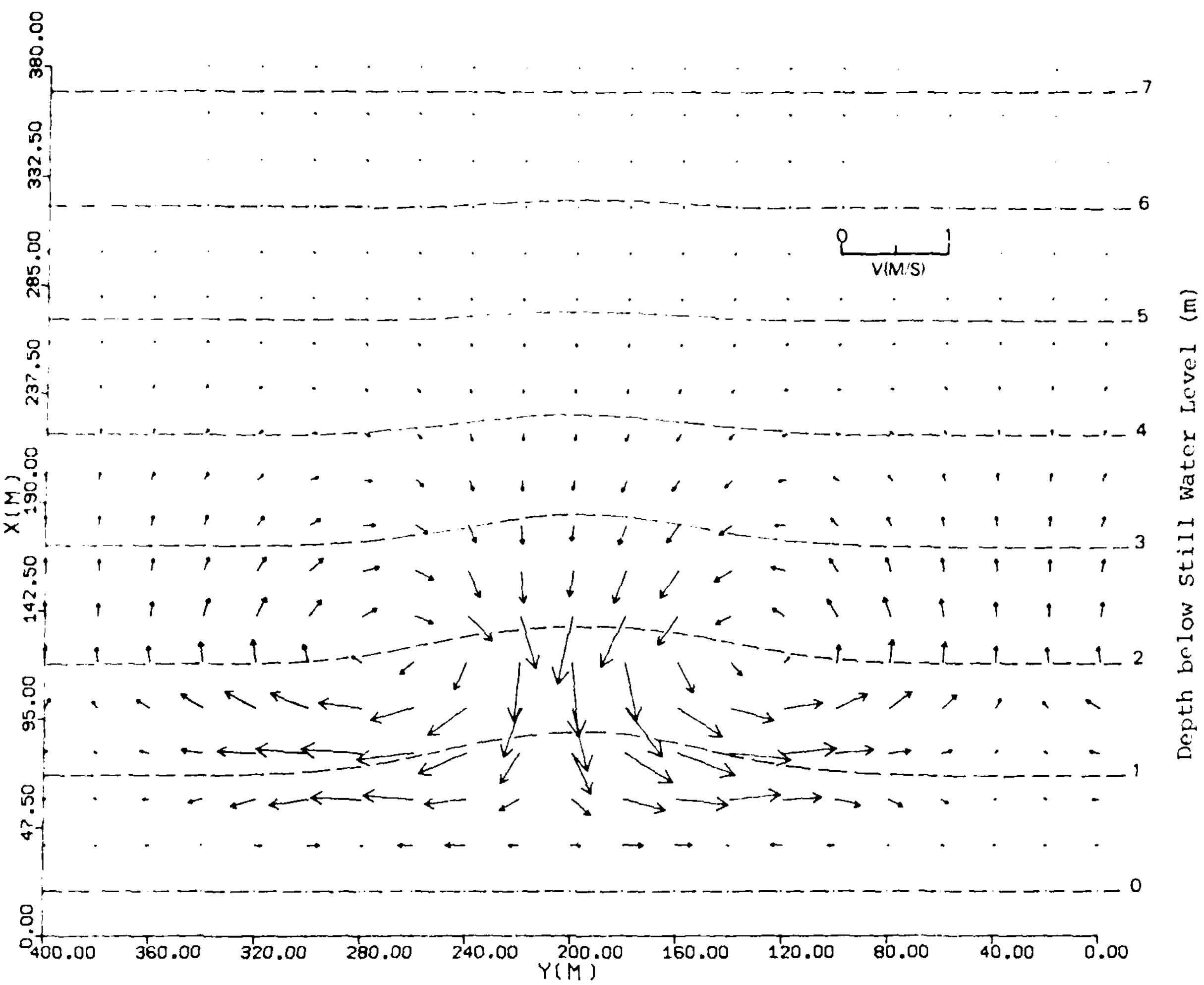


Figure 5-17. Currents Induced by Bulge on a Plane Beach Nonlinear Model: $T = 10.0$ s, $H_o = 1.0$ m, $\theta_o = 180^o$.

level determined by the decay of wave energy, leading to a steady state circulation pattern.

## 2.5 Intersecting Waves Application

Ebersole and Dalrymple have discussed the application of the model to the case of intersecting wave trains of the same frequency on a plane beach, which provides a mechanism for generating rip currents, as shown by Dalrymple (1975). The purpose of this application was to investigate the effect of the convective acceleration terms in the model. The following derivation closely follows the work of Dalrymple.

Given two intersecting wave trains A and B with amplitudes a and b and a common frequency, $\sigma$, in terms of the coordinate system shown in Figure 5-18, the free surface displacements for the two wave trains can be written as,

$$\eta_A = a \cos(k \cos \alpha x + k \sin \alpha y + \sigma t)$$

$$\eta_B = b \cos(k \cos \beta x + k \sin \beta y + \sigma t) \quad .$$

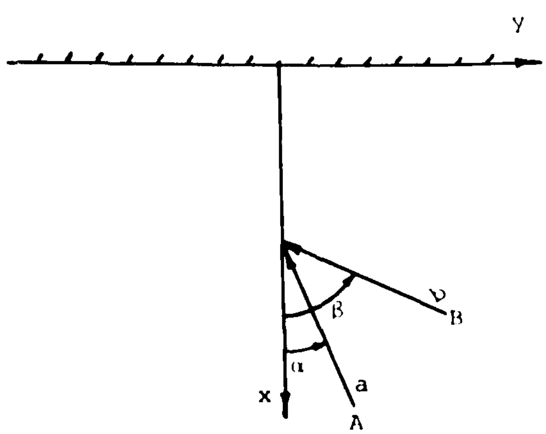


Figure 5-18. Wave Angles for Intersecting Waves.

The total free surface $\eta_T = \eta_1 + \eta_2$ can then be written as,

$$\eta_T = 2a \cos \{\frac{k}{2}(\cos\alpha + \cos \beta)x + \frac{k}{2}(\sin\alpha + \sin \beta)y + \sigma t\} \cdot$$
$$\cos \{\frac{k}{2}(\cos\alpha - \cos \beta)x + \frac{k}{2}(\sin\alpha - \sin \beta)y\}$$
$$+ (b-a)\cos \{k \cos \beta x + k \sin \beta y + \sigma t\} \quad . \qquad (5.2)$$

Using the linearized dynamic free surface boundary condition the velocity potential $\phi_T$ can be shown to equal,

$$\phi_T = \frac{2ag}{\sigma} \frac{\cosh k(h+z)}{\cosh kh} \sin\{\frac{k}{2}(\cos\alpha + \cos \beta)x + \frac{k}{2}(\sin\alpha + \sin \beta) + \sigma t\} \cdot$$
$$\cos \{\frac{k}{2}(\cos\alpha - \cos \beta)x + \frac{k}{2}(\sin\alpha - \sin \beta)y\}$$
$$+ \frac{(b-a)}{\sigma} \frac{\cosh k(h+z)}{\cosh kh} \sin \{k \cos \beta x + k \sin \beta y + \sigma t\} \quad .$$

From the velocity potential the total orbital velocities can be found from,

$$u = -\frac{\partial\phi}{\partial x} \quad , \quad v = -\frac{\partial\phi}{\partial y} \quad , \quad w = -\frac{\partial\phi}{\partial z} \quad .$$

The radiation stresses, which are essentially the forcing terms, are defined as,

$$S_{xx} = \int_{-h}^{0} \overline{\rho u^2} dz + \int_{-h}^{\eta} \overline{P} dz - \frac{1}{2} \rho g (h+\overline{\eta})^2 + \frac{1}{2} \rho g \overline{\eta^2}$$

$$S_{yy} = \int_{-h}^{0} \overline{\rho v^2} dz + \int_{-h}^{\eta} \overline{P} dz - \frac{1}{2} \rho g (h+\overline{\eta})^2 + \frac{1}{2} \rho g \overline{\eta^2}$$

$$S_{xy} = \int_{-h}^{0} \overline{\rho uv}\, dz$$

where

$$\overline{P} = \rho g(\overline{\eta}-z) + \frac{\partial}{\partial x}\int_{z}^{0} \overline{\rho uw}\, dz + \frac{\partial}{\partial y}\int_{z}^{0} \overline{\rho vw}\, dz - \overline{\rho w^2} \quad .$$

The radiation stresses are found to be given by

$$S_{xx} = \frac{\rho g}{4\sinh 2kh} [a^2\cos^2\alpha + b^2\cos^2\beta + 2ab\cos\alpha\cos\beta\cos\{2\psi\}] \cdot$$

$$\{2kh+\sinh 2kh\} - \frac{\rho g\ ab}{8\sinh 2kh} (\cos\beta - \cos\alpha)^2\cos\{2\psi\} \cdot$$

$$\{2kh\cosh 2kh-\sinh 2kh\} - \frac{\rho g\ ab}{8\sinh 2kh} (\sin\alpha-\sin\beta)^2\cos\{2\psi\} \cdot$$

$$\{2kh\cosh 2kh-\sinh 2kh\} - \frac{\rho g}{4\sinh 2kh} [a^2+b^2+2ab\ \cos\{2\psi\}] \cdot$$

$$\{\sinh 2kh-2kh\} + \rho gab\cos^2\psi + \frac{1}{4}\rho g(b-a)^2$$

$$S_{yy} = \frac{\rho g}{4\sinh 2kh} [a^2\sin^2\alpha+b^2\sin^2\beta+2ab\sin\alpha\sin\beta\cos\{2\psi\}] \cdot \{2kh+\sinh 2kh\}$$

$$- \frac{\rho g\ ab}{8\sinh 2kh} (\cos\beta-\cos\alpha)^2\cos\{2\psi\} \cdot \{2kh\cosh 2kh-\sinh 2kh\}$$

$$- \frac{\rho g\ ab}{8\sinh 2kh} (\sin\alpha-\sin\beta)^2\cos\{2\psi\} \cdot \{2kh\cosh 2kh-\sinh 2kh\}$$

$$- \frac{\rho g}{4\sinh 2kh} [a^2+b^2+2ab\cos\{2\psi\}] \cdot \{\sinh 2kh-2kh\}$$

$$+ \rho gab\cos^2\psi + \frac{1}{4}\rho g(b-a)^2$$

$$S_{xy} = \frac{\rho g}{4\sinh 2kh} [a^2\sin\alpha\cos\alpha+b^2\cos\beta\sin\beta+ab\cos\{2\psi\}\sin(\alpha+\beta)] \cdot$$

$$\{2kh+\sinh 2kh\}$$

where the expression "$\psi$" is defined as,

$$\psi \equiv \frac{k}{2}(\cos\alpha-\cos\beta)x + \frac{k}{2}(\sin\alpha-\sin\beta)y \quad .$$

The time independent mean free surface displacement, $\bar{\eta}$, is defined by

$$\bar{\eta} \equiv -\frac{1}{2g}\,\overline{\{u^2+v^2+w^2\}}_{z=0}$$

where "——" denotes the time average over one wave period. Substituting the expressions for the velocity components u, v, and w from the velocity potential $\phi_T$, $\bar{\eta}$ can be written as,

$$\bar{\eta} = \frac{-k}{2\sinh 2kh}\,[a^2+b^2+2ab\cos\{2\psi\}\cdot(\cos(\alpha-\beta)\cosh^2 kh-\sinh^2 kh] \tag{5.3}$$

where "$\psi$" is the same quantity defined previously. Notice that the mean free surface displacement is modulated in the x and y directions by,

$$\cos\{k(\cos\alpha-\cos\beta)x + k(\sin\alpha-\sin\beta)y\} \quad .$$

Using Snell's Law which states

$$k_o \sin\alpha_o = k \sin\alpha \quad \text{and} \quad k_o \sin\beta_o = k \sin\beta \quad ,$$

and using the fact that $k_o \equiv \frac{2\pi}{L_o}$, where "o" denotes deep water values for the wave length, L, and the wave angles, $\alpha$ and $\beta$, we see that there is a periodicity of the mean displacement in the longshore direction with a periodic spacing, $\ell$, given by,

$$\ell = \frac{L_o}{\sin\alpha_o - \sin\beta_o}$$

This periodicity in water level and wave height causes water to be driven from regions of high mean water level displacement to regions of lower displacement, resulting in the formation of circulation cells.

In order to attempt to model this phenomena, certain simplifications to the model had to be made. Since the refraction and shoaling routines borrowed from the work of Noda, *et al.*, could not treat more than one wave train, they were replaced with routines governed by Snell's Law neglecting wave-current interaction. Again a quadratic, "exact," bottom friction was used including velocities due to mean currents and, this time, the two wave trains. In the momentum equations the advective acceleration terms were retained, horizontal mixing was neglected, and the radiation stresses were calculated using the results presented earlier in this section. The wave height used in calculating the radiation stresses and the bottom frictional stresses is given by

$$H_T = 2.0 \sqrt{a^2+b^2+2ab \cos[k(\cos\alpha-\cos\beta)x + k(\sin\alpha-\sin\beta)y]} \ .$$

Two runs are presented here using different combinations of wave heights and wave angles. The remainder of the input data for both runs, however, was the same. The waves were run on a plane beach with a slope of 0.025. The planform area of interest was comprised of 25 grids in the x direction with an $\Delta x$ grid size of 5.0 meters, and 21 grids in the longshore direction with a $\Delta y$ grid size of 4.0 meters. The time step was chosen to be 0.2 seconds and the model was run for 1500 iterations for both cases. A wave period of 7.159366 seconds was used, which resulted in theoretical rip spacings of 80.0 meters. The bottom friction factor was set equal to 0.12 to allow the system to reach steady state after the 1500 iterations and to decrease the magnitude of the resultant currents.

The first case used waves of equal heights and equal angles to either side of the beach normal. The deep water wave heights were 0.25 meters and the deep water angles were ± 30.0 degrees. For this case, referring to Eq. (5.3), $a=b$ and $\alpha=-\beta$ resulting in a free surface displacement given by

$$\eta_T = 2a \cos(k_o \sin \alpha_o y)\cos(k \cos \alpha x + \sigma t) \quad .$$

This free surface describes a wave train moving in the -x direction with a modulated wave height that is periodic in the longshore direction only. The periodicity in wave height is the driving mechanism producing the rip current perpendicular to the beach, as shown in Figure 5-19. Note the constricted width of the rip current in relation to the width of the inflow region. This is a result of the convective acceleration terms. Also note the weak rip head where the currents diverge from the rip axis and return towards shore.

In the second case, the waves, A and B, had different heights, 0.1 and 0.4 meters, and wave angles of 30.0 and -30.0 degrees, respectively. The resulting circulation pattern is shown in Figure 5-20, and consists of a meandering current with alternating regions of strong and weak longshore velocity along the beach. This circulation would lend itself well to the formation of rythmic beach features. Looking at Eq. (5.2), we see that there is a non-zero term,

$$(b-a)\cos\{k \cos \beta x + k \sin \beta y + \sigma t\}$$

which is a wave train at an angle to the beach normal with height 2(b-a). This wave is present in addition to the normal wave train with the modulated height from the first case, causing a longshore current which is superimposed on the cellular circulation.

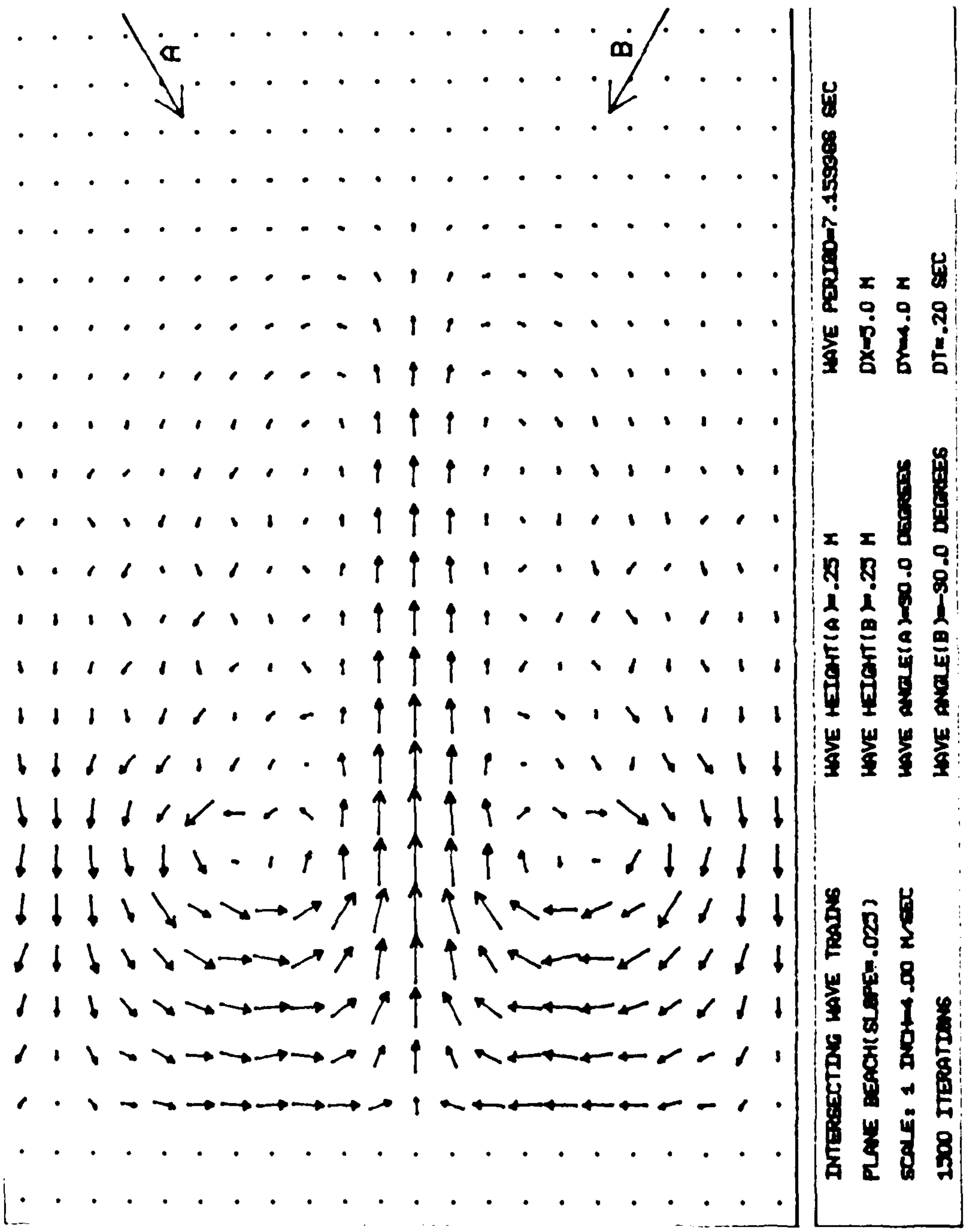


Figure 5-19. Current Vector Plot for Intersecting Waves, Case 1. Nonlinear Model

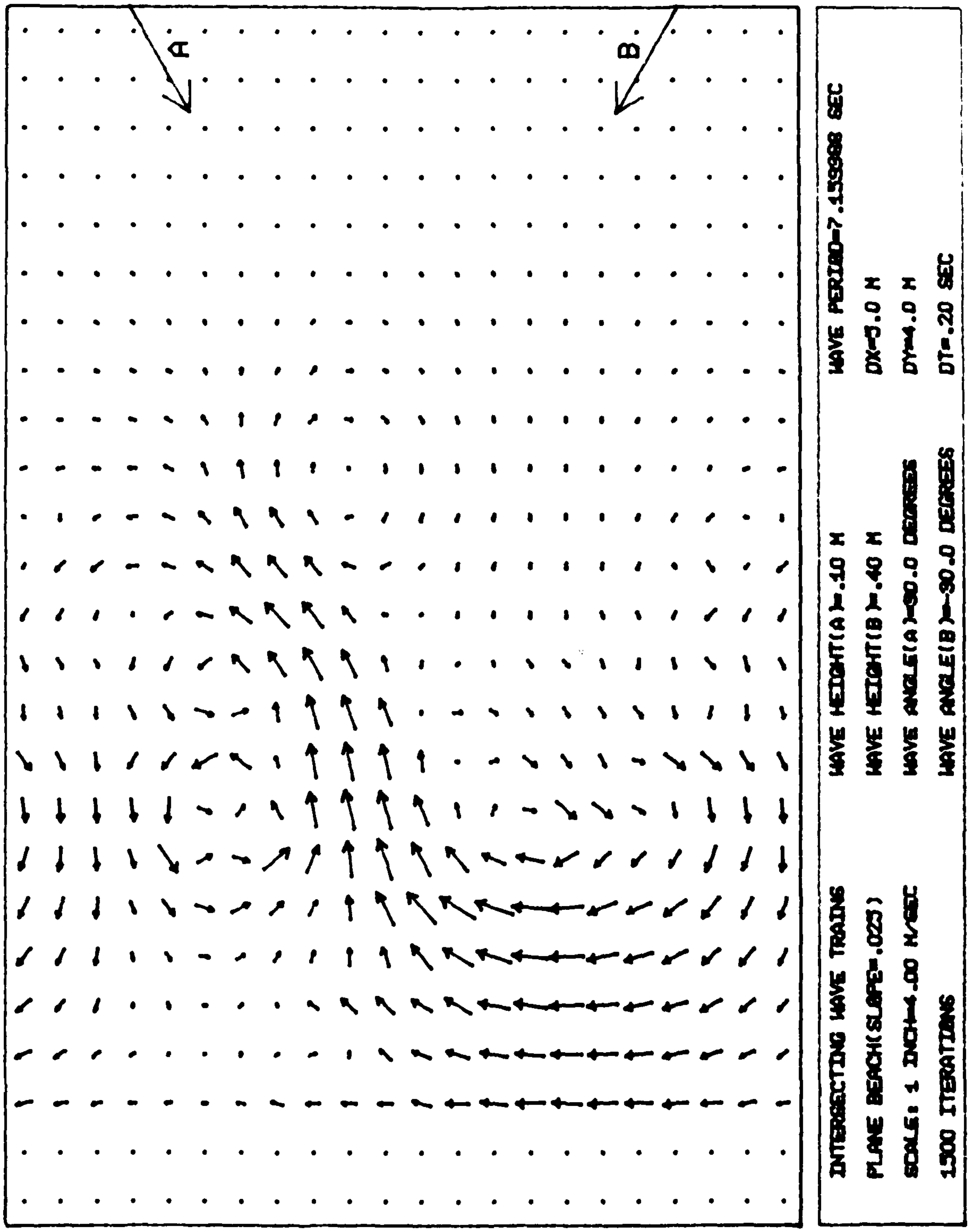


Figure 5-20. Current Vector Plot for the Meandering Circulation Pattern. Nonlinear Model.

## Chapter VI

## CONCLUSIONS

In this report, the theoretical background and numerical formulation of two models for nearshore circulation have been reviewed. A review of the application of the models to plane beach problems has shown that the models successfully reproduce the characteristics of known analytic solutions. The comments of Basco (1981), who expressed the opinion that the models are invalid due to the effect of numerical viscosity on the calculated velocity profiles, can be seen to be incorrect upon inspection of Figure 5-5, which demonstrates the steep drop in longshore current at the breaker line in the absence of a prescribed lateral mixing. In addition, Figure 5-1 shows that the model reproduces the sharp drop in wave set down at the breaker line, further indicating that the model is capable of reproducing the distinct features of analytic solutions, if the grid scheme chosen is fine enough to resolve the features. It is apparent that any numerical diffusion of solutions for $\overline{\eta}$ or V is confined to one or two grid rows, and can be made insignificant by choosing the grid size small enough. It should also be remarked that the slight decrease in the longshore velocity below the purely linear profile predicted by Longuet-Higgins (1970a) has been explained to be a result of wave-current interaction (Dalrymple, 1980) included in both models, and of finite angle of wave incidence (Liu and Dalrymple, 1978; Krauss and Sasaki, 1979), included in the nonlinear model. In conclusion, there appears to be no discrepancy between numerical solutions using a fine grid and the corresponding analytic solutions.

In practical applications, grid spacings are often chosen which lead to some false numerical averaging of the solutions. In the linear model, this averaging manifests itself most obviously as a smoothing of the longshore profile across the breaker line in the same manner as would be induced by lateral mixing effects (see Figure 4-14). This indicates that the mixing coefficients included in the nonlinear model should be smaller than expected on physical grounds in order to compensate for the numerical effects. With the choice of a friction factor based on the formulae of Jonsson (1966) or Kajiura (1968), the model is then seen to produce realistic current profiles, both in form and magnitude, for the field site chosen. However, it should be noted that no detailed data set currently exists which satisfies the requirement of a monochromatic input wave condition, and which represents a field case for which model results are fairly reliable, such as the absence of a large longshore bar.

The numerical models are shown to be successful predictors of nearshore dynamics in situations dominated by refraction and weak wave-current interaction effects. In this regard, it is noted that the model as currently formulated cannot handle certain effects, such as the influence of finite barriers in the wave field, or strong interaction of waves and opposing currents. The modelling of both of these effects requires the inclusion of a capability for handling wave diffraction.

Finally, the present models require an input wave condition based on a monochromatic wave, whereas wave trains in nature tend to include a spectrum of waves. In the case where the incident wave spectrum is sufficiently narrow-banded in frequency, the incident wave can be represented as a wave of single frequency with a modulated amplitude; such an effect can be modelled after modification of the programs to handle a time varying deepwater wave height. However, modelling of broad-banded spectra at the level of the treatment here remains a complex problem.

## REFERENCES


Allender, J. H., J. D. Ditmars, A. A. Frigo, and R. A. Paddock (1981), "Evaluation of a Numerical Model for Wave- and Wind-Induced Nearshore Circulation Using Field Data," Report NUREG/CR-1210, ANL/EES-TM-154, Argonne National Laboratory, Argonne, Illinois.

Basco, D. R. (1981), "Surf Zone Currents," U. S. Army Corps of Engineers, Coastal Engin. Res. Center (in preparation).

Birkemeier, W. A., and R. A. Dalrymple (1976), "Numerical Models for the Prediction of Wave Set-up and Nearshore Circulation," ONR Tech. Rept. 1, Ocean Engineering Rept. 3, Dept. of Civil Engineering, University of Delaware, Newark, DE.

Blumberg, A. F. (1977), "Numerical Tidal Model of Chesepeake Bay," ASCE J. Hydraulics Division 103, HY1, 1-9.

Bowen, A. J., and D. L. Inman (1974), "Nearshore Mixing Due to Waves and Wave-Induced Currents," Rapp. P.-v. Réun. Cons. int. Explor. Mer. 167, 6-12.

Bowen, A. J., D. L. Inman, and V. P. Simmons (1968), "Wave Set-Down and Set-up," J. Geophys. Res. 73(8), 2569-2577.

Dalrymple, R. A. (1975), "A Mechanism for Rip Current Generation on an Open Coast," J. Geophys. Res. 80(24), 3485-3487.

Dalrymple, R. A. (1978), "Rip Currents and their Causes," Proc. 16th Int. Conf. on Coastal Engineering, Hamburg.

Dalrymple, R. A. (1980), "Longshore Currents with Wave Current Interation," ASCE J. Waterway, Port, Coast. and Ocean Div. 106 WW3, 414-420.

Dalrymple, R. A., R. A. Eubanks, and W. A. Birkemeier, (1977), "Wave-Induced Circulation in Shallow Basins," ASCE J. Waterway, Port, Coast. and Ocean Div. 103 WW1, 117-135.

Dalrymple, R. A., and P. L.-F. Liu (1978), "Waves over Soft Muds: A Two Layer Fluid Model," J. Phys. Oceanogr. 8(6), 1121-1131.

Dalrymple, R. A., and C. J. Lozano (1978), "Wave-Current Interaction Models for Rip Currents," J. Geophys. Res. 83(C12), 6063-6071.

Divokey, D., B. LeMehaute, and A. Liu (1970), "Breaking Waves on Gentle Slopes," J. Geophys. Res. 75(9), 1681-1692.

Ebersole, B. A., and R. A. Dalrymple (1979), "A Numerical Model for Nearshore Circulation including Convective Accelerations and Lateral Mixing," ONR Tech. Rept. 4, Ocean Engineering Rept. 21, Dept. of Civil Engineering, University of Delaware, Newark, DE.

Gable, C. G. (ed.) (1979), "Report on Data from the Nearshore Sediment Transport Study Experiment at Torrey Pines Beach, California, November-December 1978," IMR Ref. No. 79-8, Institute of Marine Resources, University of California, La Jolla, CA.

Hildebrand, F. B. (1976), Advanced Calculus for Applications, Prentice-Hall.

James, I. D. (1974), "Non-linear Waves in the Nearshore Region: Shoaling and Set-up," Est. Coast. Mar. Sci. 2, 207-234.

Jonsson, I. G. (1966), "Wave Boundary Layers and Friction Factors," Proc. 10th Int. Conf. on Coastal Engineering, Tokyo, 127-148.

Kajiura, K. (1968), "A Model of the Bottom Boundary Layer in Water Waves," Bull. Earthquake Res. Inst. 46, 75-123.

Kraus, N. C., and T. O. Sasaki (1979), "Influence of Wave Angle and Lateral Mixing on the Longshore Current," Marine Sci. Comm. 5, 99-126.

Kurihara, Y. (1965), "On the Use of Implicit and Iterative Methods for Time Integration of the Wave Equation," Monthly Weather Rev. 93(1), 33-46.

LeBlond, P. H., and C. L. Tang (1974), "On Energy Coupling between Waves and Rip Currents," J. Geophys. Res. 79(6), 811-816.

Lilly, D. K. (1965), "On the Computational Stability of Numerical Solutions of Time-Dependent Non-Linear Geophysical Fluid Problems," Monthly Weather Rev. 93(1), 11-26.

Liu, P. L.-F. (1973), "Damping of Waves over a Porous Bed," ASCE J. Hydraulics Div. 99, HY , 2263-2271.

Liu, P. L.-F. (1982), "Finite Element Modelling of Breaking Wave-Induced Near-shore Currents," Proc. Nearshore Current Model Workshop, CERC, (in preparation) Newark, Del.

Liu, P. L.-F., and R. A. Dalrymple (1978), "Bottom Frictional Stresses and Longshore Currents Due to Waves with Large Angles of Incidence," J. Mar. Res. 36(2), 357-375.

Longuet-Higgins, M.S. (1970a), "Longshore Currents Generated by Obliquely Incident Sea Waves, 1," J. Geophys. Res. 75(33), 6778-6789.

Longuet-Higgins, M.S. (1970b), "Longshore Currents Generated by Obliquely Incident Sea Waves, 2," J. Geophys. Res. 75(33), 6790-6801.

Longuet-Higgins, M. S., and Stewart, R. W. (1969), "Radiation Stress in Water Waves: A Physical Discussion with Applications," Deep Sea. Res. 4, 529-563.

Longuet-Higgins, M. S., and J. S. Turner (1974), "An 'Entraining Plume' Model of a Spilling Breaker," J. Fluid Mech. 63(1), 1-20.

McDougall, W. G. (1979), "A Numerical Model to Predict Surf Zone Dynamics," M.C.E. Thesis, Dept. of Civil Engineering, University of Delaware, Newark, DE.

Miller, C., and A. Barcilon (1978), "Hydrodynamic Instability in the Surf Zone as a Mechanism for the Formation of Horizontal Gyres," J. Geophys. Res. 83, 4107-4116.

Noda, E. K. (1973), "Rip Currents," Proc. 13th Int. Conf. on Coastal Engineering, Vancouver, 653-668.

Noda, E. K., C. J. Sonu, V. C. Rupert, and J. I. Collins (1974), "Nearshore Circulation under Sea Breeze Conditions and Wave-Current Interaction in the Surf Zone," Tetra Tech Report TC-149-4.

Paddock, R. A., and J. D. Ditmars (1981), "Investigation of the Feasibility of Linking a Sediment Transport Model with a Nearshore Circulation Model," Report NUREG/CR-2237, ANL/EES-TM-155, Argonne National Laboratory, Argonne, Illinois.

Pawka, S. (1980), personal communication.

Pearce, B. R. (1972), "Numerical Calculation of the Response of Coastal Waters to Storm Systems with Applications to Hurricane Camille of August 17-22, 1969," College of Engineering Tech. Rept. 12, University of Florida.

Phillips, O. M. (1977), The Dynamics of the Upper Ocean, 2nd Ed., Cambridge University Press.

Roache, P. J. (1976), Computational Fluid Dynamics, Hermosa Publishers, Albuquerque.

Shore Protection Manual (1975), U.S. Army Corps of Engineers, Vol. 1, Government Printing Office.

Sonu, C. J. (1972), "Field Observations of Nearshore Circulation and Meandering Currents," J. Geophys. Res. 77(18), 3232-3247.

Sommerfeld, A. (1949), Partial Differential Equations in Physics, Academic Press, New York.

Symonds, G., D. A. Huntley, and A. J. Bowen (1982), "Two Dimensional Surf Beat: Long Wave Generation by a Time-Varying Breakpoint," J. Geophys. Res. 87(C1), 492-498.

Van Dorn, W. C. (1953), "Wind Stress on an Artificial Pond," J. Marine Res. 12, Weggel, J. R. (1972), "Maximum Breaker Height," J. Waterways, Harbors and Coastal Engineering, ASCE 98, WW4, 529-548.

Wilson, B. W. (1966), "Seiche," in Encyclopedia of Oceanography, Reinhold Publishers, New York.

Wu, J. (1968), "Laboratory Studies of Wind-Wave Interactions," J. Fluid Mech. 34(1), 91-111.

## Appendix I.

## USING THE NEARSHORE CIRCULATION PROGRAM

The nearshore circulation model as described above is supplied in two versions, referred to as the linear and the nonlinear versions. Complete listings of the programs for each version follow. The programs as written are designed to run on a Burroughs B7700. The line

$RESET FREE

which appears on the front of each program allows for the use of standard Fortran on the B7700. This line should be removed before operating the program on a different system.

The two versions of the model are currently designed to be indistinguishable to the operator, with the input file containing wave and wind information and the depth grid being of identical format for each program. The output file generated currently at a line printer is also identical for each program. The exception to the uniformity between the two models occurs in the output file stored at the end of execution for subsequent restart of the model. Since the nonlinear version of the program requires the storage of three time levels of data, two extra time levels are included in the output. Thus, the nonlinear version of the program can not be started based on intermediate results generated by the linear version, as not enough information is present. It is possible in principle to start the linear version of the program using intermediate results from the non-linear version, although at present the READ statement in the linear version is not structured to handle this option.

The circulation model is currently designed to be run as a batch job, and as such has all device number specifications for data files in the job file external to the program. This feature may have to be changed depending on the machine to be used. Currently, data files may be named arbitrarily. The program currently requirues four IO device specifications:

| Logical Device Number | Corresponding Data File |
|---|---|
| 5 | User defined input data |
| 6 | Output stream, currently directed to a line printer |
| 3 | Output file, stores results of last interation for a later restart |
| 8 | Input file used to restart the model |

It should be noted that the input file 8 used for restarting the program is identical to, and should be just a renamed version of, the output file 3 generated by the model at the point from which it is desired to continue computation.

## Structure of Input Data File 5

The input data file is structured into five groups of data. The first four groups each consist of a single line in the file, with data values entered unformatted; i.e., separated by commas with no requirements on spacing. The fifth data group consists of the depth grid, and requires more space than a single line, as explained below. The information included in the input data file is as follows.

DATA IN INPUT DATA FILE 5

1. Wave Parameters

| | |
|---|---|
| T | - Wave period (seconds) |
| HO | - Wave height (meters) |
| A | - Wave angle, measured clockwise from the +X direction (degrees) |

2. Wind Parameters

| | |
|---|---|
| WIND | - Wind speed (meters/second) |
| WINANG | - Wind angle, measured clockwise from the -X direction (degrees) |

3. Grid Parameters

| | |
|---|---|
| M | - Number of grid rows in X direction (offshore) |
| N | - Number of grid columns in Y direction (longshore) |
| DX | - Grid spacing in X direction (meters) |
| DY | - Grid spacing in Y direction (meters) |
| DT | - Size of the time step (seconds) |
| INDEX | - Specifies the input of depth information<br>=1, read data from previous run from file 8<br>=2, read depth grid from input file 5<br>=3, establish plane beach based on input beach slope |
| AM | - Beach slope (space in input file must be filled, but value is unsed only if INDEX=3) |

4. Program Control Parameters

| | |
|---|---|
| ITA | - Total number of iterations (including the accumulated total from previous runs, if previous run data is used) |
| NHIGHT | - Number of iterations over which the deep water wave builds up |

ID - Determine if dissipation of wave energy is to be included
=0, no dissipation
=1, dissipation due to viscosity and bottom permeability is included

KSKIP - Determine frequency of printed iterations in output file 6

5. Depth Grid (required if INDEX=2)

D - Local water depth with respect to still water level at each grid center.

The depth grid D is input in an unformatted string of length M*N, starting with the fifth line of the input file 5 and continuing to as many lines as necessary. The data values are read off of an established grid row-wise in the +Y direction, starting at the inshore end of the grid.

Coordinate System Used in the Program

The input depth grid and wave and wind parameters should be established using the coordinates shown in Figure 2-1. The models require that the bathymetry be periodic in the longshore direction. Accordingly, for an input depth grid of size (M, N), where (I, J) are X and Y indices and (M, N) are the maximum values of (I, J), the laterally bordering depth values should satisfy the requirement:

$$D(I,N) = D(I,1) \quad .$$

If this condition is not met on input, D(I,1) is redefined to be equal to D(I,N). Both models create two additional rows in the Y direction, (N+1) and (N+2). The grid storage requirement for all variables is thus M by (N+2), with a current maximum of 50 by 50. The maximum may be enlarged or decreased by alteration of all COMMON and DIMENSION statements in either program.

Wave angle and wind angle are defined as shown in Figure 2-1. Wave angle is measured clockwise from the +X direction. Waves approaching the beach from the right of directly offshore have wave angles > 180°. Wind angle is given clockwise from the -X direction, so that winds approaching shore from the right of normal have wind directions greater than 0°.

The program requires that incident waves have longshore components propagating in the +Y direction. For the case of wave angles = $180° - \theta$, the program flips the depth grid over and rotates the wave and wind directions through $360° - 2\theta$ degrees, and runs the program for waves approaching at $180° + \theta$ and a mirror image depth grid.

## Error Messages from the Circulation Models

Each version of the nearshore circulation model will generate various error messages when fatal conditions are met during execution. The messages are, for the most part, identical from either program and correspond to equivalent situations within the programs. A list of possible internally occurring errors leading to the printing of a message follows.

1. Failure of iteration scheme to converge on a wave height at a grid point will cause the message

RELAXATION FOR THE WAVE HEIGHT FAILED TO CONVERGE

followed by an indication of the row and number of iterations tried. This condition arises in the subroutine HEIGHT. Occurrence of the condition does not lead to termination of the program; iteration continues with the last wave height calculated and the entire iteration is tried again at the next time step.

2. Failure of iteration scheme to converge on a wave angle at a grid point will cause the message

RELAXATION FOR THETA FAILED AFTER -- ITERATIONS

with an indication given of the number of iterations tried. This condition could arise if the magnitude of a current directed against the general direction of wave travel was too strong. The condition arises in the subroutine ANGLE and causes termination of the program.

3. If a negative wave number RK is calculated, the message

RK IS NEGATIVE

is printed, and the program is terminated. This condition occurs in the subroutine WVNUM.

LINEAR MODEL

```
$RESET FREE
C*-----------------------------------------------------------------
C*
C*    NEARSHORE CIRCULATION MODEL --- LINEAR VERSION
C*
C*    THIS COMPUTER PROGRAM IS A NUMERICAL MODEL TO PREDICT SURF-ZONE
C*    DYNAMICS, GIVEN A FIXED, PERIODIC TOPOGRAPHY AND DEEPWATER
C*    MONOCHROMATIC WAVE CONDITIONS AS INPUT.
C*    THE REFRACTION PROGRAM INCLUDING WAVE-CURRENT INTERACTION IS BASED
C*    ON THE PROGRAM OF NODA ET AL(TETRA TECH 1974).  THE CURRENT
C*    PROGRAM IS AN UPDATED VERSION OF THE MODEL DEVELOPED BY
C*    BIRKEMEIER AND DALRYMPLE(UNIV. OF DEL. 1977).
C*
C*-----------------------------------------------------------------
      COMMON D(50,50),U(50,50),V(50,50),Z(50,50),SI(50,50),CO(50,50),
     *H(50,50),CG(50,50),S(50,50),HBREAK(50,50),IB(50,50),DDDX(50,50),
     *DDDY(50,50),W(50,50),Y(50,50)
      COMMON/VAL/ETA(50,50)
      COMMON/STRESS/SIGXX(50,50),SIGYY(50,50),SIGXY(50,50),TAUBX(50,50),
     *TAUBY(50,50),TAUSX(50,50),TAUSY(50,50)
      COMMON/REF/ZZ(50,50),HNEW(50,50),RKA(50,50)
      COMMON/CONST/ G,PI,PI2,RAD,EPS,DX,DY,DT,DX2,DY2,T,SIGMA,
     *M,N,N1,N2,M1,M2,AM,DD,IT,RHO,IWET,IDRY,ID
      DIMENSION DST(50,50)
C*-----------------------------------------------------------------
C*
C*    NOTES ON RUNNING THE CIRCULATION PROGRAM
C*
C*    1. WAVE ANGLE IS MEASURED CLOCKWISE FROM THE +X DIRECTION
C*
C*    2. WIND ANGLE IS MEASURED CLOCKWISE FROM THE -X DIRECTION
C*
C*    3. ALL INPUT AND OUTPUT DATA IS IN MKS UNITS
C*
C*    4. THE DEPTH GRID IS OFFSET BY -DY FROM ALL THE OTHER VARIABLE
C*       FIELDS
C*
C*-----------------------------------------------------------------
C*
C*    DEFINITIONS OF QUANTITIES USED IN PROGRAM
C*
C*    1. CONSTANTS
C*
C*       CF - BOTTOM FRICTION FACTOR (DARCY TYPE)
C*       VANCON - WIND SHEAR FACTOR (VAN DORN TYPE)
C*
C*    2. VARIABLE ARRAYS (VALUE AT EACH GRID LOCATION)
C*
C*       D - TOTAL WATER DEPTH (D(SW)+ETA)
C*       ETA - DEVIATION OF MEAN WATER LEVEL FROM STILL WATER LEVEL
C*       Z - WAVE ANGLE
C*       CO - COS(Z)
C*       SI - SIN(Z)
C*       H - WAVE HEIGHT
C*       HBREAK - LOCAL BREAKING WAVE HEIGHT
C*       IB - BREAKING INDEX
C*            IB=0, WAVE IS BREAKING LOCALLY
C*            IB=1, WAVE IS NOT BREAKING LOCALLY
C*       DDDX,DDDY - LOCAL DERIVATIVES OF THE TOTAL DEPTH
```

```
C*      CG - GROUP VELOCITY
C*      RKA - WAVE NUMBER
C*      U,V - X,Y VELOCITIES AT SIDES OF GRID BLOCKS
C*      W,Y - X,Y VELOCITIES AT CENTERS OF GRID BLOCKS
C*            NOTE THAT THE U,V AND W,Y ARRAYS ARE INTERCHANGED
C*            IN SEVERAL SUBROUTINES THROUGH THE COMMON STATEMENTS
C*      SIGXX,SIGXY,SIGYY - RADIATION STRESSES
C*      TAUBX,TAUBY - BOTTOM STRESSES
C*      TAUSX,TAUSY - SURFACE STRESSES
C*
C*   3. LOCALLY DEFINED VARIABLES
C*
C*      DUDX,DVDX - VELOCITY GRADIENT COMPONANTS
C*      DCDX,DCDY - WAVE CELERITY GRADIENT COMPONANTS
C*      DCGDX,DCGDY - GROUP VELOCITY GRADIENT COMPONANTS
C*      DTDX,DTDY - WAVE ANGLE GRADIENT COMPONANTS
C*      EPS - ACCURACY VALUE USED IN THE RELAXATION SCHEMES
C*
C*
C*
C*-------------------------------------------------------------------
C*
C*   VARIABLES TO BE READ INTO PROGRAM
C*
C*   1. WAVE PARAMETERS
C*
C*      T       - WAVE PERIOD (SECONDS)
C*      HO      - WAVE HEIGHT (METERS)
C*      A       - WAVE ANGLE, CLOCKWISE FROM +X (DEGREES)
C*
C*   2. WIND PARAMETERS
C*
C*      WIND    - WIND SPEED (METERS/SECOND)
C*      WINANG  - WIND ANGLE, CLOCKWISE FROM -X (DEGREES)
C*
C*   3. GRID PARAMETERS
C*
C*      M       - NUMBER OF GRIDS IN X DIRECTION (OFFSHORE)
C*      N       - NUMBER OF GRIDS IN Y DIRECTION (LONGSHORE)
C*      DX      - GRID SPACING IN X DIRECTION (METERS)
C*      DY      - GRID SPACING IN Y DIRECTION (METERS)
C*      DT      - TIME STEP<DX/SQRT(2*G*DMAX) (SECONDS)
C*      INDEX   - SPECIFY INPUT OF DEPTH INFORMATON
C*                =1, READ DATA FROM PREVIOUS RUN
C*                =2, READ DEPTH GRID FROM INPUT DATA FILE
C*                =3, ESTABLISH PLANE BEACH BASED ON INPUT BEACH SLOPE
C*      AM      - BEACH SLOPE (REQUIRED IF INDEX=3)
C*
C*   4. PROGRAM CONTROL PARAMETERS
C*
C*      ITA     - TOTAL NUMBER OF ITERATIONS (INCLUDING ACCUMULATED
C*                TOTAL OF PREVIOUS RUNS, IF PREVIOUS RUN DATA IS
C*                USED)
C*      NHIGHT  - NUMBER OF ITERATIONS OVER WHICH THE DEEPWATER WAVE
C*                HEIGHT IS BUILT UP
C*      ID      - DETERMINE IF DISSAPATION OF WAVE ENERGY IS TO BE
C*                INCLUDED
C*                =0, NO DISSIPATION
C*                =1, DISSIPATION DUE TO VISCOSITY AND BOTTOM PERM-
C*                    EABILITY
C*      KSKIP   - DETERMINE FREQUENCY OF PRINTED ITERATIONS
C*
```

```
C*     5. DEPTH GRID (IF INDEX=2)
C*
C*        D        - LOCAL WATER DEPTH W/R MEAN WATER LEVEL.
C*                   SEE USERS MANUAL FOR INPUT FORMAT
C*
C*-------------------------------------------------------------------
C*
C*     DEFINE CONSTANTS
C*-------------------------------------------------------------------
       RHO=1000.
       G=9.8
       PI=3.1415927
       PI2=2.*PI
       RAD=180.0/PI
       CF=0.015
       DD=0.0
C*----------------------------------------------------------------
C*     READ INPUT DATA
C*
C*     1. WAVE PARAMETERS
       READ(5,/) T,HO,A
C*     2. WIND PARAMETERS
       READ(5,/) WIND,WINANG
C*     3. GRID PARAMETERS
       READ(5,/) M,N,DX,DY,DT,INDEX,AM
C*     4. PROGRAM CONTROL PARAMETERS
       READ(5,/) ITA,NHIGHT,ID,KSKIP
C*----------------------------------------------------------------
C*     WRITE INPUT DATA ON OUTPUT FILE AS HEADER
C*----------------------------------------------------------------
       WRITE(6,102)M,N,ITA
       WRITE(6,101)DX,DY,DT
       WRITE(6,119) T,HO,A,AM
       WRITE(6,114) WIND,WINANG
       WRITE(6,115) INDEX,ID
       WRITE(6,117) NHIGHT
       WRITE(6,116) CF,DD
       ITO=0
       HEIGHT=HO
       DELTAT=DT
       WINANG=WINANG/RAD
       N2=N+2
       N1=N+1
       M2=M-2
       M1=M-1
       DX2=DX*2.
       DY2=DY*2.
       SIGMA=PI2/T
       EPS=0.01
C*------------------------------------------------------------------
C*     ESTABLISH BOTTOM TOPOGRAPHY BASED ON VALUE OF INDEX
C*------------------------------------------------------------------
       GO TO (1,2,3) INDEX
C*------------------------------------------------------------------
C*     INDEX=1, READ DATA FROM FILE 8 FOR PREVIOUS RUN OF MODEL
C*------------------------------------------------------------------
     1 READ(8,113)
      *((ETA(I,J),J=1,N2),I=1,M),((D(I,J),J=1,N2),I=1,M),
      *((U(I,J),J=1,N2),I=1,M),((V(I,J),J=1,N2),I=1,M),
      *((Z(I,J),J=1,N2),I=1,M),((H(I,J),J=1,N2),I=1,M),
      *((W(I,J),J=1,N2),I=1,M),((Y(I,J),J=1,N2),I=1,M),
      *((RKA(I,J),J=1,N2),I=1,M)
```

```
      READ(8,107)ITO
      DO 10 I=1,M
      DO 10 J=1,N2
      CO(I,J)=COS(Z(I,J))
      SI(I,J)=SIN(Z(I,J))
   10 CONTINUE
C*--------------------------------------------------------------------
C*    IF WAVE ANGLE IS LESS THAN 180 DEGREES, VARIABLE FIELDS WERE
C*    FLIPPED DURING PREVIOUS RUN.  ROTATE THE WAVE AND WIND ANGLES
C*--------------------------------------------------------------------
      IF(A.GE.180.) GO TO 42
      A=360.-A
      WINANG=PI2-WINANG
      GO TO 42
C*--------------------------------------------------------------------
C*    INDEX=2, READ IN DEPTH GRID FROM INPUT DATA FILE 5
C*--------------------------------------------------------------------
    2 READ(5,/,END=99)((D(I,J),J=1,N),I=1,M)
   99 WRITE(6,120) I,J
C*--------------------------------------------------------------------
C*    IF WAVE ANGLE IS LESS THAN 180 DEG., FLIP THE INPUT DEPTH
C*    GRID AND ROTATE THE WAVE AND WIND ANGLES
C*--------------------------------------------------------------------
      IF(A.GT.180.) GO TO 22
      A=360.-A
      WINANG=PI2-WINANG
      DO 21 I=1,M
      DO 20 J=1,N
   20 DST(I,J)=D(I,J)
      DO 21 J=1,N
      K=(N-J)+1
   21 D(I,K)=DST(I,J)
   22 DO 23 I=1,M
      D(I,1)=D(I,N)
      D(I,N2)=D(I,3)
      D(I,N1)=D(I,2)
   23 CONTINUE
      GO TO 41
C*--------------------------------------------------------------------
C*    INDEX=3, ESTABLISH PLANE BEACH BASED ON VALUE OF AM READ ABOVE
C*--------------------------------------------------------------------
    3 DO 31 J=1,N2
      DO 31 I=1,M
      D(I,J)=((FLOAT(I-2)*DX)*AM)
   31 CONTINUE
C*--------------------------------------------------------------------
C*    IF WAVE ANGLE IS LESS THAN 180 DEGREES, ROTATE THE WAVE AND WIND
C*    ANGLES
C*--------------------------------------------------------------------
      IF(A.GE.180.) GO TO 41
      A=360.-A
      WINANG=PI2-WINANG
   41 WRITE(6,108)
      WRITE(6,103)((D(I,J),J=1,N1),I=1,M)
      DO 65 I=1,M
      DO 65 J=1,N2
      ETA(I,J)=0.0
      U(I,J)=0.0
      V(I,J)=0.0
   65 CONTINUE
   42 DO 15 I=1,M
      IF(D(I,1).GT.DD) GO TO 95
```

```
   15 CONTINUE
   95 IWET=I
      IDRY=IWET-1
C*------------------------------------------------------------------
C*    MAIN PROGRAM LOOP FOR EACH ITERATION
C*------------------------------------------------------------------
      DO 4 IT=(1+ITO),ITA
      L=AMOD(FLOAT(IT),FLOAT(KSKIP))
      HO=HEIGHT*TANH(FLOAT(IT)/(FLOAT(NHIGHT)/2.0))
      IF(IT.LE.(NHIGHT*2.0)) GO TO 12
      GO TO 13
   12 CALL DGRAD
      CALL REFRAC(A,HO,IT,INDEX,NHIGHT,CF)
   13 CALL TAUSB(WIND,WINANG,CF,ITO)
      CALL UCALC
      CALL ETAS
      SUM=0.0
      DO 86 I=1,M
      DO 86 J=2,N
      SUM=SUM+0.5*(W(I,J)**2+Y(I,J)**2)*D(I,J-1)
      SUM=SUM+G*ETA(I,J)*(D(I,J-1)-0.5*ETA(I,J))
   86 CONTINUE
C*--------------------------------------------------------------------
C*    WRITE SUM AFTER EACH ITERATION
C*--------------------------------------------------------------------
      WRITE(6,100) SUM
      IF(L.NE.0)GO TO 4
C*--------------------------------------------------------------------
C*    WRITE WAVE HEIGHT, WAVE ANGLE, VELOCITIES, AND SETUP AT
C*    KSKIP INTERVALS
C*--------------------------------------------------------------------
      WRITE(6,109)
      WRITE(6,110)IT,HO
      WRITE(6,111)
      WRITE(6,112)
      WRITE(6,103)((H(I,J),J=1,N1),I=1,M)
      DO 401 I=1,M
      DO 401 J=1,N1
  401 ZZ(I,J)=360.0-Z(I,J)*RAD
      WRITE(6,118)
      WRITE(6,103)((ZZ(I,J),J=1,N1),I=1,M)
      WRITE (6,104)
      WRITE (6,103) ((U(I,J), J = 1,N1),I=1,M)
      WRITE (6,105)
      WRITE (6,103) ((V(I,J), J = 1,N1),I=1,M)
      WRITE (6,106)
      WRITE(6,103) ((ETA(I,J),J=1,N1),I=1,M)
    4 CONTINUE
C*------------------------------------------------------------------
C*    WRITE THE RESULTS OF THE LAST ITERATION INTO AN OUTPUT FILE
C*    TO BE USED FOR A SUBSEQUENT STARTUP
C*------------------------------------------------------------------
      WRITE(3,113)
     *((ETA(I,J),J=1,N2),I=1,M),((D(I,J),J=1,N2),I=1,M),
     *((U(I,J),J=1,N2),I=1,M),((V(I,J),J=1,N2),I=1,M),
     *((Z(I,J),J=1,N2),I=1,M),((H(I,J),J=1,N2),I=1,M),
     *((W(I,J),J=1,N2),I=1,M),((Y(I,J),J=1,N2),I=1,M)
     *,((RKA(I,J),J=1,N2),I=1,M)
      WRITE(3,107)ITA
      LOCK 3
  100 FORMAT(1X,"THE TOTAL ENERGY IS",F14.2)
  101 FORMAT (/,1X,'DX=',I5,3X,'DY=',I5,3X,3X,'DT=',F5.2)
```

```
  102 FORMAT(1X,"M=",I5,3X,"N=",I5,3X,"ITERATIONS =",I5)
  103 FORMAT(1X,11F10.4)
  104 FORMAT ( 10X,12HX - VELOCITY)
  105 FORMAT ( 10X,12HY - VELOCITY)
  106 FORMAT (10X,10HETA VALUES)
  107 FORMAT(I5)
  108 FORMAT (//' THE AUGMENTED MATRIX OF WATER DEPTH IN METERS'/)
  109 FORMAT('******************************',/)
  110 FORMAT(10X,'ITERATION NUMBER',I6,10X,'WAVE HEIGHT=',F10.5,/)
  111 FORMAT (1X,'******************************',/)
  112 FORMAT (5X,'WAVE HEIGHTS',/)
  113 FORMAT(15F8.4)
  114 FORMAT (1X,'WIND SPEED =',F7.3,'M/SEC',5X,'WIND ANGLE =',F7.
     *3,' DEGREES')
  115 FORMAT(5X,'INDEX =',I5,3X,'ID =',I5)
  116 FORMAT(10X,4HCF =,F10.3,5X,4HDD =,F10.3)
  117 FORMAT(10X,'WAVE HEIGHT BUILDS UP FIRST',I3,' ITERATIONS')
  118 FORMAT(2X,'WAVE ANGLE (DEGREES)')
  119 FORMAT(1X,'WAVE PARAMETERS',/2X,'PERIOD =',F7.2,'  HEIGHT =',F7
     *.2,3X,7HANGLE =,F7.2,1X,7HDEGREES,4X,12HBEACH SLOPE=,F7.4)
 120  FORMAT(" INPUT DEPTH GRID TOO SMALL. LAST I,J VALUES ARE"/
     12X,I2,2X,I2)
      STOP
      END
C*---------------------------------------------------------------------
C*
      SUBROUTINE REFRAC(THETAO,HH,ITER,INDEX,NHIGHT,CF)
C*
C*    REFRAC CONTROLS THE CALCULATION OF WAVE ANGLE AND WAVE HEIGHT
C*    FOR EACH ITERATION
C*
C*---------------------------------------------------------------------
      COMMON D(50,50),U(50,50),V(50,50),Z(50,50),SI(50,50),CO(50,50),
     *H(50,50),CG(50,50),S(50,50),HBREAK(50,50),IB(50,50),DDDX(50,50)
     *,DDDY(50,50)
      COMMON/STRESS/SIGX(50,50),SIGY(50,50),SIGXY(50,50),TAUBX(50,50),
     *TAUBY(50,50),TAUSX(50,50),TAUSY(50,50)
      COMMON/CONST/ G,PI,PI2,RAD,EPS,DX,DY,DT,DX2,DY2,T,SIGMA,
     *M,N,N1,N2,M1,M2,AM,DD,IT,RHO,IWET,IDRY,ID
      IF (ITER.GT.(NHIGHT)) GO TO 600
C*---------------------------------------------------------------------
C*    CALL SNELL DURING BUILDUP OF DEEP WATER WAVE
C*---------------------------------------------------------------------
      THETA=PI2-THETAO/RAD
      CALL SNELL (THETA,HH,ITER)
  600 DO 50 I=1,IDRY
      DO 50 J=1,N2
      H(I,J)=0.0
      Z(I,J)=PI
      SI(I,J)=0.0
      CO(I,J)=-1.0
   50 CONTINUE
      CALL ANGLE(25)
      CALL HEIGHT(25,CF)
C*---------------------------------------------------------------------
C*    CALCULATE THE RADIATION STRESSES
C*---------------------------------------------------------------------
      DO 57 I=IWET,M1
      DO 21 J=3,N1
      ENERGY=0.125*RHO*G*(H(I,J)**2)
      SIGX(I,J)=SIGX(I,J)*ENERGY
      SIGY(I,J)=SIGY(I,J)*ENERGY
```

```
      SIGXY(I,J)=SIGXY(I,J)*ENERGY
   21 CONTINUE
      SIGX(I,1)=SIGX(I,N)
      SIGY(I,1)=SIGY(I,N)
      SIGXY(I,1)=SIGXY(I,N)
      SIGX(I,2)=SIGX(I,N1)
      SIGY(I,2)=SIGY(I,N1)
      SIGXY(I,2)=SIGXY(I,N1)
      SIGX(I,N2)=SIGX(I,3)
      SIGY(I,N2)=SIGY(I,3)
      SIGXY(I,N2)=SIGXY(I,3)
   57 CONTINUE
      DO 59 J=3,N1
      SIGXY(M,J)=2.0*SIGXY(M1,J)-SIGXY(M2,J)
   59 CONTINUE
      SIGXY(M,1)=SIGXY(M,N)
      SIGXY(M,2)=SIGXY(M,N1)
      SIGXY(M,N2)=SIGXY(M,3)
      RETURN
      END
C*-----------------------------------------------------------------
C*
      SUBROUTINE GROUP(I,J,DCGDX,DCGDY,FF)
C*
C*    GROUP CALCULATES THE GROUP VELOCITY, WAVE CELERITY, AND
C*    THEIR SPATIAL DERIVATIVES
C*
C*-------------------------------------------------------------------
      COMMON D(50,50),W(50,50),Y(50,50),Z(50,50),SI(50,50),CO(50,50),
     *H(50,50),CG(50,50),S(50,50),HBREAK(50,50),IB(50,50),DDDX(50,50)
     *,DDDY(50,50),U(50,50),V(50,50)
      COMMON/CONST/ G,PI,PI2,RAD,EPS,DX,DY,DT,DX2,DY2,T,SIGMA,
     *M,N,N1,N2,M1,M2,AM,DD,IT,RHO,IWET,IDRY,ID
      COMMON/REF/ZZ(50,50),HNEW(50,50),RKA(50,50)
C*------------------------------------------------------------------
C*    STATEMENT FUNCTIONS DUDX,DUDY,DVDX,DVDY,DTDX,DTDY,E,DKDX,DKDY
C*------------------------------------------------------------------
      DUDX(I,J)=(W(I+1,J)-W(I,J))/DX
      DUDY(I,J)=(U(I,J+1)-U(I,J-1))/DY2
      DVDX(I,J)=(V(I+1,J)-V(I-1,J))/DX2
      DVDY(I,J)=(Y(I,J+1)-Y(I,J))/DY
      DTDX(I,J)=(Z(I+1,J)-Z(I-1,J))/DX2
      DTDY(I,J)=(Z(I,J+1)-Z(I,J-1))/DY2
      E(I,J)=U(I,J)*COSI+V(I,J)*SINI+0.5*A*(1.0+ARG2/SINH2)/RK
      DKDX(I,J)=RK*((U(I,J)*SINI-V(I,J)*COSI)*DTDX(I,J)-(COSI*DUDX(I,J)+
     *SINI*DVDX(I,J))-A*DDDX(I,J-1)/SINH2)/EE
      DKDY(I,J)=RK*((U(I,J)*SINI-V(I,J)*COSI)*DTDY(I,J) -(COSI*DUDY(I,J)
     * +SINI*DVDY(I,J))-A*DDDY(I,J-1)/SINH2)/EE
      JJ=J-1
      DEP=D(I,JJ)
      COSI=CO(I,J)
      SINI=SI(I,J)
      DCGDX=0.0
      DCGDY=0.0
C*------------------------------------------------------------------
C*    CHECK FOR DRY LAND
C*------------------------------------------------------------------
      IF(DEP.LE.DD) RETURN
      CALL WVNUM(DEP,COSI,SINI,U(I,J),V(I,J),RK,A)
      RKA(I,J) = RK
      IF (J.EQ.N) RKA(I,1)=RKA(I,J)
      IF (J.EQ.2) RKA(I,N1)=RKA(I,J)
```

```
      IF (J.EQ.3) RKA(I,N2)=RKA(I,J)
      TA=TANH(RK*DEP)
      HBREAK(I,J)=0.12*PI2*TA/RK
      COSH1=COSH(RK*DEP)
      SECHSQ=1.0/(COSH1**2)
      ARG2=2.0*RK*DEP
      SINH2=SINH(ARG2)
      COSH2=COSH(ARG2)
      SINHSQ=SINH2**2
      EE=E(I,J)
      C=SQRT(G*TA/RK)
      FF=0.5*(1.0+ARG2/SINH2)
      CG(I,J)=FF*C
      P=C*(SINH2-ARG2*COSH2)/SINHSQ
      DKDDX=RK*DDDX(I,JJ)+DEP*DKDX(I,J)
      DKDDY=RK*DDDY(I,JJ)+DEP*DKDY(I,J)
      Q=0.5*G/(C*RK**2)
      DCDX=Q*(RK*SECHSQ*DKDDX-TA*DKDX(I,J))
      DCDY=Q*(RK*SECHSQ*DKDDY-TA*DKDY(I,J))
      DCGDX=P*DKDDX+FF*DCDX
      DCGDY=P*DKDDY+FF*DCDY
      RETURN
      END
C*-----------------------------------------------------------------
C*
      SUBROUTINE HEIGHT(ITMAX,CF)
C*
C*    HEIGHT CALCULATES THE WAVE HEIGHT
C*
C*-----------------------------------------------------------------
      COMMON D(50,50),W(50,50),Y(50,50),Z(50,50),SI(50,50),CO(50,50),
     *H(50,50),CG(50,50),S(50,50),HBREAK(50,50),IB(50,50),DDDX(50,50)
     *,DDDY(50,50),U(50,50),V(50,50)
      COMMON/CONST/ G,PI,PI2,RAD,EPS,DX,DY,DT,DX2,DY2,T,SIGMA,
     *M,N,N1,N2,M1,M2,AM,DD,IT,RHO,IWET,IDRY,ID
      COMMON/STRESS/SIGX(50,50),SIGY(50,50),SIGXY(50,50),TAUBX(50,50),
     *TAUBY(50,50),TAUSX(50,50),TAUSY(50,50)
      COMMON/REF/ZZ(50,50),HNEW(50,50),RKA(50,50)
       VISCOS=1.0E-05
       PERM=1.06E-09
      DO 500 I=2,M1
      DO 500 J=2,N1
      IF(D(I,J-1).LE.DD) GO TO 499
      CALL GROUP(I,J,DCGDX,DCGDY,FF)
      DUDX=(W(I+1,J)-W(I,J))/DX
      DUDY=(U(I,J+1)-U(I,J-1))/DY2
      DVDX=(V(I+1,J)-V(I-1,J))/DX2
      DVDY=(Y(I,J+1)-Y(I,J))/DY
      DTDX=(Z(I+1,J)-Z(I-1,J))/DX2
      DTDY=(Z(I,J+1)-Z(I,J-1))/DY2
  501 SS2=SI(I,J)**2
      CC2=CO(I,J)**2
      CH=COSH(RKA(I,J)*D(I,J-1))
      IF(ID.EQ.1) GO TO 301
      X=0.0
      GO TO 302
 301  X=RKA(I,J)*CF*SIGMA*H(I,J)/(6.*PI*(CH**3.-CH))
      X=X+G*PERM*RKA(I,J)/(VISCOS*CH*CH)
 302  NA=N1
      NB=N2
      SIGXX=(2.0*FF-0.5)*CC2+(FF-0.5)*SS2
      SIGYY=(2.0*FF-0.5)*SS2+(FF-0.5)*CC2
```

```
      SIGX(I,J) = SIGXX
      SIGY(I,J) = SIGYY
      TAUXY=FF*SI(I,J)*CO(I,J)
      SIGXY(I,J)=TAUXY
      S(I,J)=CG(I,J)*(SI(I,J)*DTDX-CO(I,J)*DTDY)-(DUDX+DVDY)-(CO(I,J)*DC
     *GDX+SI(I,J)*DCGDY)-(SIGXX*DUDX+TAUXY*DUDY+TAUXY*DVDX+SIGYY*DVDY)-X
      GO TO 500
  499 H(I,J)=0.0
      SIGXY(I,J)=0.0
  500 CONTINUE
      DO 510 II=1,M2
      I=M-II
      DO 580 ITT=1,ITMAX
      IFLAG=1
      DO 520 J=2,N1
      IF(D(I,J-1) .LE. DD) GO TO 520
      IB(I,J)=1
      CC1=(V(I,J)+CG(I,J)*SI(I,J))/DY
      CC2=(U(I,J)+CG(I,J)*CO(I,J))/DX
      HNEW(I,J)= (CC1*H(I,J-1)-CC2*H(I+1,J))/(CC1-CC2-S(I,J)/2.0)
      IF (HNEW(I,J) .LT. 0.0) GO TO 810
      IF(HNEW(I,J).LE.HBREAK(I,J)) GO TO 850
  810 HNEW(I,J)=HBREAK(I,J)
      IB(I,J)=0
  850 CONTINUE
      IF(ABS(HNEW(I,J)-H(I,J)).GT.(EPS*ABS(HNEW(I,J)))) IFLAG=0
C*-----------------------------------------------------------------
C*    BOUNDARY CONDITIONS
C*-----------------------------------------------------------------
      IF(J.NE.2) GO TO 800
      HNEW(I,N1)=HNEW(I,J)
      IB(I,N1)=IB(I,J)
      GO TO 520
  800 IF(J.NE.3) GO TO 801
      HNEW(I,N2)=HNEW(I,J)
      IB(I,N2)=IB(I,J)
  801 IF(J.NE.N) GO TO 802
      HNEW(I,1)=HNEW(I,J)
      IB(I,1)=IB(I,J)
      GO TO 520
  802 IF(J.NE.N1) GO TO 520
      HNEW(I,2)=HNEW(I,J)
      IB(I,2)=IB(I,J)
  520 CONTINUE
      DO 625 J=1,N2
      H(I,J)=HNEW(I,J)
  625 CONTINUE
      IF(IFLAG.EQ.1) GO TO 570
  580 CONTINUE
      WRITE(6,540) I,ITT
  540 FORMAT(' RELAXATION FOR THE WAVE HEIGHT FAILED TO CONVERGE',
     *'ON ROW ',I5,'AFTER',I6,'ITERATIONS')
      WRITE(6,541)(H(I,J),J=1,N2    )
  541 FORMAT('  LAST VALUES OF H ARE'/,10F13.5)
C     RETURN
  570 CONTINUE
  510 CONTINUE
      RETURN
      END
C*-----------------------------------------------------------------
C*
      SUBROUTINE ANGLE(ITMAX)
```

```
C*
C*    ANGLE CALCULATES THE LOCAL WAVE DIRECTION
C*
C*-----------------------------------------------------------------------
      COMMON D(50,50),W(50,50),Y(50,50),Z(50,50),SI(50,50),CO(50,50),
     *H(50,50),CG(50,50),S(50,50),HBREAK(50,50),IB(50,50),DDDX(50,50)
     *,DDDY(50,50),U(50,50),V(50,50)
      COMMON/CONST/ G,PI,PI2,RAD,EPS,DX,DY,DT,DX2,DY2,T,SIGMA,
     *M,N,N1,N2,M1,M2,AM,DD,IT,RHO,IWET,IDRY,ID
C*-----------------------------------------------------------------------
C*    DEFINE STATEMENT FUNCTIONS - C,SS,DUDX,DUDY,DVDX,DVDY,DKDX,
C*    DKDY,FAC,F
C*-----------------------------------------------------------------------
      C(I,J)=0.25*(CO(I+1,J)+CO(I-1,J)+CO(I,J+1)+CO(I,J-1))+0.125*((Z(I
     *+1,J)-Z(I-1,J))*(SI(I+1,J)-SI(I-1,J))+ (Z(I,J+1)-Z(I,J-1))*(SI(I,
     *J+1)-SI(I,J-1)))
      SS(I,J)=0.25*(SI(I+1,J)+SI(I-1,J)+SI(I,J+1)+SI(I,J-1))+0.125*((Z(I
     *+1,J)-Z(I-1,J))*(CO(I-1,J)-CO(I+1,J)) + (Z(I,J+1)-Z(I,J-1))*(CO(I,
     *J-1)-CO(I,J+1)))
      DUDX(I,J)=(W(I+1,J)-W(I,J))/DX
      DUDY(I,J)=(U(I,J+1)-U(I,J-1))/DY2
      DVDX(I,J)=(V(I+1,J)-V(I-1,J))/DX2
      DVDY(I,J)=(Y(I,J+1)-Y(I,J))/DY
      F(I,J)=U(I,J)*COSI+V(I,J)*SINI + 0.5*A*(1.0 + ARG2/SINH2)/RK
      DKDY(I,J)=(-(COSI*DUDY(I,J) + SINI*DVDY(I,J))-A*DDDY(I,J-1)/SINH2)
     */FF
      DKDX(I,J)=(-(COSI*DUDX(I,J)+SINI*DVDX(I,J))-A*DDDX(I,J-1)/SINH2)/F
     *F
      FAC(I,J)=U(I,J)*SINI-V(I,J)*COSI
      DO 200 ITT=1,ITMAX
      MWET=M-IWET
      IFLAG=1
      DO 210 II=1,MWET
      I=M-II
      DO 210 J=2,N1
      IF(D(I,J-1).LE.DD) GO TO 210
      COSI=C(I,J)
      SINI=SS(I,J)
      JJ=J-1
      CALL WVNUM(D(I,JJ),COSI,SINI,U(I,J),V(I,J),RK,A)
      ARG2=2.0*RK*D(I,JJ)
      SINH2=SINH(ARG2)
      FF=F(I,J)
      IF(FF.GT.0.0) GO TO 450
      WRITE(6,451) I,J,D(I,JJ),COSI,SINI,U(I,J),V(I,J),RK,A
  451 FORMAT(10X'FF IS NEGATIVE--OUTPUT I,J,D,COSI,SINI,U,V,RK,A'/,
     *2I5,7E13.4)
      GO TO 210
  450 FACI=FAC(I,J)
      DEN1=(SINI-COSI*FACI/FF)/DY
      DEN2=(COSI+SINI*FACI/FF)/DX
      DEN=DEN1-DEN2
      ZNEW=(COSI*DKDY(I,J)-SINI*DKDX(I,J)+Z(I,J-1)*DEN1-Z(I+1,J)*
     *DEN2)/DEN
      IF(ABS(ZNEW-Z(I,J)).GT.(EPS*ABS(ZNEW))) IFLAG=0
      Z(I,J)=ZNEW
      CO(I,J)=COS(Z(I,J))
      SI(I,J)=SIN(Z(I,J))
      IF(J.NE.2) GO TO 400
      Z(I,N1)=Z(I,2)
      CO(I,N1)=CO(I,2)
      SI(I,N1)=SI(I,2)
```

```
      GO TO 210
  400 IF(J.NE.3) GO TO 401
      Z(I,N2)=Z(I,3)
      CO(I,N2)=CO(I,3)
      SI(I,N2)=SI(I,3)
      GO TO 210
  401 IF(J.NE.N) GO TO 402
      Z(I,1)=Z(I,N)
      CO(I,1)=CO(I,N)
      SI(I,1)=SI(I,N)
      GO TO 210
  402 CONTINUE
      IF(J.NE.N1) GO TO 210
      Z(I,2)=Z(I,N1)
      CO(I,2)=CO(I,N1)
      SI(I,2)=SI(I,N1)
  210 CONTINUE
      IF(IFLAG.EQ.1) GO TO 250
  200 CONTINUE
      WRITE(6,220) ITMAX
  220 FORMAT(" RELAXATION FOR THETA FAILED AFTER",I4,3X,
     *"ITERATIONS")
      STOP
  250 CONTINUE
      RETURN
      END
C*-----------------------------------------------------------------
C*
      SUBROUTINE WVNUM(D,COSI,SINI,U,V,RK,A)
C*
C*    WVNUM CALCULATES THE WAVE NUMBER INCLUDING THE EFFECTS OF
C*    WAVE-CURRENT INTERACTION
C*
C*-----------------------------------------------------------------
      COMMON/CONST/ G,PI,PI2,RAD,EPS,DX,DY,DT,DX2,DY2,T,SIGMA,
     *M,N,N1,N2,M1,M2,AM,DD,IT,RHO,IWET,IDRY,ID
      EPSK=0.001
      RK=PI2/(T*SQRT(G*D))
      DO 1 I=1,50
      A=SIGMA-U*RK*COSI-RK*V*SINI
      A2=A**2
      ARG=RK*D
      F1=EXP(ARG)
      F2=1.0/F1
      SECH=2.0/(F1+F2)
      SECH2=SECH**2
      TT=TANH(ARG)
      FK=G*RK*TT-A2
      FFK=G*(ARG*SECH2+TT)+2.0*(U*COSI+V*SINI)*A
      RKNEW=RK-FK/FFK
      IF(ABS(RKNEW-RK).LE.(ABS(EPSK*RKNEW)))GO TO 3
      RK=RKNEW
    1 CONTINUE
      WRITE(6,2)I,RK,T,D,U,V
    2 FORMAT(" ITERATION FOR K FAILED TO CONVERGE: I,K,D,U,V"
     *,I6,5F10.5)
      CALL EXIT
      RETURN
    3 RK=RKNEW
      A=SIGMA-RK*U*COSI-RK*V*SINI
C*------------------------------------------------------------------
C*    CHECK IF RK NEGATIVE; THIS CONDITION MAY ARRISE IF CURRENT IS
```

```
C*    TOO STRONG
C*-----------------------------------------------------------------
      IF(RK.GT.0.0)GO TO 5
      WRITE(6,4)D,COSI,SINI,U,V,RK,A
    4 FORMAT(" RK IS NEGATIVE: D,COSI,SINI,U,V,RK,A",
     *7F10.5)
      CALL EXIT
    5 RETURN
      END
C*------------------------------------------------------------------
C*
      SUBROUTINE SNELL(THETAO,HH,ITER)
C*
C*    SNELL CALCULATES THE FIRST GUESS AT THE REFRACTION ANGLE
C*    AT EACH GRID BY SNELL'S LAW, FOR EACH ITERATION IN WHICH THE
C*    DEEPWATER WAVE HEIGHT IS BUILDING UP
C*
C*    SNELL ALSO CALCULATES THE WAVE HEIGHT AT THE M GRID ROW
C*
C*-----------------------------------------------------------------
      COMMON D(50,50),U(50,50),V(50,50),Z(50,50),SI(50,50),CO(50,50),
     *H(50,50),CG(50,50),S(50,50),HBREAK(50,50),IB(50,50),DDDX(50,50)
     *,DDDY(50,50)
      COMMON/CONST/ G,PI,PI2,RAD,EPS,DX,DY,DT,DX2,DY2,T,SIGMA,
     *M,N,N1,N2,M1,M2,AM,DD,IT,RHO,IWET,IDRY,ID
      I=IDRY
   30 I=I+1
      IF(ITER.GT.1) I=M
      DO 600 J=2,N1
      CALL WVNUM(D(I,J-1),-1.0,0.0,0.0,0.0,RK,A)
      AA = RK* D(I,J-1)
      ANG = ARSIN(SIN(THETAO)*TANH(AA))
      ANG = PI-ANG
      ARG = 2.0*AA
      SHOAL = SQRT(1.0/(TANH(AA)*(1.0+ARG/SINH(ARG))))
      REF = SQRT(COS(THETAO)/COS(ANG))
      WVHT = HH*SHOAL*REF
      HB = 0.12*TANH(AA)*PI2/RK
      IF(WVHT .GT. HB) WVHT = HB
      IN = 1
      IF(WVHT .GT. HB) IN = 0
      SS = SIN(ANG)
      CC = COS(ANG)
   43 CONTINUE
      H(I,J) = WVHT
      IB(I,J) = IN
      Z(I,J) = ANG
      SI(I,J) = SS
      CO(I,J) = CC
  600 CONTINUE
      IF(I.EQ.M) GO TO 85
      GO TO 30
   85 CONTINUE
C*-----------------------------------------------------------------
C*    BOUNDARY CONDITIONS
C*-----------------------------------------------------------------
      L = 1
      K = N
      J = 1
   45 DO 60 I = 1,M
      H(I,J) = H(I,K)
      IB (I,J) = IB(I,K)
```

```
      Z(I,J)=Z(I,K)
      SI(I,J) = SI(I,K)
   60 CO(I,J) = CO(I,K)
      L = L+1
      IF (L .GT. 3) RETURN
      IF (L .EQ. 3)  GO TO 610
      L = 2
      J = 2
      K=N1
      GO TO 45
  610 J = N2
      K = 3
      GO TO 45
      RETURN
      END
C*-------------------------------------------------------------------
C*
      SUBROUTINE DGRAD
C*
C*    DGRAD CALCULATES THE SPATIAL GRADIENTS IN DEPTH AFTER EACH
C*    UPDATING OF THE TOTAL DEPTH
C*
C*-------------------------------------------------------------------
      COMMON D(50,50),U(50,50),V(50,50),Z(50,50),SI(50,50),CO(50,50),
     *H(50,50),CG(50,50),S(50,50),HBREAK(50,50),IB(50,50),DDDX(50,50)
     *,DDDY(50,50)
      COMMON/CONST/ G,PI,PI2,RAD,EPS,DX,DY,DT,DX2,DY2,T,SIGMA,
     *M,N,N1,N2,M1,M2,AM,DD,IT,RHO,IWET,IDRY,ID
      DO 1 I = 2,M1
      DO 1 J = 2,N1
      DDDX(I,J) =-(D(I-1,J)-D(I+1,J))/(2.*DX)
      DDDY(I,J) =-(D(I,J-1)-D(I,J+1))/(2.*DY)
    1 CONTINUE
      DO 2 I = 1,M
      DDDX(I,1)=DDDX(I,N)
      DDDY(I,1)=DDDY(I,N)
      DDDX(I,2)=DDDX(I,N1)
      DDDY(I,2)=DDDY(I,N1)
      DDDX(I,N2)=DDDX(I,3)
      DDDY(I,N2)=DDDY(I,3)
    2 CONTINUE
      RETURN
      END
C*-------------------------------------------------------------
C*
      SUBROUTINE TAUSB (WIND, WINANG, CF,ITO)
C*
C*    THIS SUBROUTINE CALCULATES SURFACE SHEAR STRESS BY VAN DORN'S
C*    METHOD, AND AN AVERAGE BOTTOM SHEAR STRESS USING A SMALL
C*    CURRENT ASSUMPTION
C*
C*-----------------------------------------------------------------
      COMMON D(50,50),U(50,50),V(50,50),Z(50,50),SI(50,50),CO(50,50),
     *H(50,50),CG(50,50),S(50,50),HBREAK(50,50),IB(50,50),DDDX(50,50),
     *DDDY(50,50),W(50,50),Y(50,50)
      COMMON/VAL/ETA(50,50)
      COMMON/STRESS/SIGXX(50,50),SIGYY(50,50),SIGXY(50,50),TAUBX(50,50),
     *TAUBY(50,50),TAUSX(50,50),TAUSY(50,50)
      COMMON/REF/ZZ(50,50),HNEW(50,50),RKA(50,50)
      COMMON/CONST/ G,PI,PI2,RAD,EPS,DX,DY,DT,DX2,DY2,T,SIGMA,
     *M,N,N1,N2,M1,M2,AM,DD,IT,RHO,IWET,IDRY,ID
C*-----------------------------------------------------------------
```

```
C*    CALCULATE WIND SHEAR STRESS
C*-----------------------------------------------------------------------
      IF(IT.GT.ITO+1) GO TO 21
      VANCON=1.1E-06
      IF (WIND .GE.7.2) VANCON = 1.1E-06+2.5E-06*((1.-7.2/WIND)**2.)
      WINDX = WIND*COS(WINANG)
      WINDY = WIND*SIN(WINANG)
      CON1  = RHO*VANCON*ABS(WIND)
      DO 20 J = 1,N2
      DO 20 I = 2, M
      TAUSX(I,J) =- CON1 *WINDX
      TAUSY(I,J) = CON1 *WINDY
   20 CONTINUE
C*----------------------------------------------------------------------
C*    CALCULATE BOTTOM FRICTION AT EACH GRID POINT
C*-----------------------------------------------------------------------
 21   DO 40 J = 2,N1
      K = J-1
      DO 40 I = IWET,M1
      TAUBX(I,J) = (.5*CF*RHO*H(I,J)*W(I,J))/(T*SINH(RKA(I,J)*D(I,K)))
      TAUBY(I,J) = (.25*CF*RHO*H(I,J)*Y(I,J))/(T*SINH(RKA(I,J)*D(I,K)))
   40 CONTINUE
      DO 100 I = 1,M
      TAUBX(I,1) = TAUBX(I,N)
      TAUBX(I,N1) = TAUBX( I,2)
      TAUBX(I,N2) = TAUBX(I,3)
      TAUBY(I,1) = TAUBY(I,N)
      TAUBY(I,N1) = TAUBY( I,2)
      TAUBY(I,N2) = TAUBY(I,3)
  100 CONTINUE
      RETURN
      END
C*----------------------------------------------------------------------
      SUBROUTINE UCALC
C*
C*    THIS SUBROUTINE CALCULATES THE MEAN HORIZONTAL VELOCITIES
C*    USING THE FINITE DIFFERENCE EQUATIONS
C*
C*    NOTE THAT ALL DEPTHS USED ARE OFFSET BY -DY
C*
C*----------------------------------------------------------------------
      COMMON D(50,50),U(50,50),V(50,50),Z(50,50),SI(50,50),CO(50,50),
     *H(50,50),CG(50,50),S(50,50),HBREAK(50,50),IB(50,50),DDDX(50,50),
     *DDDY(50,50),W(50,50),Y(50,50)
      COMMON/VAL/ETA(50,50)
      COMMON/STRESS/SIGXX(50,50),SIGYY(50,50),SIGXY(50,50),TAUBX(50,50),
     *TAUBY(50,50),TAUSX(50,50),TAUSY(50,50)
      COMMON/REF/ZZ(50,50),HNEW(50,50),RKA(50,50)
      COMMON/CONST/G,PI,PI2,RAD,EPS,DX,DY,DT,DX2,DY2,T,SIGMA,
     *M,N,N1,N2,M1,M2,AM,DD,IT,RHO,IWET,IDRY,ID
      DO 21 J=3,N1
      K=J-1
      DO 21 I=IWET,M-1
      DBAR = (D(I,K)+D(I-1,K))/2.
      U(I,J) = U(I,J) +DT*((ETA(I-1,J) - ETA(I,J))*G/DX+(SIGXX(I-1,J)-SI
     1GXX(I,J))/(DX*RHO*DBAR )  - (SIGXY(I,J+1)-SIGXY(I,J-1)+SIGXY(I-1,J
     2+1)-SIGXY(I-1,J-1))/(4.*DY*RHO*DBAR)+(TAUSX(I,J)+TAUSX(I-1,J))/(2.
     3*RHO*DBAR)-(TAUBX(I,J)+TAUBX(I-1,J))/(2.*RHO*DBAR))
      U(IWET,J)=0.0
      DBAR = (D(I,K) + D(I,K-1))/2.0
      V(I,J)=V(I,J) +DT*((ETA(I,J-1)-ETA(I,J))*G/DY-(SIGXY(I+1,J-1)-SIGX
     1Y(I-1,J-1))/(4.*DX*RHO*DBAR)-(SIGXY(I+1,J)-SIGXY(I-1,J))/(4.*DX*RH
```

```
      2O*DBAR)+(SIGYY(I,J-1) - SIGYY(I,J))/(DY*RHO*DBAR)+(TAUSY(I,J) + TA
      3USY(I,J-1))/(2.*RHO*DBAR) - (TAUBY(I,J) + TAUBY(I,J-1))/(2.*RHO*DB
      4AR))
   21 CONTINUE
C*-----------------------------------------------------------------
C*    BOUNDARY CONDITIONS
C*-----------------------------------------------------------------
      DO 60 I=1,M
      V(I,N2) = V(I,3)
      U(I,N2) = U(I,3)
      V(I,2) = V(I,N1)
      U(I,2) = U(I,N1)
      V(I,1) = V(I,N)
   60 U(I,1) = U(I,N)
      DO 69 I=1,M1
      DO 69 J=2,N1
      U(M,J)=0.0
      W(I,J)=(U(I,J)+U(I+1,J))/2.0
      Y(I,J)=(V(I,J)+V(I,J+1))/2.0
   69 CONTINUE
      DO 79 I=1,M
      Y(I,N2)=Y(I,3)
      W(I,N2)=W(I,3)
      Y(I,1)=Y(I,N)
   79 W(I,1)=W(I,N)
      DO 80 J=1,N+2
   80 Y(M,J)=(V(M,J)+V(M,J+1))/2.0
      RETURN
      END
C*-----------------------------------------------------------------
C*
      SUBROUTINE ETAS
C*
C*    ETAS CALCULATES THE CORRECTION TO SETUP AND TOTAL DEPTH BASED
C*    ON CONSERVATION OF MASS
C*
C*-----------------------------------------------------------------
      COMMON D(50,50),U(50,50),V(50,50),Z(50,50),SI(50,50),CO(50,50),
     *H(50,50),CG(50,50),S(50,50),HBREAK(50,50),IB(50,50),DDDX(50,50),
     *DDDY(50,50),W(50,50),Y(50,50)
      COMMON/VAL/ETA(50,50)
      COMMON/STRESS/SIGXX(50,50),SIGYY(50,50),SIGXY(50,50),TAUBX(50,50),
     *TAUBY(50,50),TAUSX(50,50),TAUSY(50,50)
      COMMON/REF/ZZ(50,50),HNEW(50,50),RKA(50,50)
      COMMON/CONST/ G,PI,PI2,RAD,EPS,DX,DY,DT,DX2,DY2,T,SIGMA,
     *M,N,N1,N2,M1,M2,AM,DD,IT,RHO,IWET,IDRY,ID
      DO 1 J = 3,N1
      K = J-1
      DO 1 I=IWET,M1
      ETAOLD = ETA(I,J)
      ETA(I,J)=ETAOLD+DT*(U(I,J)*(D(I,K)+D(I-1,K))/(2.*DX)    - U(I+1,J)
     1*(D(I,K)+D(I+1,K))/(2.*DX)+V(I,J)*(D(I,K-1)+D(I,K))/(2.*DY) - V(I,
     2J+1)*(D(I,K+1)+D(I,K))/(2.*DY))
      D(I,K) = D(I,K) - ETAOLD + ETA(I,J)
    1 CONTINUE
C*-----------------------------------------------------------------
C*    BOUNDARY CONDITIONS
C*-----------------------------------------------------------------
      DO 2 I = 1,M
      D(I,1)=D(I,N)
      D(I,N2) = D(I,3)
      D(I,N1) = D(I,2)
```

```
      ETA(I,N2) = ETA(I,3)
      ETA(I,2) = ETA(I,N1)
    2 ETA(I,1) = ETA(I,N)
      DO 3 I=1,M
      IF(D(I,1).GT.DD) GO TO 4
    3 CONTINUE
    4 IWET=I
      IDRY=IWET-1
      RETURN
      END
```

NONLINEAR MODEL

```
$RESET FREE
C*---------------------------------------------------------------
C*
C*    NEARSHORE CIRCULATION MODEL --- NONLINEAR VERSION
C*
C*    THIS PROGRAM IS A NUMERICAL MODEL TO PREDICT SURF ZONE DYNAMICS,
C*    GIVEN A PERIODIC DEPTH GRID AND MONOCHROMATIC WAVE FIELD AS INPUT.
C*    THE REFRACTION PROGRAM, INCLUDING THE EFFECTS OF WAVE-CURRENT
C*    INTERACTION, WAS DEVELOPED BY NODA ET. AL. (1974).  THE LINEAR
C*    VERSION OF THIS PROGRAM WAS DEVELOPED BY BIRKEMEIER AND DALRYMPLE
C*    (1977).  THE PRESENT NONLINEAR VERSION UTILISES THE FULL NON-
C*    LINEAR MOMENTUM EQUATIONS (EBERSOLE AND DALRYMPLE(1979).  BOTTOM
C*    FRICTION IS CALCULATED USING THE METHOD DEVELOPED BY DALRYMPLE AND
C*    LIU
C*
C*-----------------------------------------------------------------
      COMMON D(50,50),U(50,50),V(50,50),Z(50,50),SI(50,50),CO(50,50),
     *H(50,50),CG(50,50),S(50,50),HBREAK(50,50),IB(50,50),DDDX(50,50),
     *DDDY(50,50),W(50,50),Y(50,50)
      COMMON/VAL/DP1(50,50),DM1(50,50),UP1(50,50),UM1(50,50),
     *VP1(50,50),VM1(50,50),ETAP1(50,50),ETAM1(50,50),ETA(50,50)
      COMMON/STRESS/SIGXX(50,50),SIGYY(50,50),SIGXY(50,50),TAUBX(50,50),
     *TAUBY(50,50),TAUSX(50,50),TAUSY(50,50)
      COMMON/REF/ZZ(50,50),HNEW(50,50),RKA(50,50)
      COMMON/EDDY/EX(50,50),EY,VCON
      COMMON/CONST/ G,PI,PI2,RAD,EPSH,EPSA,DX,DY,DT,DX2,DY2,T,SIGMA,
     *M,N,N1,N2,M1,M2,AM,DD,IT,RHO,IWET,IDRY,ID
      DIMENSION DST(50,50)
C*-----------------------------------------------------------------
C*
C*    NOTES ON RUNNING THE PROGRAM
C*
C*    1. WAVE ANGLE IS MEASURED CLOCKWISE FROM THE +X DIRECTION
C*
C*    2. WIND ANGLE IS MEASURED CLOCKWISE FROM THE -X DIRECTION
C*
C*    3. ALL INPUT AND OUTPUT VARIABLES ARE IN MKS UNITS
C*
C*    4. THE DEPTH GRID IS OFFSET -DY FROM ALL OTHER VARIABLE GRIDS
C*
C*-----------------------------------------------------------------
C*
C*    DEFINITIONS OF QUANTITIES USED IN PROGRAM
C*
C*    1. CONSTANTS
C*
C*       CF - BOTTOM FRICTION COEFFICIENT (DARCY TYPE)
C*       VANCON - WIND SHEAR COEFFICIENT (VAN DORN TYPE)
C*       EY - LATERAL EDDY COEFFICIENT, LONGSHORE DIRECTION
C*       VCON - EDDY VISCOSITY COEFFICIENT, OFFSHORE DIRECTION
C*
C*    2. VARIABLE ARRAYS (VALUE AT EACH GRID LOCATION)
C*
C*       D - TOTAL WATER DEPTH, STILL WATER + SETUP(ETA)
C*       DDDX,DDDY - LOCAL DERIVATIVES OF THE TOTAL DEPTH
C*       ETA - DEVIATION OF MEAN WATER LEVEL FROM STILL WATER LEVEL
C*       Z - WAVE ANGLE
C*       CO - COS(Z)
C*       SI - SIN(Z)
```

```
C*      H - WAVE HEIGHT
C*      HBREAK - LOCAL BREAKING WAVE HEIGHT
C*      IB - BREAKING INDEX
C*           IB=O, WAVE IS BREAKING LOCALLY
C*           IB=1, WAVE IS NOT BREAKING LOCALLY
C*      CG - GROUP VELOCITY
C*      RKA - WAVE NUMBER
C*      U,V - X,Y VELOCITIES AT SIDES OF GRID BLOCKS
C*      W,Y - X,Y VELOCITIES AT CENTERS OF GRID BLOCKS
C*            NOTE THAT THE U,V AND W,Y ARRAYS ARE INTERCHANGED
C*            IN SEVERAL SUBROUTINES THROUGH THE COMMON STATEMENTS
C*      SIGX,SIGXY,SIGY - RADIATION STRESSES
C*      TAUBX,TAUBY - BOTTOM STRESSES
C*      TAUSX,TAUSY - SURFACE STRESSES
C*      EX - LATERAL EDDY COEFFICIENT, OFFSHORE DIRECTION
C*
C*   3. LOCALLY DEFINED VARIABLES
C*
C*      DUDX,DVDX - VELOCITY GRADIENT COMPONANTS
C*      DCDX,DCDY - WAVE CELERITY GRADIENT COMPONANTS
C*      DCGDX,DCGDY - GROUP VELOCITY GRADIENT COMPONANTS
C*      DTDX,DTDY - WAVE ANGLE GRADIENT COMPONANTS
C*      EPS - ACCURACY VALUE USED IN RELAXATION SCHEMES
C*
C*-------------------------------------------------------------
C*
C*   VARIABLES TO BE READ INTO PROGRAM
C*
C*   1. WAVE PARAMETERS (DEEPWATER)
C*
C*      T        - WAVE PERIOD (SECONDS)
C*      HO       - WAVE HEIGHT (METERS)
C*      A        - WAVE ANGLE, CLOCKWISE FROM +X (DEGREES)
C*
C*   2. WIND PARAMETERS
C*
C*      WIND     - WIN SPEED (METERS/SECOND)
C*      WINANG   - WIND ANGLE, CLOCKWISE FROM -X (DEGREES)
C*
C*   3. GRID PARAMETERS
C*
C*      M        - NUMBER OF GRIDS IN X DIRECTION
C*      N        - NUMBER OF GRIDS IN Y DIRECTION
C*      DX       - GRID SPACING IN X DIRECTION (METERS)
C*      DY       - GRID SPACING IN Y DIRECTION (METERS)
C*      DT       - TIME STEP, <DX/SQRT(2*G*DMAX) (SECONDS)
C*      INDEX    - SPECIFY INPUT OF DEPTH INFORMATION
C*                 =1, READ DATA FROM PREVIOUS RUN
C*                 =2, READ DEPTH GRID FROM INPUT DATA FILE
C*                 =3, ESTABLISH PLANE BEACH BASED ON INPUT BEACH SLOPE
C*      AM       - BEACH SLOPE
C*
C*   4. PROGRAM CONTROL PARAMETERS
C*
C*      ITA      - TOTAL NUMBER OF ITERATIONS (INCLUDING ACCUMULATED
C*                 TOTAL OF PREVIOUS RUNS IF INDEX=1 IS USED)
C*      NHIGHT   - NUMBER OF ITERATIONS OVER WHICH THE DEEP WATER WAVE
C*                 HEIGHT IS BUILT UP
C*      ID       - DETERMINE IF DISSAPATION OF WAVE ENERGY IS TO BE
C*                 INCLUDED
C*                 =O, NO DISSAPATION
C*                 =1, DISSAPATION DUE TO VISCOSITY AND BOTTOM PERM-
```

```
C*                      -EABILITY
C*       KSKIP    - DETERMINE FREQUENCY OF PRINTED ITERATIONS
C*
C*    5. DEPTH GRID (IF INDEX=2)
C*
C*       D        - LOCAL WATER DEPTH W/R MEAN WATER LEVEL.
C*                  SEE USERS MANUAL FOR INPUT FORMAT
C*
C*-----------------------------------------------------------
      RHO=1000.
      G=9.81
      PI=3.1415927
      PI2=PI *2.0
      RAD=180.0/PI
      CF=0.010
      DD=0.0
      EY=0.25
      VCON=0.0025
C*-----------------------------------------------------------------
C*    READ INPUT DATA
C*
C*    1. WAVE PARAMETERS
      READ(5,/)T,HO,A
C*    2. WIND PARAMETERS
      READ(5,/)WIND,WINANG
C*    3. GRID PARAMETERS
      READ(5,/)M,N,DX,DY,DT,INDEX,AM
C*    4. PROGRAM CONTROL PARAMETERS
      READ(5,/)ITA,NHIGHT,ID,KSKIP
C*-----------------------------------------------------------------
C*    WRITE INPUT DATA ONTO OUTPUT FILE 6 AS HEADER
C*-----------------------------------------------------------------
      WRITE(6,104)M,N,ITA
      WRITE(6,102)DX,DY,DT
      WRITE(6,105) T,HO,A,AM
      WRITE(6,106) WIND,WINANG
      WRITE(6,119) IDDEX,IN,MM
      WRITE(6,121) NHIGHT
      WRITE(6,120) CF,DD
      WRITE(6,123) EY,VCON
      ITO=0
      HGT=HO
      DELTAT=DT
      WINANG=WINANG/RAD
      N2=N+2
      N1=N+1
      M2=M-2
      M1=M-1
      DX2=DX*2.
      DY2=DY*2.
      SIGMA=PI2/T
      EPSH=0.001
      EPSA=0.01
C*-------------------------------------------------------------
C*    ESTABLISH BOTTOM TOPOGRAPHY, BASED ON VALUE OF "INDEX"
C*-------------------------------------------------------------
      GO TO (1,2,3) INDEX
C*---------------------------------------------------------------
C*    INDEX=1, READ DATA FROM FIE 8 FOR PREVIOUS RUN OF MODEL
C*----------------------------------------------------------------
    1 READ(8,116)
     *((ETA(I,J),J=1,N2),I=1,M),((D(I,J),J=1,N2),I=1,M),
```

```
     *((U(I,J),J=1,N2),I=1,M),((V(I,J),J=1,N2),I=1,M),
     *((UM1(I,J),J=1,N2),I=1,M),((VM1(I,J),J=1,N2),I=1,M),
     *((DM1(I,J),J=1,N2),I=1,M),((ETAM1(I,J),J=1,N2),I=1,M),
     *((Z(I,J),J=1,N2),I=1,M),((H(I,J),J=1,N2),I=1,M),
     *((W(I,J),J=1,N2),I=1,M),((Y(I,J),J=1,N2),I=1,M)
     *,((RKA(I,J),J=1,N2),I=1,M)
      READ(8,118)((SIGXX(I,J),J=1,N2),I=1,M),
     *((SIGXY(I,J),J=1,N2),I=1,M),((SIGYY(I,J),J=1,N2),I=1,M)
      READ(8,117)ITO
      DO 450 I=1,M
      DO 450 J=1,N2
      CO(I,J)=COS(Z(I,J))
      SI(I,J)=SIN(Z(I,J))
  450 CONTINUE
C*------------------------------------------------------------------
C*    IF WAVE ANGLE IS LESS THAN 180 DEGREES, VARIABLE GRIDS WERE
C*    FLIPPED IN PREVIOUS RUN.  ROTATE WAVE AND WIND ANGLES
C*------------------------------------------------------------------
      IF(A.GE.180.) GO TO 31
      A=360.-A
      WINANG=PI2-WINANG
      GO TO 31
C*------------------------------------------------------------------
C*    INDEX=2, READ DEPTH GRID FROM INPUT FILE 5
C*-----------------------------------------------------------------
    2 READ (5,/) ((D(I,J),J=1,N),I=1,M)
C*-------------------------------------------------------------------
C*    IF WAVE ANGLE IS LESS THAN 180 DEGREES, FLIP THE INPUT DEPTH
C*    GRID AND ROTATE THE WAVE AND WIND ANGLES
C*-------------------------------------------------------------------
      IF(A.GT.180.) GO TO 161
      A=360.-A
      WINANG=PI2-WINANG
      DO 158 I=1,M
      DO 159 J=1,N
  159 DST(I,J)=D(I,J)
      DO 158 J=1,N
      K=(N-J)+1
  158 D(I,K)=DST(I,J)
  161 DO 160 I=1,M
      D(I,1)=D(I,N)
      D(I,N2)=D(I,3)
      D(I,N1)=D(I,2)
  160 CONTINUE
      GO TO 146
C*-------------------------------------------------------------------
C*    INDEX=3, ESTABLISH PLANE BEACH
C*------------------------------------------------------------------
    3 DO 30 J=1,N2
      DO 30 I=1,M
      D(I,J)=((FLOAT(I-2)*DX)*AM)
   30 CONTINUE
C*-------------------------------------------------------------------
C*    IF WAVE ANGLE IS LESS THAN 180 DEGREES, ROTATE WAVE AND WIND ANGLE
C*--------------------------------------------------------------------
      IF(A.GE.180.) GO TO 146
      A=360.-A
      WINANG=PI2-WINANG
C*-------------------------------------------------------------------
C*    WRITE DEPTH GRID ON OUTPUT IF INDEX=2 OR 3
C*-------------------------------------------------------------------
  146 WRITE(6,108)
```

```
      WRITE(6,103)((D(I,J),J=1,N1),I=1,M)
C*-----------------------------------------------------------------
C*    INITIALIZE ARRAYS
C*-----------------------------------------------------------------
      DO 65 I=1,M
      DO 65 J=1,N2
      ETA(I,J)=0.0
      U(I,J)=0.0
      V(I,J)=0.0
      ETAM1(I,J)=0.0
      DM1(I,J)=D(I,J)
      UM1(I,J)=0.0
      VM1(I,J)=0.0
   65 CONTINUE
   31 DO 15 I=1,M
      IF(D(I,1).GT.DD) GO TO 95
   15 CONTINUE
   95 IWET=I
      IDRY=IWET-1
C*-----------------------------------------------------------------
C*    MAIN PROGRAM LOOP FOR EACH ITERATION
C*--------------------------------------------------------------
      IT=ITO
      IF(ITO.NE.0) GO TO 4
      HO=HGT*TANH(1.0/FLOAT(NHIGHT))
      CALL DGRAD
      CALL REFRAC(A,HO,1,NHIGHT,CF)
      CALL TAUSB(WIND,WINANG,CF,ITO)
      TSTEP=DT*0.5
      CALL CONTIN
      CALL ETAS(ETA,TSTEP)
      CALL MOMEN
      CALL UCALC(D,U,V,TSTEP)
      CALL ROLBAC
    4 DO 5 IT=(1+ITO),ITA
      L=AMOD(FLOAT(IT),FLOAT(KSKIP))
      MCOUNT=AMOD(FLOAT(IT),10.0)
      HO=HGT*TANH(FLOAT(IT)/(FLOAT(NHIGHT)/2.0))
C     IF(IT.LE.((NHIGHT*2.0)+5)) GO TO 12
C     GO TO 13
   12 CALL DGRAD
      ITP1=IT+1
      CALL REFRAC(A,HO,ITP1,NHIGHT,CF)
   13 CALL TAUSB(WIND,WINANG,CF,ITO)
      IF(IT.EQ.1) GO TO 51
      GO TO 52
   51 TSTEP=DT
      CALL CONTIN
      CALL ETAS(ETAM1,TSTEP)
      CALL MOMEN
      CALL UCALC(DM1,UM1,VM1,TSTEP)
      DO 66 I=1,M
      DO 66 J=1,N2
      ETA(I,J)=ETAP1(I,J)
      D(I,J)=DP1(I,J)
      U(I,J)=UP1(I,J)
      V(I,J)=VP1(I,J)
   66 CONTINUE
      GO TO 18
   52 TSTEP=DT*2.0
      CALL CONTIN
      CALL ETAS(ETAM1,TSTEP)
```

```
      CALL MOMEN
      CALL UCALC(DM1,UM1,VM1,TSTEP)
      IF(MCOUNT.EQ.O) GO TO 53
      CALL ROLBAC
      GO TO 18
   53 CALL ROLBAC
      TSTEP=DT
      CALL CONTIN
      CALL ETAS(ETAM1,TSTEP)
      CALL MOMEN
      CALL UCALC(DM1,UM1,VM1,TSTEP)
      DO 57 I=1,M
      DO 57 J=1,N2
      ETA(I,J)=ETAP1(I,J)
      D(I,J)=DP1(I,J)
      U(I,J)=UP1(I,J)
      V(I,J)=VP1(I,J)
   57 CONTINUE
   18 CONTINUE
      SUM=0.0
      DO 86 I=1,M
      DO 86 J=2,N
      SUM=SUM+0.5*(W(I,J)**2+Y(I,J)**2)*D(I,J-1)
      SUM=SUM+G*ETA(I,J)*(D(I,J-1)-0.5*ETA(I,J))
   86 CONTINUE
      WRITE(6,101) SUM
      IF(L.NE.0)GO TO 5
      WRITE(6,112)
      WRITE(6,113)IT,HO
      WRITE(6,114)
      WRITE(6,115)
      WRITE(6,103)((H(I,J),J=1,N1),I=1,M)
      DO 401 I=1,M
      DO 401 J=1,N2
  401 ZZ(I,J)=360.0-Z(I,J)*RAD
      WRITE(6,122)
      WRITE(6,109)((ZZ(I,J),J=1,N1),I=1,M)
      WRITE (6,107)
      WRITE (6,103) ((U(I,J), J = 1,N1),I=1,M)
      WRITE (6,110)
      WRITE (6,103) ((V(I,J), J = 1,N1),I=1,M)
      WRITE (6,111)
      WRITE(6,103) ((ETA(I,J),J=1,N1),I=1,M)
    5 CONTINUE
C*-----------------------------------------------------------------
C     THE FOLLOWING WRITE STATEMENTS WRITE OUT THE RESULTS OF
C     THE LAST ITERATION ONTO AN OUTPUT FILE TO BE USED FOR A
C     SUBSEQUENT START-UP
C*-------------------------------------------------------------------
      WRITE(3,116)
     *((ETA(I,J),J=1,N2),I=1,M),((D(I,J),J=1,N2),I=1,M),
     *((U(I,J),J=1,N2),I=1,M),((V(I,J),J=1,N2),I=1,M),
     *((UM1(I,J),J=1,N2),I=1,M),((VM1(I,J),J=1,N2),I=1,M),
     *((DM1(I,J),J=1,N2),I=1,M),((ETAM1(I,J),J=1,N2),I=1,M),
     *((Z(I,J),J=1,N2),I=1,M),((H(I,J),J=1,N2),I=1,M),
     *((W(I,J),J=1,N2),I=1,M),((Y(I,J),J=1,N2),I=1,M)
     *,((RKA(I,J),J=1,N2),I=1,M)
      WRITE(3,118)((SIGXX(I,J),J=1,N2),I=1,M),
     *((SIGXY(I,J),J=1,N2),I=1,M),((SIGYY(I,J),J=1,N2),I=1,M)
      WRITE(3,117)ITA
      LOCK 3
  101 FORMAT(1X,"THE TOTAL ENERGY IS",F14.2)
```

```
  102 FORMAT (/,1X,'DX=',F4.1,3X,'DY=',F4.1,3X,'DT=',F5.2)
  103 FORMAT(11F10.4)
  104 FORMAT(1X,"M=",I5,3X,"N=",I5,3X,"ITERATIONS =",I5)
  105 FORMAT(1X,'WAVE PARAMETERS',/2X,'PERIOD =',F7.2,'   HEIGHT =',F7
     *.2,3X,7HANGLE =,F7.2,1X,7HDEGREES,4X,12HBEACH SLOPE=,F7.4)
  106 FORMAT (1X,'WIND SPEED =',F7.3,'M/SEC',5X,'WIND ANGLE =',F7.
     *3,' DEGREES')
  108 FORMAT (//' THE AUGMENTED MATRIX OF WATER DEPTH IN METERS'/)
  109 FORMAT(15F8.3)
  107 FORMAT ( 10X,12HX - VELOCITY)
  110 FORMAT ( 10X,12HY - VELOCITY)
  111 FORMAT (10X,10HETA VALUES)
  112 FORMAT('******************************',/)
  113 FORMAT(10X,'ITERATION NUMBER',I6,10X,'WAVE HEIGHT=',F10.5,/)
  114 FORMAT (1X,'******************************',/)
  115 FORMAT (5X,'WAVE HEIGHTS',/)
  116 FORMAT(15F8.4)
  117 FORMAT(I5)
  118 FORMAT(10F12.2)
  119 FORMAT(5X,'IDDEX =',I5,3X,'IN ='I5,3X,'MM='
     *,I5)
  120 FORMAT(10X,4HCF =,F10.3,5X,4HDD =,F10.3)
  121 FORMAT(10X,'WAVE HEIGHT BUILDS UP FIRST',I3,' ITERATIONS')
  122 FORMAT(2X,'WAVE ANGLE (DEGREES)')
  123 FORMAT(10X,'EY =',F3.1,',   VCON= ',F6.4)
      STOP
      END
C*-------------------------------------------------------------------
C*
      SUBROUTINE REFRAC(THETAO,HH,ITER,NHIGHT,CF)
C*
C*    REFRAC CONTROLS THE CALCULATION OF WAVE HEIGHT AND DIRECTION
C*
C*-------------------------------------------------------------------
      COMMON D(50,50),U(50,50),V(50,50),Z(50,50),SI(50,50),CO(50,50),
     *H(50,50),CG(50,50),S(50,50),HBREAK(50,50),IB(50,50),DDDX(50,50)
     *,DDDY(50,50)
      COMMON/STRESS/SIGX(50,50),SIGY(50,50),SIGXY(50,50),TAUBX(50,50),
     *TAUBY(50,50),TAUSX(50,50),TAUSY(50,50)
      COMMON/CONST/ G,PI,PI2,RAD,EPSH,EPSA,DX,DY,DT,DX2,DY2,T,SIGMA,
     *M,N,N1,N2,M1,M2,AM,DD,IT,RHO,IWET,IDRY,ID
      IF (ITER.GT.NHIGHT) GO TO 1
C*-----------------------------------------------------------------------
C*    CALL SNELL DURING THE BUILDUP OF THE DEEPWATER WAVE
C*-----------------------------------------------------------------------
      THETA=PI2-THETAO/RAD
      CALL SNELL (THETA,HH,ITER)
    1 DO 2 I=1,IDRY
      DO 2 J=1,N2
      H(I,J)=0.0
      Z(I,J)=PI
      SI(I,J)=0.0
      CO(I,J)=-1.0
    2 CONTINUE
C*----------------------------------------------------------------------
C*    CALCULATE WAVE ANGLE AND WAVE HEIGHT AT EACH GRID
C*----------------------------------------------------------------------
      CALL ANGLE(25)
      CALL HEIGHT(25,CF)
C*----------------------------------------------------------------------
C*    CALCULATE THE RADIATION STRESSES
C*----------------------------------------------------------------------
```

```
      DO 4 I=IWET,M1
      DO 3 J=3,N1
      ENERGY=0.125*RHO*G*(H(I,J)**2)
      SIGX(I,J)=SIGX(I,J)*ENERGY
      SIGY(I,J)=SIGY(I,J)*ENERGY
      SIGXY(I,J)=SIGXY(I,J)*ENERGY
    3 CONTINUE
      SIGX(I,1)=SIGX(I,N)
      SIGY(I,1)=SIGY(I,N)
      SIGXY(I,1)=SIGXY(I,N)
      SIGX(I,2)=SIGX(I,N1)
      SIGY(I,2)=SIGY(I,N1)
      SIGXY(I,2)=SIGXY(I,N1)
      SIGX(I,N2)=SIGX(I,3)
      SIGY(I,N2)=SIGY(I,3)
      SIGXY(I,N2)=SIGXY(I,3)
    4 CONTINUE
      DO 5 J=3,N1
      SIGXY(M,J)=2.0*SIGXY(M1,J)-SIGXY(M2,J)
    5 CONTINUE
      SIGXY(M,1)=SIGXY(M,N)
      SIGXY(M,2)=SIGXY(M,N1)
      SIGXY(M,N2)=SIGXY(M,3)
      RETURN
      END
C*-----------------------------------------------------------------
C*
      SUBROUTINE GROUP(I,J,DCGDX,DCGDY,FF)
C*
C*     THIS SUBROUTINE CALCULATES THE GROUP VELOCITY ,WAVE CELERITY
C*     AND THEIR SPATIAL DERIVATIVES.
C*
C*-----------------------------------------------------------------
      COMMON D(50,50),W(50,50),Y(50,50),Z(50,50),SI(50,50),CO(50,50),
     *H(50,50),CG(50,50),S(50,50),HBREAK(50,50),IB(50,50),DDDX(50,50)
     *,DDDY(50,50),U(50,50),V(50,50)
      COMMON/CONST/ G,PI,PI2,RAD,EPSH,EPSA,DX,DY,DT,DX2,DY2,T,SIGMA,
     *M,N,N1,N2,M1,M2,AM,DD,IT,RHO,IWET,IDRY,ID
      COMMON/REF/ZZ(50,50),HNEW(50,50),RKA(50,50)
      DUDX(I,J)=(W(I+1,J)-W(I,J))/DX
      DUDY(I,J)=(U(I,J+1)-U(I,J-1))/DY2
      DVDX(I,J)=(V(I+1,J)-V(I-1,J))/DX2
      DVDY(I,J)=(Y(I,J+1)-Y(I,J))/DY
      DTDX(I,J)=(Z(I+1,J)-Z(I-1,J))/DX2
      DTDY(I,J)=(Z(I,J+1)-Z(I,J-1))/DY2
      E(I,J)=U(I,J)*COSI+V(I,J)*SINI+0.5*A*(1.0+ARG2/SINH2)/RK
      DKDX(I,J)=RK*((U(I,J)*SINI-V(I,J)*COSI)*DTDX(I,J)-(COSI*DUDX(I,J)+
     *SINI*DVDX(I,J))-A*DDDX(I,J-1)/SINH2)/EE
      DKDY(I,J)=RK*((U(I,J)*SINI-V(I,J)*COSI)*DTDY(I,J)-(COSI*DUDY(I,J)
     * +SINI*DVDY(I,J))-A*DDDY(I,J-1)/SINH2)/EE
      JJ=J-1
      DEP=D(I,JJ)
      COSI=CO(I,J)
      SINI=SI(I,J)
      DCGDX=0.0
      DCGDY=0.0
C*  CHECK FOR DRY LAND
      IF(DEP.LE.DD) RETURN
      CALL WVNUM(DEP,COSI,SINI,U(I,J),V(I,J),RK,A)
      RKA(I,J) = RK
      IF (J.EQ.N) RKA(I,1)=RKA(I,J)
      IF (J.EQ.2) RKA(I,N1)=RKA(I,J)
```

```
      IF (J.EQ.3) RKA(I,N2)=RKA(I,J)
      TA=TANH(RK*DEP)
      HBREAK(I,J)=0.12*PI2*TA/RK
      COSH1=COSH(RK*DEP)
      SECHSQ=1.0/(COSH1**2)
      ARG2=2.0*RK*DEP
      SINH2=SINH(ARG2)
      COSH2=COSH(ARG2)
      SINHSQ=SINH2**2
      EE=E(I,J)
      C=SQRT(G*TA/RK)
      FF=0.5*(1.0+ARG2/SINH2)
      CG(I,J)=FF*C
      P=C*(SINH2-ARG2*COSH2)/SINHSQ
      DKDDX=RK*DDDX(I,JJ)+DEP*DKDX(I,J)
      DKDDY=RK*DDDY(I,JJ)+DEP*DKDY(I,J)
      Q=0.5*G/(C*RK**2)
      DCDX=Q*(RK*SECHSQ*DKDDX-TA*DKDX(I,J))
      DCDY=Q*(RK*SECHSQ*DKDDY-TA*DKDY(I,J))
      DCGDX=P*DKDDX+FF*DCDX
      DCGDY=P*DKDDY+FF*DCDY
      RETURN
      END
C*-----------------------------------------------------------------
C*
      SUBROUTINE HEIGHT(ITMAX,CF)
C
C*    HEIGHT CALCULATES THE LOCAL WAVE HEIGHT AT EACH GRID LOCATION
C*
C*-----------------------------------------------------------------
      COMMON D(50,50),W(50,50),Y(50,50),Z(50,50),SI(50,50),CO(50,50),
     *H(50,50),CG(50,50),S(50,50),HBREAK(50,50),IB(50,50),DDDX(50,50)
     *,DDDY(50,50),U(50,50),V(50,50)
      COMMON/CONST/ G,PI,PI2,RAD,EPSH,EPSA,DX,DY,DT,DX2,DY2,T,SIGMA,
     *M,N,N1,N2,M1,M2,AM,DD,IT,RHO,IWET,IDRY,ID
      COMMON/STRESS/SIGX(50,50),SIGY(50,50),SIGXY(50,50),TAUBX(50,50),
     *TAUBY(50,50),TAUSX(50,50),TAUSY(50,50)
      COMMON/REF/ZZ(50,50),HNEW(50,50),RKA(50,50)
       VISCOS=1.0E-05
       PERM=1.06E-09
      DO 500 I=2,M1
      DO 500 J=2,N1
      IF(D(I,J-1).LE.DD) GO TO 499
      CALL GROUP(I,J,DCGDX,DCGDY,FF)
      DUDX=(W(I+1,J)-W(I,J))/DX
      DUDY=(U(I,J+1)-U(I,J-1))/DY2
      DVDX=(V(I+1,J)-V(I-1,J))/DX2
      DVDY=(Y(I,J+1)-Y(I,J))/DY
      DTDX=(Z(I+1,J)-Z(I-1,J))/DX2
      DTDY=(Z(I,J+1)-Z(I,J-1))/DY2
  501 SS2=SI(I,J)**2
      CC2=CO(I,J)**2
       CH=COSH(RKA(I,J)*D(I,J-1))
      IF(ID.EQ.1) GO TO 301
      X=0.0
      GO TO 302
 301  X=RKA(I,J)*CF*SIGMA*H(I,J)/(6.*PI*(CH**3.-CH))
      X=X+G*PERM*RKA(1,J)/(VISCOS*CH*CH)
 302  NA=N1
      NB=N2
      SIGXX=(2.0*FF-0.5)*CC2+(FF-0.5)*SS2
      SIGYY=(2.0*FF-0.5)*SS2+(FF-0.5)*CC2
```

```
      SIGX(I,J) = SIGXX
      SIGY(I,J) = SIGYY
      TAUXY=FF*SI(I,J)*CO(I,J)
      SIGXY(I,J)=TAUXY
      S(I,J)=CG(I,J)*(SI(I,J)*DTDX-CO(I,J)*DTDY)-(DUDX+DVDY)-(CO(I,J)*DC
     *GDX+SI(I,J)*DCGDY)-(SIGXX*DUDX+TAUXY*DUDY+TAUXY*DVDX+SIGYY*DVDY)-X
      GO TO 500
  499 H(I,J)=0.0
      SIGXY(I,J)=0.0
  500 CONTINUE
      DO 510 II=1,M2
      I=M-II
      DO 580 ITT=1,ITMAX
      IFLAG=1
      DO 520 J=2,N1
      IF(D(I,J-1) .LE. DD) GO TO 520
      IB(I,J)=1
      CC1=(V(I,J)+CG(I,J)*SI(I,J))/DY
      CC2=(U(I,J)+CG(I,J)*CO(I,J))/DX
      HNEW(I,J)= (CC1*H(I,J-1)-CC2*H(I+1,J))/(CC1-CC2-S(I,J)/2.0)
      IF (HNEW(I,J) .LT. 0.0) GO TO 810
      IF(HNEW(I,J).LE.HBREAK(I,J)) GO TO 850
  810 HNEW(I,J)=HBREAK(I,J)
      IB(I,J)=0
  850 CONTINUE
      IF(ABS(HNEW(I,J)-H(I,J)).GT.(EPSH*ABS(HNEW(I,J)))) IFLAG=0
C*     BOUNDARY CONDITIONS
      IF(J.NE.2) GO TO 800
      HNEW(I,N1)=HNEW(I,J)
      IB(I,N1)=IB(I,J)
      GO TO 520
  800 IF(J.NE.3) GO TO 801
      HNEW(I,N2)=HNEW(I,J)
      IB(I,N2)=IB(I,J)
  801 IF(J.NE.N) GO TO 802
      HNEW(I,1)=HNEW(I,J)
      IB(I,1)=IB(I,J)
      GO TO 520
  802 IF(J.NE.N1) GO TO 520
      HNEW(I,2)=HNEW(I,J)
      IB(I,2)=IB(I,J)
  520 CONTINUE
      DO 625 J=1,N2
      H(I,J)=HNEW(I,J)
  625 CONTINUE
      IF(IFLAG.EQ.1) GO TO 570
  580 CONTINUE
      WRITE(6,540) I,ITT
  540 FORMAT(' RELAXATION FOR THE WAVE HEIGHT FAILED TO CONVERGE',
     *'ON ROW ',I5,'AFTER',I6,'ITERATIONS')
      WRITE(6,541)(H(I,J),J=1,N2    )
  541 FORMAT('  LAST VALUES OF H ARE'/,10F13.5)
C     RETURN
  570 CONTINUE
  510 CONTINUE
      RETURN
      END
C*-----------------------------------------------------------------
C*
      SUBROUTINE ANGLE(ITMAX)
C*
C*    ANGLE CALCULATES THE LOCAL WAVE DIRECTION AT EACH GRID LOCATION
```

```
C*
C*-----------------------------------------------------------------
      COMMON D(50,50),W(50,50),Y(50,50),Z(50,50),SI(50,50),CO(50,50),
     *H(50,50),CG(50,50),S(50,50),HBREAK(50,50),IB(50,50),DDDX(50,50)
     *,DDDY(50,50),U(50,50),V(50,50)
      COMMON/CONST/ G,PI,PI2,RAD,EPSH,EPSA,DX,DY,DT,DX2,DY2,T,SIGMA,
     *M,N,N1,N2,M1,M2,AM,DD,IT,RHO,IWET,IDRY,ID
C*-------------------------------------------------------------
C*    DEFINE STATEMENT FUNCTIONS C,SS,DUDX,DUDY,DVDX,DVDY,DKDX
C*    DKDY,FAC,F
C*-------------------------------------------------------------
      C(I,J)=0.25*(CO(I+1,J)+CO(I-1,J)+CO(I,J+1)+CO(I,J-1))+0.125*((Z(I
     *+1,J)-Z(I-1,J))*(SI(I+1,J)-SI(I-1,J))+ (Z(I,J+1)-Z(I,J-1))*(SI(I,
     *J+1)-SI(I,J-1)))
      SS(I,J)=0.25*(SI(I+1,J)+SI(I-1,J)+SI(I,J+1)+SI(I,J-1))+0.125*((Z(I
     *+1,J)-Z(I-1,J))*(CO(I-1,J)-CO(I+1,J)) + (Z(I,J+1)-Z(I,J-1))*(CO(I,
     *J-1)-CO(I,J+1)))
      DUDX(I,J)=(W(I+1,J)-W(I,J))/DX
      DUDY(I,J)=(U(I,J+1)-U(I,J-1))/DY2
      DVDX(I,J)=(V(I+1,J)-V(I-1,J))/DX2
      DVDY(I,J)=(Y(I,J+1)-Y(I,J))/DY
      F(I,J)=U(I,J)*COSI+V(I,J)*SINI + 0.5*A*(1.0 + ARG2/SINH2)/RK
      DKDY(I,J)=(-(COSI*DUDY(I,J) + SINI*DVDY(I,J))-A*DDDY(I,J-1)/SINH2)
     */FF
      DKDX(I,J)=(-(COSI*DUDX(I,J)+SINI*DVDX(I,J))-A*DDDX(I,J-1)/SINH2)/F
     *F
      FAC(I,J)=U(I,J)*SINI-V(I,J)*COSI
      DO 200 ITT=1,ITMAX
      MWET=M-IWET
      IFLAG=1
      DO 210 II=1,MWET
      I=M-II
      DO 210 J=2,N1
      IF(D(I,J-1).LE.DD) GO TO 210
      COSI=C(I,J)
      SINI=SS(I,J)
      JJ=J-1
      CALL WVNUM(D(I,JJ),COSI,SINI,U(I,J),V(I,J),RK,A)
      ARG2=2.0*RK*D(I,JJ)
      SINH2=SINH(ARG2)
      FF=F(I,J)
      IF(FF.GT.0.0) GO TO 450
      WRITE(6,451) I,J,D(I,JJ),COSI,SINI,U(I,J),V(I,J),RK,A
  451 FORMAT(10X'FF IS NEGATIVE--OUTPUT I,J,D,COSI,SINI,U,V,RK,A'/,
     *2I5,7E13.4)
      GO TO 210
  450 FACI=FAC(I,J)
      DEN1=(SINI-COSI*FACI/FF)/DY
      DEN2=(COSI+SINI*FACI/FF)/DX
      DEN=DEN1-DEN2
      ZNEW=(COSI*DKDY(I,J)-SINI*DKDX(I,J)+Z(I,J-1)*DEN1-Z(I+1,J)*
     *DEN2)/DEN
      IF(ABS(ZNEW-Z(I,J)).GT.(EPSA*ABS(ZNEW))) IFLAG=0
      Z(I,J)=ZNEW
  992 CO(I,J)=COS(Z(I,J))
      SI(I,J)=SIN(Z(I,J))
      IF(J.NE.2) GO TO 400
      Z(I,N1)=Z(I,2)
      CO(I,N1)=CO(I,2)
      SI(I,N1)=SI(I,2)
      GO TO 210
  400 IF(J.NE.3) GO TO 401
```

```
      Z(I,N2)=Z(I,3)
      CO(I,N2)=CO(I,3)
      SI(I,N2)=SI(I,3)
      GO TO 210
  401 IF(J.NE.N) GO TO 402
      Z(I,1)=Z(I,N)
      CO(I,1)=CO(I,N)
      SI(I,1)=SI(I,N)
      GO TO 210
  402 CONTINUE
      IF(J.NE.N1) GO TO 210
      Z(I,2)=Z(I,N1)
      CO(I,2)=CO(I,N1)
      SI(I,2)=SI(I,N1)
  210 CONTINUE
      IF(IFLAG.EQ.1) GO TO 250
  200 CONTINUE
      WRITE(6,220) ITMAX
  220 FORMAT(" RELAXATION FOR THETA FAILED AFTER",I4,3X,
     *"ITERATIONS")
      STOP
  250 CONTINUE
      RETURN
      END
C*-----------------------------------------------------------------
C*
      SUBROUTINE WVNUM(D,COSI,SINI,U,V,RK,A)
C*
C*    SUBROUTINE WVNUM COMPUTES WAVE NUMBER INCLUDING WAVE-
C*    CURRENT INTERACTION.
C*
C*-----------------------------------------------------------------
      COMMON/CONST/ G,PI,PI2,RAD,EPSH,EPSA,DX,DY,DT,DX2,DY2,T,SIGMA,
     *M,N,N1,N2,M1,M2,AM,DD,IT,RHO,IWET,IDRY,ID
      EPSK=0.001
      RK=PI2/(T*SQRT(G*D))
      DO 100I=1,50
      A=SIGMA-U*RK*COSI-RK*V*SINI
      A2=A**2
      ARG=RK*D
      F1=EXP(ARG)
      F2=1 O/F1
      SECH=2.0/(F1+F2)
      SECH2=SECH**2
      TT=TANH(ARG)
      FK=G*RK*TT-A2
      FFK=G*(ARG*SECH2+TT)+2.0*(U*COSI+V*SINI)*A
      RKNEW=RK-FK/FFK
      IF(ABS(RKNEW-RK).LE.(ABS(EPSK*RKNEW)))GO TO 110
      RK=RKNEW
  100 CONTINUE
      WRITE(6,101)I,RK,T,D,U,V
  101 FORMAT(" INTERATION FOR K FAILED TO CONVERGE: I,K,D,U,V"
     *,I6,5F10.5)
      CALL EXIT
      RETURN
  110 RK=RKNEW
      A=SIGMA-RK*U*COSI-RK*V*SINI
C*-----------------------------------------------------------------
C*    CHECK IF RK NEGATIVE, THIS CONDITION CAN ARISE IF LOCAL CURRENT
C*    IS TOO STRONG
C*-----------------------------------------------------------------
```

```
      IF(RK.GT.0.0)GO TO 120
      WRITE(6,130)D,COSI,SINI,U,V,RK,A
  130 FORMAT(" RK IS NEGATIVE: D,COSI,SINI,U,V,RK,A",
     *7F10.5)
      CALL EXIT
  120 RETURN
      END
C*--------------------------------------------------------------
C*
      SUBROUTINE SNELL (THETAO,HH,ITER)
C*
C*    SNELL CALCULATES THE FIRST GUESS OF THE REFRACTION ANGLE
C*    AT EACH GRID, AND ALSO THE WAVE HEIGHT AT THE LAST GRID(M)
C*    FOR EACH ITERATION THAT THE DEEPWATER WAVE IS BUILDING UP.
C*
C*-----------------------------------------------------------------
      COMMON D(50,50),U(50,50),V(50,50),Z(50,50),SI(50,50),CO(50,50),
     *H(50,50),CG(50,50),S(50,50),HBREAK(50,50),IB(50,50),DDDX(50,50)
     *,DDDY(50,50)
      COMMON/CONST/ G,PI,PI2,RAD,EPSH,EPSA,DX,DY,DT,DX2,DY2,T,SIGMA,
     *M,N,N1,N2,M1,M2,AM,DD,IT,RHO,IWET,IDRY,ID
      I=IDRY
   30 I=I+1
      IF(ITER.GT.1) I=M
      DO 600 J=2,N1
      CALL WVNUM(D(I,J-1),-1.0,0.0,0.0,0.0,RK,A)
      AA = RK* D(I,J-1)
      ANG = ARSIN(SIN(THETAO)*TANH(AA))
      ANG = PI-ANG
      ARG = 2.0*AA
      SHOAL = SQRT(1.0/(TANH(AA)*(1.0+ARG/SINH(ARG))))
      REF = SQRT(COS(THETAO)/COS(ANG))
      WVHT = HH*SHOAL*REF
      HB = 0.12*TANH(AA)*PI2/RK
      IF(WVHT .GT. HB) WVHT = HB
      IN = 1
      IF(WVHT .GT. HB) IN = 0
      SS = SIN(ANG)
      CC = COS(ANG)
   43 CONTINUE
      H(I,J) = WVHT
      IB(I,J) = IN
      Z(I,J) = ANG
      SI(I,J) = SS
      CO(I,J) = CC
  600 CONTINUE
      IF(I.EQ.M) GO TO 85
      GO TO 30
   85 CONTINUE
C*--------------------------------------------------------------
C*    BOUNDARY CONDITIONS
C*--------------------------------------------------------------
      L = 1
      K = N
      J = 1
   45 DO 60 I = 1,M
      H(I,J) = H(I,K)
      IB (I,J) = IB(I,K)
      Z(I,J)=Z(I,K)
      SI(I,J) = SI(I,K)
   60 CO(I,J) = CO(I,K)
      L = L+1
```

```
      IF (L .GT. 3) RETURN
      IF (L .EQ. 3)  GO TO 610
      L = 2
      J = 2
      K=N1
      GO TO 45
  610 J = N2
      K = 3
      GO TO 45
      RETURN
      END
C*-----------------------------------------------------------------
C*
      SUBROUTINE TAUSB (WIND, WINANG, CF,ITO)
C*
C*    THIS SUBROUTINE CALCULATES SURFACE SHEAR STRESS BY VAN DORN'S
C*    METHOD, AND AVERAGE BOTTOM SHEAR STRESS BY THE METHOD OF
C*    DALRYMPLE AND LIU
C*
C*    WIND SPEED MUST BE IN METERS/SECOND
C*
C*------------------------------------------------------------------
      COMMON D(50,50),U(50,50),V(50,50),Z(50,50),SI(50,50),CO(50,50),
     *H(50,50),CG(50,50),S(50,50),HBREAK(50,50),IB(50,50),DDDX(50,50),
     *DDDY(50,50),W(50,50),Y(50,50)
      COMMON/VAL/DP1(50,50),DM1(50,50),UP1(50,50),UM1(50,50),
     *VP1(50,50),VM1(50,50),ETAP1(50,50),ETAM1(50,50),ETA(50,50)
      COMMON/STRESS/SIGXX(50,50),SIGYY(50,50),SIGXY(50,50),TAUBX(50,50),
     *TAUBY(50,50),TAUSX(50,50),TAUSY(50,50)
      COMMON/REF/ZZ(50,50),HNEW(50,50),RKA(50,50)
      COMMON/CONST/ G,PI,PI2,RAD,EPSH,EPSA,DX,DY,DT,DX2,DY2,T,SIGMA,
     *M,N,N1,N2,M1,M2,AM,DD,IT,RHO,IWET,IDRY,ID
      DIMENSION B(40),F(40),GG(40)
C*------------------------------------------------------------------
C*    COMPUTE SURFACE SHEAR STRESS
C*-------------------------------------------------------------------
      IF(IT.GT.ITO+1) GO TO 1
      VANCON=1.1E-06
      IF (WIND .GE.7.2) VANCON = 1.1E-06+2.5E-06*((1.-7.2/WIND)**2.)
      WINDX = WIND*COS(WINANG)
      WINDY = WIND*SIN(WINANG)
      CON1  = RHO*VANCON*ABS(WIND)
      DO 20 J = 1,N2
      DO 20 I = 2, M
      TAUSX(I,J) =- CON1 *WINDX
      TAUSY(I,J) = CON1 *WINDY
   20 CONTINUE
C*-------------------------------------------------------------------
C*    COMPUTE BOTTOM SHEAR STRESS
C*--------------------------------------------------------------------
    1 L=16
      DELTA=PI2/L
      VALUE=(RHO*CF)/(24.0*L)
      DO 4 J=2,N1
      K=J-1
      DO 4 I=IWET,M1
      PHI=Z(I,J)-PI
      CC=COS(PHI)
      SS=SIN(PHI)
      UMAX=(PI*H(I,J))/(T*SINH(RKA(I,J)*D(I,K)))
      EXPR1=UMAX*SS
      EXPR2=UMAX*CC
```

```
      EXPR3=2.0*EXPR2
      EXPR4=2.0*EXPR1
      WM1=(UM1(I,J)+UM1(I+1,J))/2.0
      YM1=(VM1(I,J)+VM1(I,J+1))/2.0
      EXPR5=WM1**2
      EXPR6=YM1**2
      DELX=0.0
      DO 2 LL=1,L+1,1
      B(LL)=SQRT(EXPR5+EXPR6+(UMAX*COS(DELX))**2+COS(DELX)*
     *(WM1*EXPR3+YM1*EXPR4))
      GG(LL)=(YM1+EXPR1*COS(DELX))*B(LL)
      F(LL)=(WM1+EXPR2*COS(DELX))*B(LL)
      DELX=DELX+DELTA
    2 CONTINUE
      SUM=0.0
      SUMM=0.0
      DO 3 MM=2,L,2
      SUM=SUM+F(MM-1)+4.0*F(MM)+F(MM+1)
      SUMM=SUMM+GG(MM-1)+4.0*GG(MM)+GG(MM+1)
    3 CONTINUE
      TAUBX(I,J)=SUM*VALUE
      TAUBY(I,J)=SUMM*VALUE
    4 CONTINUE
   42 DO 5 I=1,M
      TAUBX(I,1) = TAUBX(I,N)
      TAUBX(I,N1) = TAUBX(I,2)
      TAUBX(I,N2) = TAUBX(I,3)
      TAUBY(I,1) = TAUBY(I,N)
      TAUBY(I,N1) = TAUBY(I,2)
      TAUBY(I,N2) = TAUBY(I,3)
    5 CONTINUE
      RETURN
      END
C*-----------------------------------------------------------------------
C*
      SUBROUTINE DGRAD
C*
C*    CALCULATE THE SPATIAL GRADIENTS IN TOTAL DEPTH AFTER EACH
C*    UPDATING OF THE TOTAL DEPTH
C*
C*-----------------------------------------------------------------------
      COMMON D(50,50),U(50,50),V(50,50),Z(50,50),SI(50,50),CO(50,50),
     *H(50,50),CG(50,50),S(50,50),HBREAK(50,50),IB(50,50),DDDX(50,50)
     *,DDDY(50,50)
      COMMON/CONST/ G,PI,PI2,RAD,EPSH,EPSA,DX,DY,DT,DX2,DY2,T,SIGMA,
     *M,N,N1,N2,M1,M2,AM,DD,IT,RHO,IWET,IDRY,ID
      DO 60 I = 2,M1
      DO 60 J = 3,N1
      DDDX(I,J) =-(D(I-1,J)-D(I+1,J))/(2.*DX)
      IF(J.EQ.N1) GO TO 61
      DDY=D(I,J-2)-8.0*D(I,J-1)+8.0*D(I,J+1)-D(I,J+2)
      DDDY(I,J)=DDY/(12.0*DY)
      GO TO 60
   61 DDY=D(I,N-1)-8.0*D(I,N)+8.0*D(I,N+2)-D(I,4)
      DDDY(I,J)=DDY/(12.0*DY)
   60 CONTINUE
      DO 70 I = 1,M
      DDDX(I,1)=DDDX(I,N)
      DDDY(I,1)=DDDY(I,N)
      DDDX(I,2)=DDDX(I,N1)
      DDDY(I,2)=DDDY(I,N1)
      DDDX(I,N2)=DDDX(I,3)
```

```
      DDDY(I,N2)=DDDY(I,3)
   70 CONTINUE
      RETURN
      END
C*-------------------------------  ----------------------------
C*
      SUBROUTINE MOMEN
C*
C*    MOMEN CALCULATES VELOCITIES USING THE FULL NONLINEAR MOMENTUM
C*    EQUATIONS
C*
C*-------------------------------------------------------------------
      COMMON D(50,50),U(50,50),V(50,50),Z(50,50),SI(50,50),CO(50,50),
     *H(50,50),CG(50,50),S(50,50),HBREAK(50,50),IB(50,50),DDDX(50,50),
     *DDDY(50,50),W(50,50),Y(50,50)
      COMMON/VAL/DP1(50,50),DM1(50,50),UP1(50,50),UM1(50,50),
     *VP1(50,50),VM1(50,50),ETAP1(50,50),ETAM1(50,50),ETA(50,50)
      COMMON/STRESS/SIGX(50,50),SIGY(50,50),SIGXY(50,50),TAUBX(50,50),
     *TAUBY(50,50),TAUSX(50,50),TAUSY(50,50)
      COMMON/EDDY/EX(50,50),EY,VCON
      COMMON/CONST/ G,PI,PI2,RAD,EPSH,EPSA,DX,DY,DT,DX2,DY2,T,SIGMA,
     *M,N,N1,N2,M1,M2,AM,DD,IT,RHO,IWET,IDRY,ID
      DO 97 I=IWET,M
      DO 96 J=3,N1
      EX(I,J)=((I-IWET+1)*DX)*VCON*SQRT(G*DM1(I,J-1))
      IF(I.GE.12) EX(I,J)=.875
   96 CONTINUE
      EX(I,N2)=EX(I,3)
      EX(I,2)=EX(I,N1)
      EX(I,1)=EX(I,N)
   97 CONTINUE
   99 DO 21 J=3,N1
      K = J-1
      DO 21 I=IWET,M1
      UP1(I,J)=(((D(I+1,K)+D(I,K))*U(I+1,J)+(D(I,K)+D(I-1,K))*
     *U(I,J))*(U(I+1,J)+U(I,J))-((D(I,K)+D(I-1,K))*U(I,J)+
     *(D(I-1,K)+D(I-2,K))*U(I-1,J))*(U(I,J)+U(I-1,J)))/(8.0*DX)
      UP1(I,J)=UP1(I,J)+(((D(I,K+1)+D(I,K))*V(I,J+1)+(D(I-1,K+1)+
     *D(I-1,K))*V(I-1,J+1))*(U(I,J)+U(I,J+1))-((D(I,K)+D(I,K-1))*
     * V(I,J)+(D(I-1,K)+D(I-1,K-1))*V(I-1,J))*(U(I,J)+U(I,J-1)))
     */(8.0*DY)
      UP1(I,J)=UP1(I,J)+(D(I,K)+D(I-1,K))*(ETA(I,J)-ETA(I-1,J))
     **(G/(DX*2.0))
      UP1(I,J)=UP1(I,J)-(TAUSX(I,J)+TAUSX(I-1,J))/(2.0*RHO)
      UP1(I,J)=UP1(I,J)+(TAUBX(I,J)+TAUBX(I-1,J))/(2.0*RHO)
      UP1(I,J)=UP1(I,J)+(SIGX(I,J)-SIGX(I-1,J))/(DX*RHO)+(SIGXY(I,
     *J+1)-SIGXY(I,J-1)+SIGXY(I-1,J+1)-SIGXY(I-1,J-1))/(4.0*DY*RHO)
      UP1(I,J)=UP1(I,J)-(DM1(I,K)+DM1(I-1,K))*((UM1(I,J+1)-
     *UM1(I,J))*EY-(UM1(I,J)-UM1(I,J-1))*EY)/(2.0*DY*DY)
      UP1(I,J)=UP1(I,J)-(DM1(I,K)+DM1(I-1,K))*((VM1(I,J+1)-
     *VM1(I-1,J+1))*(EX(I,J+1)+EX(I,J)+EX(I-1,J)+EX(I-1,J+1))-
     *(VM1(I,J)-VM1(I-1,J))*(EX(I,J)+EX(I,J-1)+EX(I-1,J-1)+
     *EX(I-1,J)))/(8.0*DX*DY)
      VP1(I,J)=(((D(I+1,K)+D(I,K))*U(I+1,J)+(D(I+1,K-1)+D(I,K-1))*
     *U(I+1,J-1))*(V(I+1,J)+V(I,J))-((D(I,K)+D(I-1,K))*U(I,J)+
     *(D(I,K-1)+D(I-1,K-1))*U(I,J-1))*(V(I,J)+V(I-1,J)))/(8.0*DX)
      IF (K.EQ.2) GO TO 83
      GO TO 84
   83 VP1(I,J)=VP1(I,J)+(((D(I,K+1)+D(I,K))*V(I,J+1)+(D(I,K)+
     *D(I,K-1))*V(I,J))*(V(I,J+1)+V(I,J))-((D(I,K)+D(I,K-1))*
     *V(I,J)+(D(I,K-1)+D(I,N-1))*V(I,J-1))*(V(I,J)+V(I,J-1)))/(8.0*DY)
      GO TO 85
```

```
   84 VP1(I,J)=VP1(I,J)+(((D(I,K+1)+D(I,K))*V(I,J+1)+(D(I,K)+
     *D(I,K-1))*V(I,J))*(V(I,J+1)+V(I,J))-((D(I,K)+D(I,K-1))*
     *V(I,J)+(D(I,K-1)+D(I,K-2))*V(I,J-1))*(V(I,J)+V(I,J-1)))/(8.0*DY)
   85 VP1(I,J)=VP1(I,J)+(D(I,K)+D(I,K-1))*(ETA(I,J)-ETA(I,J-1))*
     *(G/(2.0*DY))
      VP1(I,J)=VP1(I,J)-(TAUSY(I,J)+TAUSY(I,J-1))/(2.0*RHO)
      VP1(I,J)=VP1(I,J)+(TAUBY(I,J)+TAUBY(I,J-1))/(2.0*RHO)
      VP1(I,J)=VP1(I,J)+(SIGXY(I+1,J-1)-SIGXY(I-1,J-1)+SIGXY
     *(I+1,J)-SIGXY(I-1,J))/(4.0*RHO*DX)+(SIGY(I,J)-SIGY(I,J-1))
     */(RHO*DY)
      VP1(I,J)=VP1(I,J)-(DM1(I,K)+DM1(I,K-1))*((EX(I+1,J-1)+
     *EX(I+1,J)+EX(I,J-1)+EX(I,J))*(VM1(I+1,J)-VM1(I,J))-(
     *EX(I,J-1)+EX(I,J)+EX(I-1,J-1)+EX(I-1,J))*(VM1(I,J)-
     *VM1(I-1,J)))/(8.0*DX*DX)
      VP1(I,J)=VP1(I,J)-(DM1(I,K)+DM1(I,K-1))*((UM1(I+1,J)-
     *UM1(I+1,J-1))*EY-(UM1(I,J)-UM1(I,J-1))*EY)/(2.0*DY*DX)
   21 CONTINUE
      RETURN
      END
C*-----------------------------------------------------------------
C*
      SUBROUTINE ETAS(RETA,DELT)
C*
C*    ETAS CALCULATES THE CHANGE IN MEAN WATER LEVEL DUE TO WAVE ACTION
C*
C*-----------------------------------------------------------------
      COMMON D(50,50),U(50,50),V(50,50),Z(50,50),SI(50,50),CO(50,50),
     *H(50,50),CG(50,50),S(50,50),HBREAK(50,50),IB(50,50),DDDX(50,50),
     *DDDY(50,50),W(50,50),Y(50,50)
      COMMON/VAL/DP1(50,50),DM1(50,50),UP1(50,50),UM1(50,50),
     *VP1(50,50),VM1(50,50),ETAP1(50,50),ETAM1(50,50),ETA(50,50)
      COMMON/CONST/ G,PI,PI2,RAD,EPSH,EPSA,DX,DY,DT,DX2,DY2,T,SIGMA,
     *M,N,N1,N2,M1,M2,AM,DD,IT,RHO,IWET,IDRY,ID
      DIMENSION RETA(50,50)
      DO 20 J=2,N1
      DO 20 I=IWET,M1
      K=J-1
      ETAP1(I,J)=RETA(I,J)-(DELT*0.5)*ETAP1(I,J)
   22 DP1(I,K)=D(I,K)-ETA(I,J)+ETAP1(I,J)
   20 CONTINUE
      DO 23 J=2,N1
      K=J-1
      DO 24 I=1,IDRY
      DP1(I,K)=D(I,K)
   24 CONTINUE
      DP1(M,K)=D(M,K)
   23 CONTINUE
      DO 60 I=1,M
      ETAP1(I,N2)=ETAP1(I,3)
      ETAP1(I,N1)=ETAP1(I,2)
      ETAP1(I,1)=ETAP1(I,N)
      DP1(I,N2)=DP1(I,3)
      DP1(I,N1)=DP1(I,2)
      DP1(I,1)=DP1(I,N)
   60 CONTINUE
      DO 92 I=1,M
      IF(DP1(I,1).GT.DD) GO TO 93
   92 CONTINUE
   93 IWET=I
      IDRY=IWET-1
      RETURN
      END
```

```
C*---------------------------------------------------------------------
C*
      SUBROUTINE UCALC(TD,TU,TV,DELT)
C*
C*    UCALC CALCULATES THE DEPTH AVERAGED VELOCITIES BASED ON THE
C*    RESULTS OF SUBROUTINE MOMEN
C*
C*---------------------------------------------------------------------
      COMMON D(50,50),U(50,50),V(50,50),Z(50,50),SI(50,50),CO(50,50),
     *H(50,50),CG(50,50),S(50,50),HBREAK(50,50),IB(50,50),DDDX(50,50),
     *DDDY(50,50),W(50,50),Y(50,50)
      COMMON/VAL/DP1(50,50),DM1(50,50),UP1(50,50),UM1(50,50),
     *VP1(50,50),VM1(50,50),ETAP1(50,50),ETAM1(50,50),ETA(50,50)
      COMMON/CONST/ G,PI,PI2,RAD,EPSH,EPSA,DX,DY,DT,DX2,DY2,T,SIGMA,
     *M,N,N1,N2,M1,M2,AM,DD,IT,RHO,IWET,IDRY,ID
      DIMENSION  TD(50,50),TU(50,50),TV(50,50)
      DO 24 I=IWET,M1
      DO 24 J=3,N1
      K=J-1
      UP1(I,J)=((TD(I,K)+TD(I-1,K))*TU(I,J))/(DP1(I,K)+DP1(I-1,
     *K))-((DELT*2.0)/(DP1(I,K)+DP1(I-1,K)))*UP1(I,J)
      VP1(I,J)=((TD(I,K)+TD(I,K-1))*TV(I,J))/(DP1(I,K)+
     *DP1(I,K-1))-((DELT*2.0)/(DP1(I,K)+DP1(I,K-1)))*VP1(I,J)
   24 CONTINUE
      DO 22 J=3,N1
      DO 27 I=1,IWET
      UP1(I,J)=0.0
   27 CONTINUE
      UP1(M,J)=0.0
      VP1(M,J)=VP1(M1,J)
   22 CONTINUE
      DO 60 I=1,M
      UP1(I,N2)=UP1(I,3)
      UP1(I,2)=UP1(I,N1)
      UP1(I,1)=UP1(I,N)
      VP1(I,N2)=VP1(I,3)
      VP1(I,2)=VP1(I,N1)
      VP1(I,1)=VP1(I,N)
   60 CONTINUE
      DO 69 J=2,N1
      DO 68 I=1,M1
      W(I,J)=(UP1(I,J)+UP1(I+1,J))/2.0
      Y(I,J)=(VP1(I,J)+VP1(I,J+1))/2.0
   68 CONTINUE
      Y(M,J)=0.0
   69 CONTINUE
      DO 79 I=1,M
      W(I,N2)=W(I,3)
      W(I,2)=W(I,N1)
      W(I,1)=W(I,N)
      Y(I,N2)=Y(I,3)
      Y(I,2)=Y(I,N1)
      Y(I,1)=Y(I,N)
   79 CONTINUE
      RETURN
      END
C*---------------------------------------------------------------------
C*
      SUBROUTINE ROLBAC
C*
C*    ROLBAC UPDATES THE VALUES OF ETA,U,V,AND D FOR THE NEXT
C*    ITERATION
```

```
C*
C*-----------------------------------------------------------------
      COMMON D(50,50),U(50,50),V(50,50),Z(50,50),SI(50,50),CO(50,50),
     *H(50,50),CG(50,50),S(50,50),HBREAK(50,50),IB(50,50),DDDX(50,50),
     *DDDY(50,50),W(50,50),Y(50,50)
      COMMON/VAL/DP1(50,50),DM1(50,50),UP1(50,50),UM1(50,50),
     *VP1(50,50),VM1(50,50),ETAP1(50,50),ETAM1(50,50),ETA(50,50)
      COMMON/CONST/ G,PI,PI2,RAD,EPSH,EPSA,DX,DY,DT,DX2,DY2,T,SIGMA,
     *M,N,N1,N2,M1,M2,AM,DD,IT,RHO,IWET,IDRY,ID
      DO 1 I=1,M
      DO 1 J=1,N2
      ETAM1(I,J)=ETA(I,J)
      ETA(I,J)=ETAP1(I,J)
      UM1(I,J)=U(I,J)
      U(I,J)=UP1(I,J)
      VM1(I,J)=V(I,J)
      V(I,J)=VP1(I,J)
      D(I,J)=DP1(I,J)
      DM1(I,J)=D(I,J)
    1 CONTINUE
      RETURN
      END
C*-----------------------------------------------------------------
C*
      SUBROUTINE CONTIN
C*
C*    CONTIN CALCULATES THE FINAL CORRECTION TO TOTAL DEPTH BASED
C*    ON THE EQUATION OF CONTINUITY
C*
C*-----------------------------------------------------------------
      COMMON D(50,50),U(50,50),V(50,50),Z(50,50),SI(50,50),CO(50,50),
     *H(50,50),CG(50,50),S(50,50),HBREAK(50,50),IB(50,50),DDDX(50,50),
     *DDDY(50,50),W(50,50),Y(50,50)
      COMMON/VAL/DP1(50,50),DM1(50,50),UP1(50,50),UM1(50,50),
     *VP1(50,50),VM1(50,50),ETAP1(50,50),ETAM1(50,50),ETA(50,50)
      COMMON/CONST/ G,PI,PI2,RAD,EPSH,EPSA,DX,DY,DT,DX2,DY2,T,SIGMA,
     *M,N,N1,N2,M1,M2,AM,DD,IT,RHO,IWET,IDRY,ID
      DO 20 J=2,N1
      K=J-1
      DO 20 I=IWET,M1
      IF (K.EQ.1) GO TO 21
      ETAP1(I,J)=(((D(I+1,K)+D(I,K))*U(I+1,J)-
     *(D(I,K)+D(I-1,K))*U(I,J))/DX+((D(I,K+1)+D(I,K))*V(I,J+1)-
     *(D(I,K)+D(I,K-1))*V(I,J))/DY)
      GO TO 20
   21 ETAP1(I,J)=(((D(I+1,K)+D(I,K))*U(I+1,J)-
     *(D(I,K)+D(I-1,K))*U(I,J))/DX+((D(I,K+1)+D(I,K))*V(I,J+1)
     *-(D(I,K)+D(I,N-1))*V(I,J))/DY)
   20 CONTINUE
      RETURN
      END
```

Distribution

Office of Naval Research
Coastal Science Program
Code 42205
Arlington, VA 22217

Defense Documentation Center
Cameron Station
Alexandria, VA 22314

Director, Naval Research Lab.
ATTN: Technical Information Officer
Washington, D. C. 20375

Director
Office of Naval Research Branch Office
1030 East Green Street
Pasadena, CA 91101

Chief of Naval Research
Code 100M
Office of Naval Research
Arlington, VA 22217

Office of Naval Research
Operational Applications Division
Code 200
Arlington, VA 22217

Office of Naval Research
Scientific Liaison Officer
Scripps Institution of Oceanography
La Jolla, CA 92093

Director Naval Research Laboratory
ATTN: Library, Code 2628
Washington, D. C. 20375

ONR Scientific Liaison Group
American Embassy ~ Room A-407
APO San Francisco, CA 96503

Commander
Naval Oceanographic Office
ATTN: Library, Code 1600
Washington, D. C. 20374

Naval Oceanographic Office
Code 3001
Washington, D. C. 20374

Chief of Naval Operations
OP 987P1
Department of the Navy
Washington, D. C. 20350

Oceanographer of the Navy
Hoffman II Building
200 Stovall Street
Alexandria, VA 22322

Naval Academy Library
U. S. Naval Academy
Annapolis, MD 21402

Commanding Officer
Naval Coastal Systems Laboratory
Panama City, FL 32401

Director
Coastal Engineering Research Center
U. S. Army Corps of Engineers
Kingman Building
Fort Belvoir, VA 22060

Officer in Charge
Environmental Research Prodctn Fclty.
Naval Postgraduate School
Monterey, CA 93940

Director
Amphibious Warfare Board
U. S. Atlantic Fleet
Naval Amphibious Base
Norfolk, Little Creek, VA 23520

Commander, Amphibious Force
U. S. Pacific Fleet
Force Meteorologist
Comphibpac Code 25 5
San Diego, CA 93155

Librarian, Naval Intelligence
Support Center
4301 Suitland Road
Washington, D. C. 20390

Commanding Officer
Naval Civil Engineering Laboratory
Port Hueneme, CA 93041

Chief, Wave Dynamics Division
USAE-WES
P. O. Box 631
Vicksburg, MS 39180

Commandant
U. S. Coast Guard
ATTN: GECV/61
Washington, D. C. 20591

Office of Research and Development
%DS/62
U. S. Coast Guard
Washington, D. C. 20591

National Oceanographic Data
Center %D764
Environmental Data Services
NOAA
Washington, D. C. 20235

Prof. Dr. Fuehrboeter
Lehrstuhl F. Hydromechanik U. Kuestenw
Technische Hochschule Braunschweig
Beethovenstrasse 51A
D-3300 Braunschweig, West Germany

Prof. Dr. Walter Hansen
Direktor D. Instituts F. Meereskunde
Universitaet Hamburg
Heimhuderstrasse 71
D-2000 Hamburg 13, West Germany

Prof. Dr. Klaus Hasselmann
Institut F. Geophysik
Universitaet Hamburg
Schleuterstrasse 22
D-2000 Hamburg 13, West Germany

Coastal Studies Institute
Louisiana State University
Baton Rouge, LA 70803

Dr. Edward Thornton
Department of Oceanography
Naval Postgraduate School
Monterey, CA 93940

Dr. Douglas I. Inman
University of California A-009
Shore Processes Laboratory
La Jolla, CA 92093

Dr. Bruce Heyden
Dept. of Environmental Sciences
University of Virginia
Charlottesville, VA 22903

ATE

LMED

-8